The Study of Molecular Interactions during Zebrafish Tail Regeneration for use in Glycotherapeutics

Thesis submitted to the University of Sheffield

for the degree of MPhil

by

Philip James Jankun

Department of Biomedical Sciences

March 2017

Contents

Abstract

In recent years the field of regenerative medicine has been inundated with studies focusing on the use of stem cells. However, advances in scientific techniques have allowed us to gain insights into the regenerative process first hand. Using model organisms, such as the zebrafish and axolotl, able to replace lost tissue through epimorphic regeneration, we might eventually be able to induce the same response in mammals.

As developmental signal pathways have been shown to rely on the extracellular glycosaminoglycan, heparan sulphate (HS), to induce a robust ligand-receptor interaction, I hypothesised that this macromolecule has a role during epimorphic regeneration. Using the *dackel/ext2* mutant zebrafish, unable to synthesise HS, my work provides evidence for HS having a crucial role during epimorphic regeneration, following the amputation of their caudal fin. Carrying out *in situ* hybridisation, and chemical manipulation of developmental pathways I was also able to provide evidence for the interaction between the FGF and Wnt pathways, and also identify the Hedgehog pathway as the earliest response following zebrafish caudal fin amputation. During the study of *dackel* regeneration the Hedgehog pathway was downregulated, and the FGF10a and Wnt10a transcripts were lost. Furthermore, I came to the conclusion that FGF10 functions as a mitogen during the latter stages of epimorphic regeneration. Finally, in an attempt to rescue regeneration in *dackel* mutants, I used affinity chromatography to isolate a novel HS fraction to target the Hedgehog pathway. The disaccharide composition and protein binding analysis showed that the positive, $HS23^{+ve}$, fraction differed to the other – negative - fraction. Application of both to amputated *dackel* tails was unable to rescue regeneration. This study has highlighted the need for the Hh, Wnt, and FGF pathways, and their differing roles during larval zebrafish epimorphic regeneration, and the isolation of a Hedgehog-binding HS fraction is possible, but still possesses some level of promiscuity.

1 General Introduction

The modern era of regeneration began around the late 17th to early 18th Century with the observation of lizard tail regeneration by Melchis*é*dech Th*é*venot, and the regrowth of the crayfish limb after amputation by R*é*ne-Antoine R*é*aumer (Dinsmore, 1996). An early hypothesis for limb regeneration was that of preformation: many limbs are stored within the body, to be released after the loss of an appendage. However, more recently, thanks, in part, to the progression of sophisticated genetic techniques, we have moved away from this idea, and are gradually piecing together the complex molecular cues driving this natural phenomenon.

Regeneration covers a broad spectrum of responses, from homeostatic to the more complex epimorphic regeneration, involving the re-growth of whole limbs after amputation. In higher vertebrates, such as mice and humans, replacing damaged tissue is not uncommon, for example the gut or skin epithelium and large parts of the liver (Figure 1-1*).* However, the regenerative capacity of other vertebrates, such as urodele amphibians – salamanders and newts - is unrivalled within the animal kingdom. These lower vertebrates can replace lost lens, tails, or appendages back to a functional state (Wassmer *et al*., 2013. Brockes, 1997).

The zebrafish is a bony fish able to regenerate a broad range of structures, such as the caudal fin (Pfefferli and Jaźwińska, 2015; Poss *et al*., 2002.), much like the urodeles. Many studies investigating zebrafish regeneration focus on the adult stage, which is ideal for identifying the role of certain tissues during the regenerative response, such as bone or nerves. However, the adult zebrafish might not be as suitable for studying pathway interactions that could occur during epimorphic regeneration, as the fish require several months to reach maturity, but also take significantly longer to regenerate. Zebrafish before 5-days post fertilisation (dpf) are more suited to this, because adults can produce hundreds of eggs every week, but also, within 48 hours the

larvae have developed their major internal organs and a broad range of cells are beginning to differentiate.

The initial focus of my project was to identify the activity of developmental pathways during regeneration of the larval zebrafish caudal fin and if they could interact with one another. This was followed by the use of a mutant – *dackel/ext2* - with dramatically reduced levels of heparan sulphate to highlight how signalling events were affected in the absence of such a crucial component of the extracellular matrix, and to see if this could lead to the identification of other mutants unable to regenerate. Finally, after determining which pathway responds the earliest during caudal fin regeneration, I used my time in the Cool lab (Institute of Medical Biology (IMB), A*STAR, Singapore) to isolate, and test biochemically, a novel heparan sulphate fraction that could target the pathway with the intention of rescuing *dackel/ext2* regeneration.

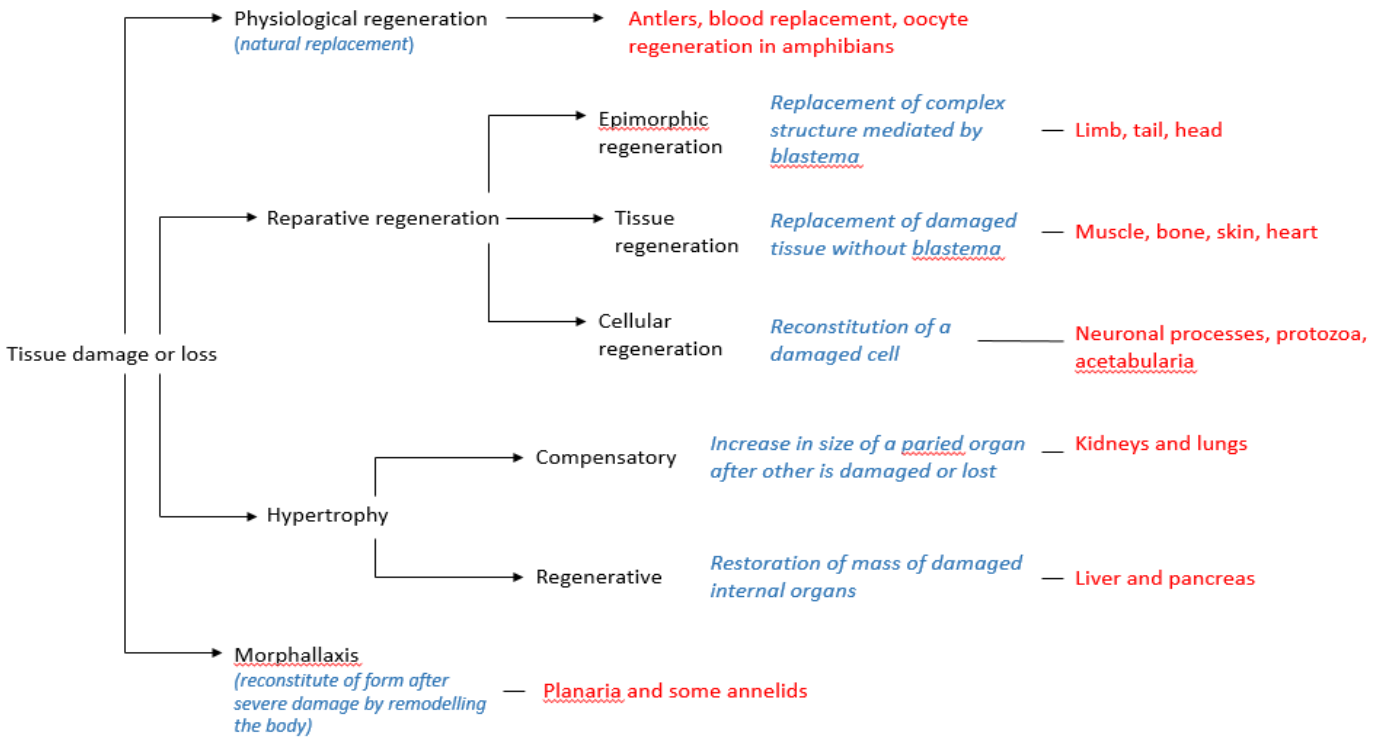

Figure 1-1. A diagram to illustrate the various types of regeneration

1.1. The three stages of epimorphic regeneration

It is widely accepted that the zebrafish regenerates its caudal fin through a process known as epimorphic regeneration – tissue replacement involving a specialised, proliferative cell mass known as the blastema. Epimorphic regeneration is well characterised; having three clearly defined stages, in the following order: wound healing, blastema formation, and regenerative outgrowth (Poss *et al*., 2003) (Figure 1-2). The time taken to regenerate their caudal fin varies from two weeks to four days for adults and juvenile zebrafish, respectively. As this project relies heavily on the use of zebrafish as the model for regeneration, from here on out the majority of the literature will refer to studies carried out using zebrafish.

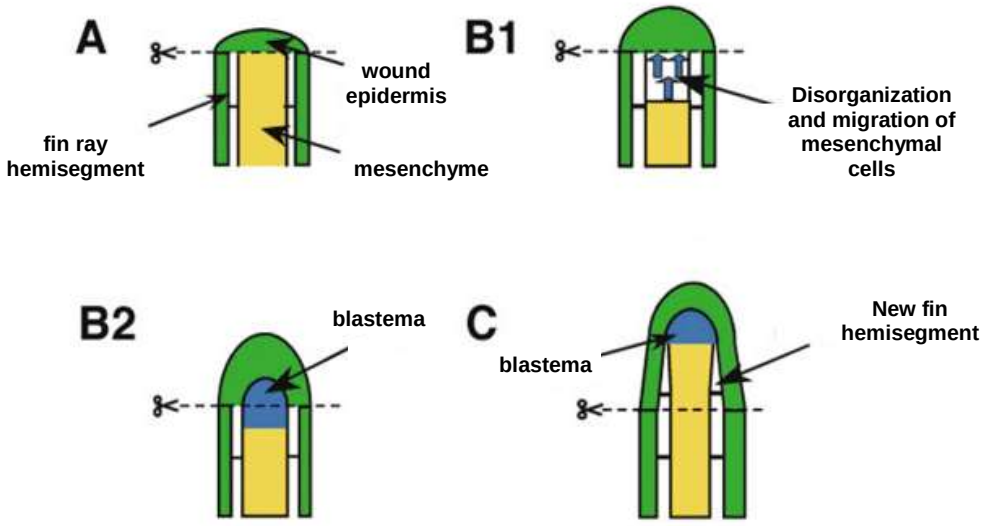

Figure 1-2. Stages of epimorphic regeneration after adult zebrafish caudal fin amputation.
(A) Immediately after amputation epithelial cells migrate to form the wound epidermis.
(B1) Tissue of the mesenchyme becomes disorganized and migrates just proximal to the wound epidermis.
(B2) The mesenchyme organises to form the blastema – a major source of new tissue growth.
(C) Regenerative outgrowth is marked by rapid proliferation and elongation of the regenerate. The whole process can take up to 2 weeks in adults and 5 days in larvae.
Image source: (Poss et al., 2003)

1.1.1. Wound epidermis formation

Immediately after the amputation of an animal's appendage – limb or fin – the epithelial cells surrounding the wound begin to migrate to close the initial wound. This stage of regeneration relies primarily on migration over proliferation (Shimokawa et al., 2012). After approximately 24 hours postamputation (hpa) the wound epithelium begins to thicken into a regenerative structure known as the wound epidermis. Schebesta et al (2006) described the transcriptional events during caudal fin regeneration using microarray and RT-PCR, and also used in situ hybridisation, to highlight the upregulation of the transcription factor, dlx5a, in the basal wound epidermis at 24 hpa (Figure 1-3). As this specialised epidermal structure matures it becomes a crucial signalling centre (Lee et al., 2009) - essential for epimorphic regeneration to progress (Thornton, 1957). It has also been likened to the apical ectodermal ridge (AER) during limb bud development.

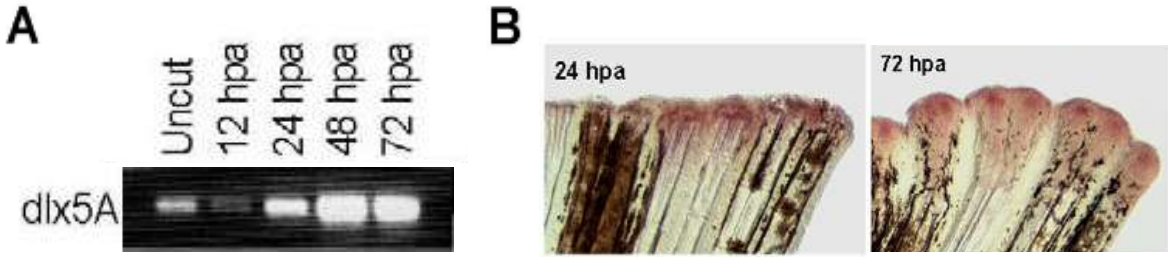

Figure 1-3. *Dlx5a* is a marker of wound epidermis formation.
(A) Semi-quantitati
ve RT-PCR shows an increase in *dlx5a* RNA by 24 hpa
(B) *In situ* hybridization detection of *dlx5a* transcripts at 24 and 72 hpa in the adult caudal fin
Figure aapted from: (Schebesta *et al*., 2006)

1.1.2. Blastema formation

The following stage of epimorphic regeneration involves the induction of a highly specialised structure - which seems to be unique to this subset of regeneration – known as the blastema; a collection of undifferentiated mesenchymal cells proximal to the wound epidermis.

The cellular origins of the blastema remain controversial within the field of regenerative biology. One theory is that it originates from stem cells, another via the contribution of dedifferentiated somatic cells. However, there is mounting evidence that blastema cells are a result of somatic cells converting to a more dedifferentiated state; highlighted, not only by the re-entry of cultured newt myotubes into the cell cycle (Tanaka *et al*., 1997), but also observations of muscle fibres changing from a mature, poly-nucleated phenotype to a relatively undifferentiated, mono-nucleated one during axolotl tail regeneration (Echeverri *et al*., 2001). Furthermore, Tu and Johnson (2011) used transposon-based lineage tracing to show that the tissues contributing towards the regrowth of zebrafish caudal fins are restricted to the fate of their tissue of origin.

A key feature of the blastema is its maintenance of a proliferative population of cells (Poleo *et al*., 2001). The retinoic acid (RA) synthesising enzyme, *aldh1a2* (*raldh2*), has been identified as a transcriptional marker for the blastema (Figure 1-4), and blocking the synthesis of RA leads to a reduction in the number of proliferating cells (Blum and Begemann, 2011). Further support for the activity of RA signalling during caudal fin regeneration is the expression of one of its receptors, RAR-γ (White *et al*., 1994). It is generally agreed that the blastema is an essential but complex structure that provides the necessary foundation for a regenerative response to be successful.

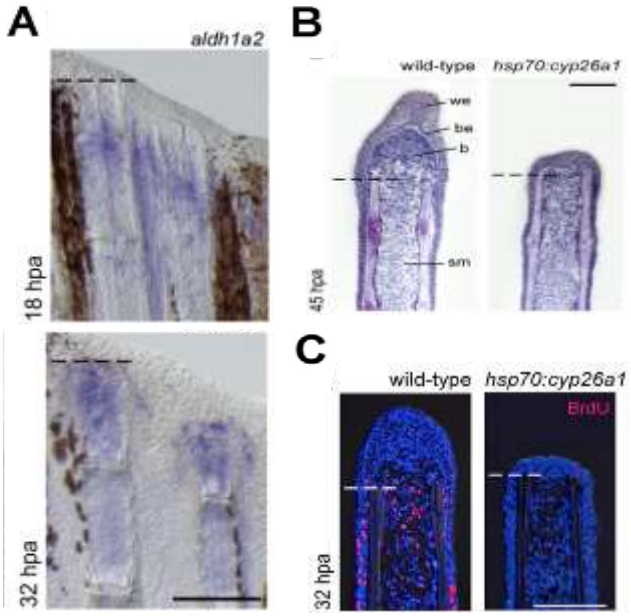

Figure 1-4. Retinoic Acid synthase, *aldh1a2*, is an important regulator of blastema function during regeneration.

(A) Detection of *aldh1a2* transcripts during adult zebrafish caudal fin regeneration.

(B) Inhibition of RA signalling through heat shock expression of an RA-degrading enzyme, *cyp26a1*, inhibits the regenerative process.

(C) Blocking RA signalling in *cyp26a1* zebrafish causes a dramatic loss of proliferating cells in the blastema and lateral epithelium.

Figure adapted from: (Blum, N. and Begemann., 2012)

1.1.3. Regenerative outgrowth

The final stage of epimorphic regeneration comprises a highly proliferative step known as regenerative outgrowth. It is in this crucial phase that the regenerating structure begins to take shape; from a regenerative stump to its original - functional - form. The switch from blastema formation to regenerative outgrowth is slight, but still crucial; the main change is the speed at which cells contributing towards regeneration divide. Nechiporuk and Keating (2002) provided evidence, using BrdU labelling, and immunostaining for phosphohistone-H3, for a dramatic reduction in the length of time blastema cells are in the G_2 phase of the cell cycle (Figure 1-5).

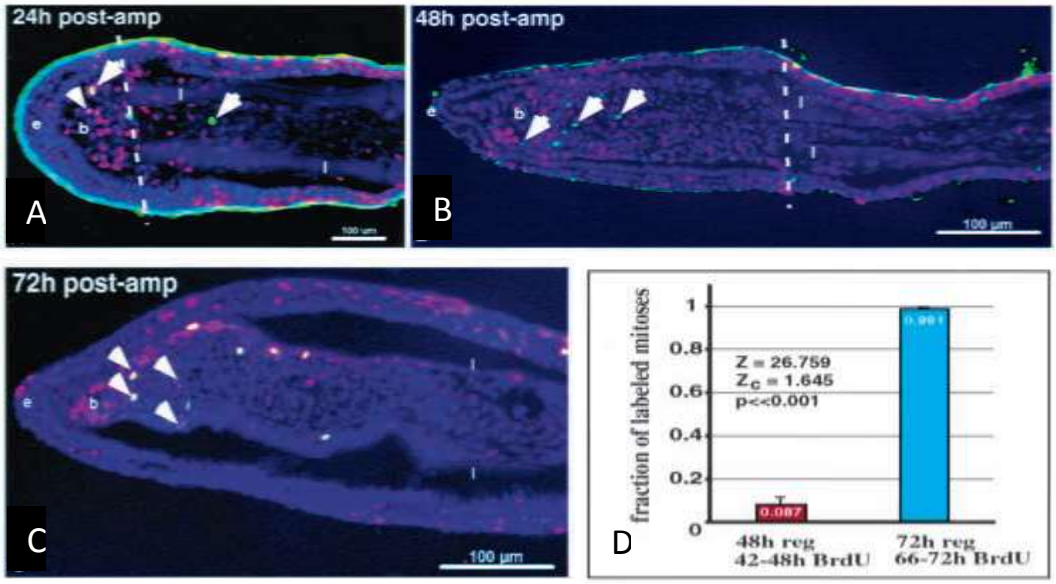

Figure 1-5. The length of the G_2 phase of mitosis shortens at the beginning of regenerative outgrowth in zebrafish adult caudal fins.
(A-C) Immunohistochemistry showing the overlap of BrdU (red) labelled cells and those undergoing mitosis (anti-phosphohistone-H3 (H3P): green label) after (A) 24, (B) 48, and (C) 72 hours postamputation. White cells highlight an overlap. (D) Quantification of BrdU+H3P+ cells of caudal fins amputated and treated with BrdU for 6 hours. Notice the increase in the ratio of BrdU-H3P overlap after 72 hours of regeneration (blue bar) even when BrdU labelling time is maintained.
Figure adapted from: (Nechiporuk and Keating., 2002).

Lastly, little is known about the morphogenesis of the caudal fin during regeneration; however, recent publications have reported on genes that, when mutated, can lead to abnormalities in fin length during development. A common theme between both mutants – *another long fin* (*alf*) and *shortfin* – is that both genes encode proteins involved in creating channels between cells: *alf,* the potassium channel, *kcnk5b* (Perathoner *et al*., 2014); *shortfin,* a connexin, *cx43* (Iovine *et al*., 2004). Therefore, the same principlr may apply during fin regeneration: exchange of molecules and/or ions between the cells contributing towards regeneration could be one mechanism involved in terminating the process at the appropriate time.

1.2. Epimorphic regeneration requires the activation of development pathways

A complex, but seemingly well-coordinated process such as the replacement of a whole limb or caudal fin, through epimorphic regeneration, undoubtedly requires guidance from a potent cocktail of molecular cues. The following three sections highlight literature that has provided evidence for the important roles played by several developmental – hedgehog, fibroblast growth factor, and wnt – pathways throughout all stages of regeneration.

1.2.1. The Fibroblast growth factor (FGF) pathway and its role during regeneration

The Fibroblast growth factor (FGF) family consists of over twenty ligands, and five receptors (FGFR1-5) that can produce isoforms through alternate splicing of their genes. Pathway activation involves the binding of a ligand dimer to the cell-surface receptor tyrosine kinase, causing dimerization and auto-phosphorylation of the intracellular domains, followed by the association of a kinase complex, leading to signal transduction. This phosphorylation cascade can transduce a signal via the MAP kinase proteins, leading to entry into the nucleus and induction of transcription, or can directly affect intracellular calcium stores through the phospholipase C (PLCγ) branch of the pathway (Figure 1-6) (Reviewed: Dailey *et al.,* 2005). The activation of this pathway is involved during early development of the mammalian lung and limbs (Bellusci *et al.,* 1997; Xu. X *et al.,* 1998). If the FGF pathway can alter the transcriptional activity of cells it directly acts upon, but also has early roles during the development of complex structures, one could assume that FGF signalling could be crucial during the regrowth of the zebrafish caudal fin.

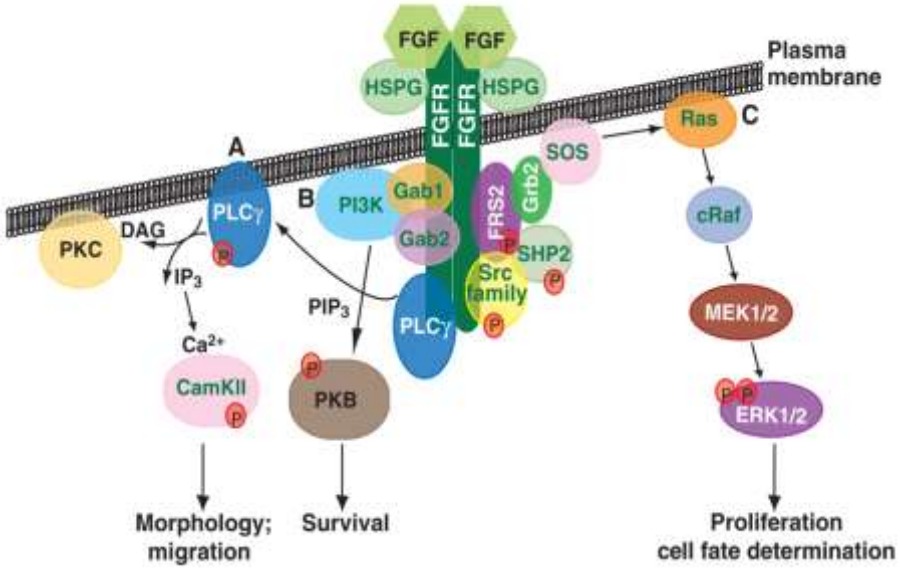

Figure 1-6. The FGF pathways control various aspects of cell behaviour.
Three canonical paths can be activated followed after auto-phosphorylation of the FGF receptor tyrosine kinase. (A) Phospholipase C induction leads to the release of intracellular calcium, followed by the activation of enzymes involved with cell migration. Another pathway is directed by the activation of phosphoinositide 3-kinase (PI3K) (B). Finally, after the recruitment of several phosphorylating enzymes, in a scaffold, to the receptor, leads to ras/ERK signal transduction (C).
Figure source: Dorey and Amaya (2010).

It has, indeed, been demonstrated that there is a direct role for the FGF pathway during adult zebrafish caudal fin regeneration (Poss *et al*., 2000a). The study used the broad-spectrum FGF inhibitor, SU5402, to show that blocking the pathway had dramatic effects on the progression of regenerative outgrowth, but also caused change at the molecular level, through downregulation of a blastema marker, *msxb* (Figure 1-7). A similar study, instead, opting for the electroporation of a morpholino targeting FGFR1, provided results supporting the findings of Poss *et al* (2000a) (Thummel *et al*., 2006). Whitehead *et al* (2005) identified, using the mutant zebrafish *devoid of blastema, dob,* an early regenerative ligand contributing to the initiation of regeneration: FGF20a. Not only did the regenerative response lack any sign of a blastema histologically, there was a significant reduction in the number of proliferating cells; a clear sign that progression to the latter

stages of the regeneration had been disrupted. Finally, Lee *et al* (2005) identified the expression of several downstream targets – *spry4*, *sef*, and *mkp3* – of the FGF pathway during a study highlighting the involvement of the FGF pathway during positional-dependent outgrowth of regenerating caudal fins: the more tissue amputated correlated with a faster regeneration time.

The ability of the FGF pathway to modulate the blastema marker, *msxb*, but also the identification of a ligand that has been linked with an early requirement during regeneration, suggests that the FGF signalling could play a crucial role across various regenerative contexts.

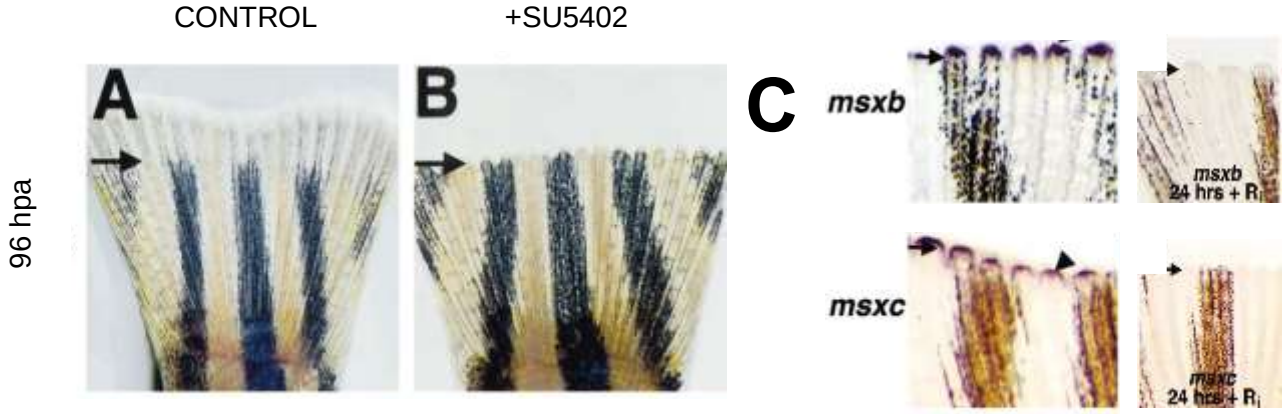

Figure 1-7. FGF signalling is crucial for the progress of regeneration beyond blastema formation.
The adult zebrafish caudal fin 96 hours after amputation in the absence (A) or presence (B) of 1.7 µM SU5402. (C) The blastema markers (*msxb* and *msxc*) are expressed at 24 hpa (left panel) are lost after 24 hours of continuous treatment with SU5402 (right panel).
Figure adapted from: (Poss *et al.*, 2000).

1.2.2. The Hedgehog pathway and its role during regeneration

The Hedgehog pathway is another early acting, essential part of whole-organism development. The Hedgehog ligands are amongst a special subset of molecular cues – morphogens. These act on cells in a concentration dependent manner. Therefore, a Hedgehog ligand can determine a range of cell phenotypes amongst an initially homogenous population depending on their distance from the morphogen's source. This is most evident during vertebrate neurogenesis within the neural tube (Roelink *et al.*, 1995).

The Hedgehog pathway has been extensively studied since its identification as an important segment polarity gene during a *drosophila* screen (Nüsslein-Volhard. C and Wieschaus. E., 1980). In the absence of the Hedgehog ligand the multi-pass transmembrane receptor, patched, inhibits pathway activation through the down regulation of smoothened at the cell surface. Once a ligand binds to patched, the inhibition imposed on smoothened is relieved, and the seven transmembrane protein is able to translocate to the cell membrane. Next, a protein complex comprised of: costal 2, a kinesin-like protein; fused, a serine/threonine kinase; protein kinase A (PKA); and cubitus interruptus (Ci), a transcription factor, binds to an intracellular region of smoothened. Fused then phosphorylates costal 2, causing the release of a full-length, active form of Ci from its complex which enters the nucleus to initiate transcription of its target genes (Figure 1-8) (Ingham *et al.*, 2011).

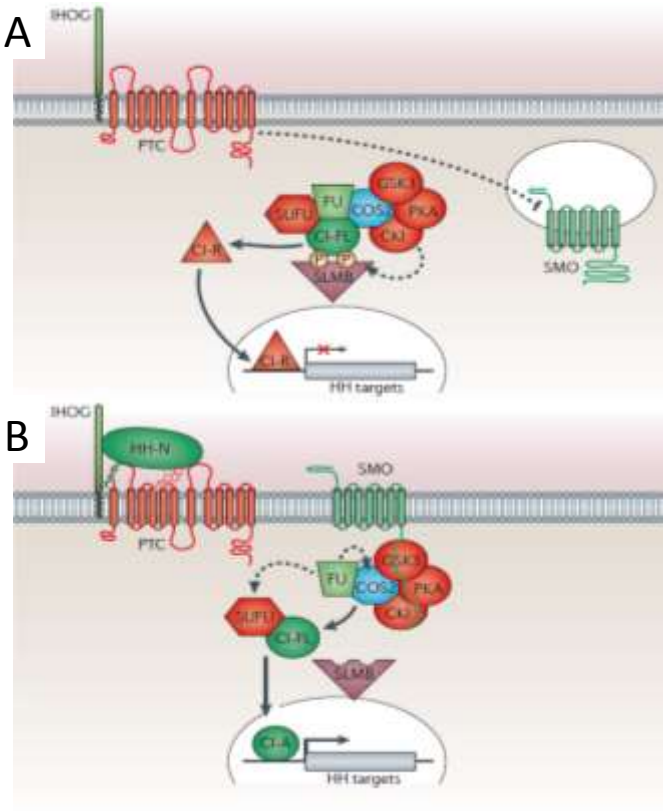

Figure 1-8. The Hedgehog (Hh) signalling pathway in *drosophila melanogaster* .
A schematic to show our knowledge of the Hedgehog pathway from lessons learned in the *drosophila*. Much of the mechanics in mammals are the same, with different nomenclature of protein components. (A) In the absence of Hh ligands, patched, the receptor, inhibits smoothened – the activator protein of the pathway. The transcription factor, cubitus interuptus (CI), is subsequently phosphorylated and sent for degradation by the costal2 (COS2), fused (FU), suppressor of fused (SUFU) destruction complex. The truncated form of CI acts as a repressor of transcription. (B) Secreted Hh ligands bind to patched and inhibits its actions upon smoothened. Smoothened migrates to the cell surface where it is phosphorylated, causing a conformational change and ability to interact with the destruction complex. CI is released in its full-length, active form, and enters the nucleus to induce the transcription of target genes.
Figure source: (Ingham *et al.*, 2011).

As a crucial developmental pathway, able to regulate the expression of various transcription factors depending upon the concentration that cells are exposed to, it is feasible that Hedgehog signalling has maintained its functionality during development, in animals able to regenerate. Schnapp *et al* (2005) identified the Hedgehog pathway to be important during axolotl tail regeneration. The group show that it is required for controlling proliferation within the blastema and during out-growth of regenerating tails, however, Hedgehog activation was only required for patterning of the limbs during regeneration. A similar experiment showed that after the induction of the Hedgehog pathway its activity was crucial for *xenopus* tail regeneration, and identified the expression of a transcript for a Hedgehog ligand, Sonic hedgehog (Shh), but also

for the patched receptor in the notochord and spinal cord, respectively (Taniguchi *et al.*, 2014). The expression of Shh has also been identified in the bony fin rays of the zebrafish caudal fin following amputation (Quint *et al.*, 2002). Furthermore, application of the Hedgehog inhibitor, cyclopamine, to the regenerating adult caudal fin, leads to a reduction in the number of proliferating cells within the mesenchyme (Figure 1-9).

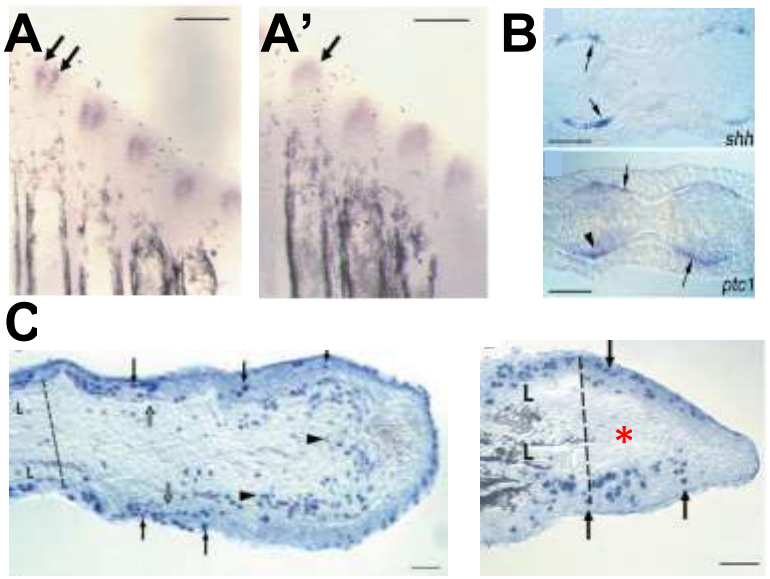

Figure 1-9. The Hedgehog pathway regulates fin ray patterning and mesenchyme proliferation during caudal fin regeneration.
Normal expression of the sonic hedgehog ligand (A) and patched (A') following 1-day of regeneration.
(B) Transverse section of a regenerating fin to show the distribution of *shh* and *ptc1*-expressing cells at 4-days post amputation (dpa)
(C) Treatment with control alkaloid, solanidine, shows no effect in the number of regenerating cells through BrdU labelling (left panel), however, in the mesenchyme of regenerates treated with cyclopamine the BrdU cells were lost (right panel, red asterisk).
Figure adapted from: (Quint *et al.*, 2002)

It is interesting to see the various roles played by the Hedgehog pathway during the regenerative process in different animal models. Studies show that Hedgehog acts in a context dependent manner: zebrafish caudal fins utilise sonic hedgehog for bone patterning, but axolotl tail regeneration fails if Hedgehog activity is chemically blocked. All the information presented, highlights the versatility of the Hedgehog pathway and thus the crucial role it could play across many, if not all, contexts of regeneration.

1.2.3. The Wnt pathway and its role during regeneration

The final developmental cues to be instigated during regeneration are the Wnts. The Wnt pathway is amongst the most diverse in terms of function. It can determine a cell's fate, induce proliferation and/or differentiation during embryogenesis. Wnt pathway transduction shares many characteristics seen after the induction of the Hedgehog pathway. In the absence of a Wnt ligand, β-catenin is phosphorylated and subsequently degraded via its association with a degradation complex - Axin, APC, and CKIα, a serine-threonine kinase. After the Wnt ligand binds to its receptor, Frizzled (Frz), the signalling complex - APC and Axin - associates with the intracellular domain of Frz, lifting the targeted degradation of β-catenin. Accumulation of intracellular β-catenin leads to its entry into the nucleus where it can disrupt binding between the transcription factor, TCF, and its inhibitor, groucho - lifting the transcriptional block (Figure 1-10) (Logan and Nusse, 2004).

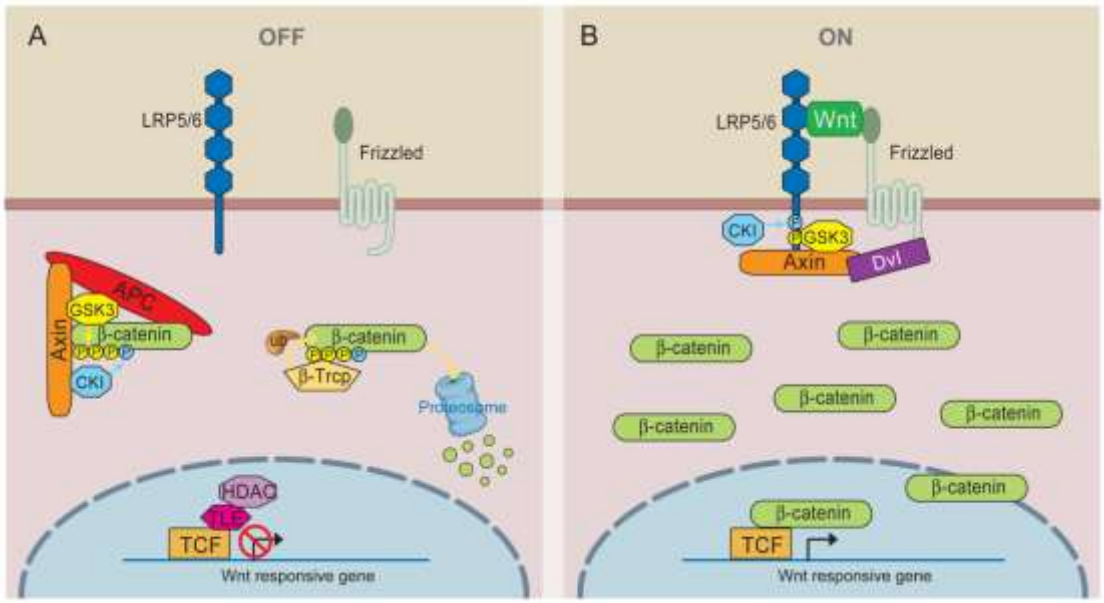

Figure 1-10. The Wnt signalling pathway.
(A) In the absence of Wnt ligand the cytoplasmic β-catenin is phosphorylated after forming a complex with Axin, APC, GSK3 and CK1, targeting it for degradation. Wnt target genes are inhibited by default through the binding of groucho/TLE to the TCF transcription factor in the nucleus. (B) Upon binding of a Wnt ligand to its receptors, LRP and frizzled, the complex containing APC and Axin is recruited to the intracellular cell-surface by dishevelled, preventing the phosphorylation and subsequent degradation of β-catenin, which causes its accumulation in the cytoplasm, followed by its entry into the nucleus, releasing the inhibition of groucho/TLE. β-catenin acts as a coactivator with the already present TCF transcription factor to transcribe Wnt-target genes.
Figure source: (MacDonald *et al.*, 2009)

Wnt signalling has been shown to have an important role during urodele limb and zebrafish caudal fin regeneration. In the *Xenopus laevis* limb bud, Yokoyama *et al* (2007) were able to block the regenerative process after inducing the expression of a Wnt inhibitor - dikkopf-1 - prior to its amputation. They also saw, even after induction of Dkk-1 expression, that the development of un-amputated limb buds was not impeded. In the adult zebrafish caudal fin, Poss *et al* (2000b) identified the transcripts of the Wnt target gene, *lef1*, in cells of the epidermal layers, but also later on in presumptive bone-forming cells, scleroblasts. Furthermore, the same group saw an upregulation in *wnt5* and *wnt3a* transcripts at 24- and 96-hours postamputation, respectively. Stoick-Cooper *et al* (2007) identified the expression of another Wnt target gene, *axin2*, during

caudal fin regeneration. They went on, using two heat shock-inducible transgenic lines, hs-Dkk1 and hs-ΔTCF, to downregulate Wnt activity. Inhibition of the Wnt pathway after blastema formation saw zebrafish regenerate substantially more of their tails than those inhibited during or prior to blastema formation. Blocking the Wnt pathway also reduced the number of proliferating cells during regenerative outgrowth (Figure 1-11). Finally, Stoick-Cooper *et al* (2007) provided evidence for the opposing roles of different Wnt pathways during regeneration. Using the heat-shock inducible Wnt5a zebrafish transgenic line, the group found that over-activation of the non-canonical Wnt pathway perturbed caudal fin regeneration.

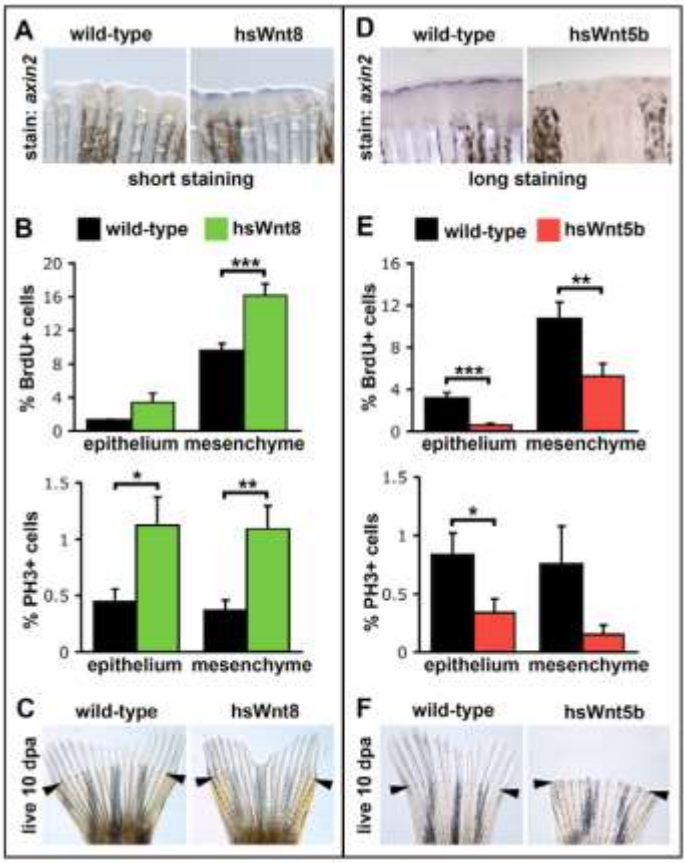

Figure 1-11. Opposing roles of the canonical and non-canonical Wnt pathways during caudal fin regeneration.

Detection of the canonical Wnt read-out, *axin2*, 6 hours after heat shock-induction of (A) Wnt8 or (D) Wnt5b in 3 dpa caudal fins. The difference in proliferation, detected through BrdU labelling or phosphohistone-H3 immunohistochemistry, after overexpression of (B) Wnt8 or (E) Wnt5b during caudal fin regeneration. Observation of the gross morphology of caudal fins continuously overexpressing (C) Wnt8 or (F) Wnt5b for 10 days post amputation.

Figure source: (Stoick-Cooper *et al*., 2007)

There is substantial evidence for the role of several Wnt ligands during caudal fin regeneration, but also a varied response depending upon canonical or non-canonical pathway activation. This highlights the array of prompts a large group of Wnt proteins could provide during the regenerative process in zebrafish larval tails.

1.3. Heparan sulphate is an important modulator of signal pathways

For a ligand to have a meaningful interaction with the appropriate receptor it is sometimes necessary for an extracellular macromolecule to intervene. A glycosaminoglycan, such as heparan sulphate, is an ideal candidate for such a role, and has already been cited to interact with an array of extracellular proteins. To this end, this section will highlight the ability of heparan sulphate (HS) to interact with ligands of the pathways shown to have an important role during regeneration.

1.3.1. Stages of heparan sulphate (HS) synthesis

HS is a glycosaminoglycan (GAG) comprised of between 50 and 200 disaccharide - glucosamine and hexuronic acid – repeats (Figure 1-12). It is an unbranched polysaccharide, modified through various enzymatic reactions to create a biologically active macromolecule. HS chains are found *in vivo* as heparan sulphate proteoglycans (HSPGs); whereby one or several HS chains are synthesised onto a core – glypican, syndecan, perlecan, or aggrecan – protein, which dictates whether they are destined to be cell-surface bound or released into the extracellular matrix (Reviewed here: Sarrazin *et al.*, 2013). As the synthesis of GAGs do not follow a template, like that of DNA replication, little is known about how a cell decides upon the type of chain - and with which modifications - to produce. However, three clearly defined stages have been identified during HS chain synthesis: initiation, polymerisation, and modification (Figure 1-12).

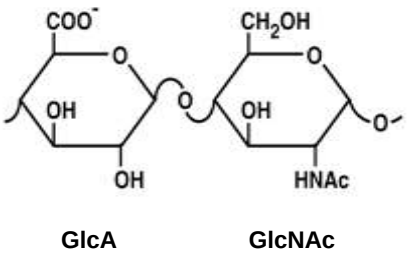

Figure 1-12. The core disaccharide repeats of the HS chain.

The two main saccharides, N-acetylated glucosamine (GlcNAc) and glucuronic acid (GlcA), form the initial HS chains prior to their modification.

Figure source: (Esko and Lindahl, 2001).

1.3.1.1. Chain initiation

HS biosynthesis is initiated by the attachment of a xylose residue, followed by the formation of a tetrasaccharide linker by the addition of two galactose and a final glucuronic acid (Xylose-Galactose-Galactose-Glucuronic acid) (Figure 1-13A). The next step is crucial for determining the synthesis of HS over other GAGs, such as chondroitin or dermatan sulphate. An enzyme from the exostosin family, Exostosin-like 3, attaches the first N-acetylglucosamine to the linker region, allowing for the progression of the chains to the polymerisation step.

1.3.1.2. Chain polymerisation

The next stage of HS synthesis – chain polymerisation (Figure 1-13B) - involves a family of glycosyltransferase enzymes, known as exostosins (EXT) because, when mutated, these genes are known to cause a condition sometimes referred to as hereditary multiple exostoses (HME); characterised by cartilage capped bony protrusions of long bone growth plates (Solomon., 1963). The two enzymes responsible for the addition of disaccharide repeats to the HS chain are exostosin 1 and 2 (EXT1/2), which are able to catalyse the addition of either saccharide: N-acetyl glucosamine (GlcNac) and glucuronic acid (GlcA) (Kim *et al.*, 2003). Furthermore, Busse *et al.*

(2007) provided evidence for the EXT1 and 2 enzymes forming a complex in the Golgi apparatus, but also that a bias may exist when it comes to their transferase abilities: EXT1 shows a higher GlcNac/GlcA transferase activity over EXT2 when expressed separately, but together show an even higher activity. Finally, Stickens *et al*. (2005) observed that mice expressing a truncated *Ext2* gene showed a significant reduction in HS synthesis, but also develop osteochondromas similar to those seen in HME patients. This suggests that the main function of EXT2 is to modify the catalytic properties of EXT1 during HS chain polymerisation.

1.3.1.3. Chain modification

It is generally accepted that as the HS chain undergoes polymerisation there is some overlap with the beginning of the chain modification step: almost immediately after the first sugars are added the modifying enzymes begin altering the disaccharide units (Figure 1-13C). The modification sequence seems to be well-organised – one modification must be done before the following can begin. There are up to six ways in which the chain can be modified, in the following order: removal of the N-acetyl group from subsets of GlcNAc residues, sulphation of deacetylated glucosamine, epimerisation of GlcA to iduronic acid (IdoA) within the GlcNS domains, 2-O-sulphation of IdoA, addition of 6-O-sulphate groups, and a rare 3-O-sulphation of glucosamine (Reviewed here: Esko and Selleck, 2002).

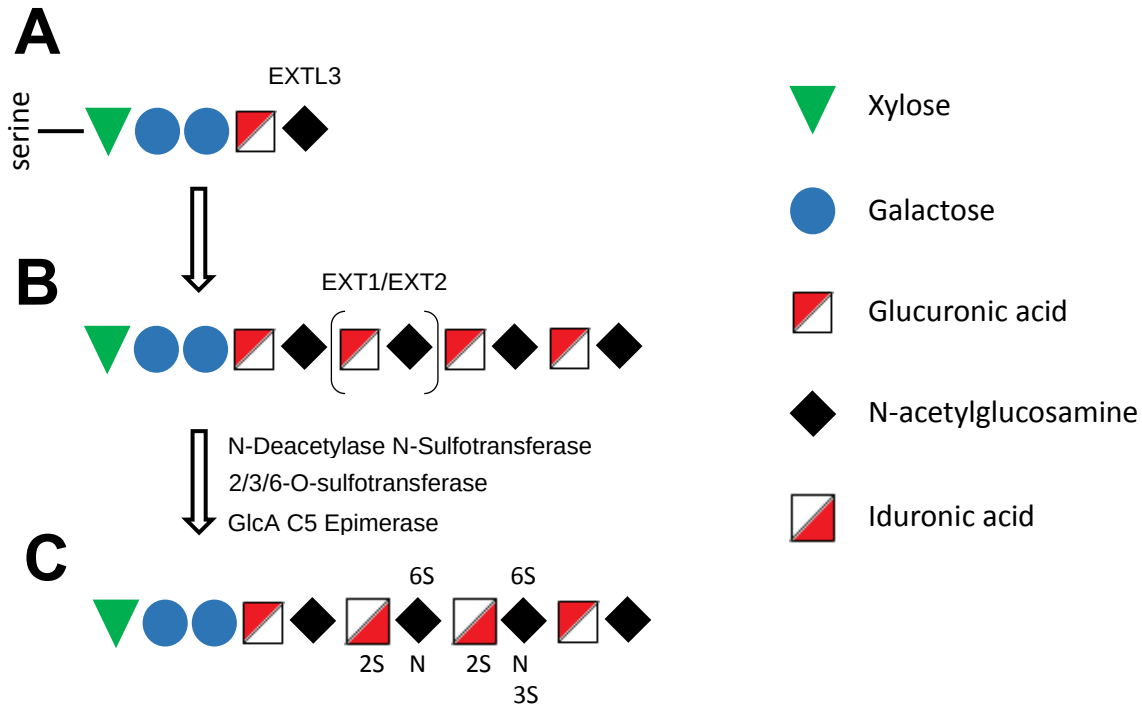

Figure 1-13. The three stages of HS chain synthesis.

(A) Synthesis of the GAG chain begins with the addition of a tetrasaccharide linker to a serine residue of the core protein. Determination of HS synthesis occurs upon addition of an N-acetylglucosamine. (B) Addition of the saccharide units are catalysed by the glycosyltransferases, EXT1/EXT2, during polymerisation. (C) Modification of the core sugars begins with substitution of acetyl groups with sulphates, followed by epimerisation of glucuronic acid to iduronic acid, and further sulphation of saccharide units within the region of modifications.

After the final modification the HS chains are highly heterogeneous: some areas are concentrated with sulphated residues, whereas the regions between contain negligible to non-existent levels. These differences in sulphation give the chains their polyanionic charge, but also enough flexibility to interact with a plethora of proteins involved in cell-cell signalling.

1.3.2. The *dackel/ext2* mutant

The *dackel* mutant was identified during a screen to uncover genes that affected fin development (Van Eeden *et al*., 1996). Normal zebrafish initially develop a pair of pectoral fins and a caudal fin fold and, later in development, a pelvic, dorsal and anal fin form. Amongst the

118 mutants that caused defects in larval fin development, there were several with very specific changes, such as the complete absence of pectoral fins in 3.5-day-old *dackel* larvae (Figure 1-14A). It wasn't until eight years after this initial screen that the *dackel* gene was identified as a homolog for one of the crucial glycosyltransferases during HS chain polymerisation, EXT2 (Lee *et al.*, 2004). The same group also saw that the ventrotemporal and dorsonasal axons were disorganised within the developing optic tract of *dackel* zebrafish compared to wild-type.

During normal development of the long bones in mammals, chondrocytes within the growth plate organise into columns that resemble a stack of pennies; however, in patients with HME the chondrocytes are highly disorganised. This chondrocyte phenotype has been witnessed in the *dackel* zebrafish mutant: the pre-cartilage condensate presented irregular chondrocyte stacking within the ceratobranchial arch (Figure 1-14B) (Clément *et al*., 2008). Clément *et al*. (2008) also saw a reduction in the amount of HS produced using immunohistochemistry. In a study to understand the absence of the pectoral fin, Grandel *et al*. (2000) came to the conclusion that fish lacking the *ext2* gene failed to maintain the signalling of the apical ectodermal ridge (AER) beyond the first 10 hours of pectoral fin development, leading to a truncation in its proximodistal axis. They went on to state that *ext2* was not part of the *syu-fgf4* feedback loop, because they could detect the *syu* target, *ptc1*, but also, application of an FGF4-soaked bead induced *syu/shha* expression. It was suggested that there was an *syu/shha*-independent route for the maintenance of important *hox* genes during pectoral fin development which were determined through an *ext2*-dependent pathway.

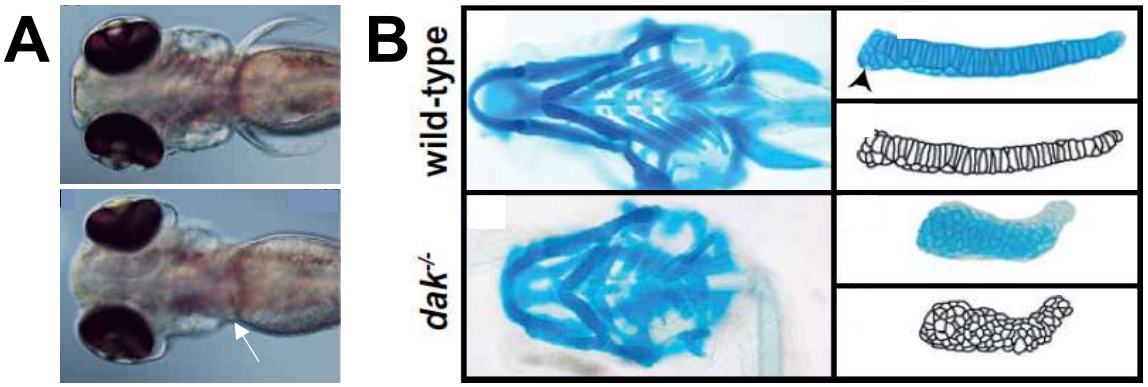

Figure 1-14. The *dackel/ext2* zebrafish phenotype and its similarity to chondrocyte defects seen in patients with HME.
(A) Dorsal aspect of a wild-type zebrafish (top) and *dackel* mutant (bottom). White arrow highlights where the pectoral fin should be.
(B) The *dackel* mutant has dysmorphic cartilage condensates similar to the chondrocytes seen in the growth plate of patients with HME
In all images anterior is to the left and posterior to the right.
Figure adapted from: (A) (Grandel *et al*., 2000) (B) (Clément *et al*., 2008).

As we have the benefit of applying what we know now to previous studies, it is clear that Ext2-dependent synthesis of HS is crucial for the modulation of developmental pathways. This is evident through the various developmental defects, but also diseases such as HME, borne from the lack of a functional EXT2 protein. The use of zebrafish as a model for disease was highlighted during experiments carried out by Clément *et al*. (2008), whereby the *dackel/ext2* mutant phenotype is not too dissimilar to the way HME manifests in human growth plates.

1.3.3. HS modulates developmental pathways

Previous experiments have used HS-defective mutants to understand the progression of human diseases, such as HME, but also to identify the signalling events disrupted during pectoral fin development. It is evident from these findings that the presence of HS chains are crucial for normal animal development and homeostasis. The next topic in this chapter highlights several

molecular pathways - previously identified to be important during epimorphic regeneration – with which HS has been shown to interact.

1.3.3.1. HS chains can interact with the FGF pathway

Ever since the purification of the acidic and basic FGF ligands, FGF1 and 2, respectively, from bovine neural tissue using affinity chromatography and the highly sulphated HS analogue, heparin (Lobb and Fett, 1984), the interactions between GAGs and growth factors have been the focus of many studies. The crystal structure of the interaction between FGF2 and FGFR1, in the presence of a heparin oligosaccharide, has been published (Schlessinger *et al*., 2000). The study showed a dimeric 2:2:2 heparin:FGF2:FGFR1 ternary complex, with heparin binding 1:1:1 to both the ligand and receptor through hydrogen bonds, but also the heparin can interact with the receptors of both ternary heparin-FGF2-FGFR1 complexes, suggesting that this HS analogue is involved in stabilizing the FGFR dimer for a stronger transduction of the pathway. Rapraeger *et al*. (1991) were able to provide evidence for the requirement of cell surface HS for FGF2-dependent proliferation, and inhibition of differentiation, in MM14 myoblasts. Culturing cells in chlorate to block the sulphation of HS chains reduced FGF2 binding, causing myoblasts to stop proliferating, leading to increased differentiation. The ability of HS chains to enhance the signal potential of FGFs has been heavily linked to the levels of their 6-O-sulphation (Pye *et al.*, 1998).

Studies using animal models harbouring mutations within genes encoding enzymes involved during HS synthesis can shed light on the ability of HS chains to interact with different pathways. Using flies mutated in either the *sugarless* or *sulfateless* genes – encoding the UDP-glucosamine dehydrogenase and N-deacetylase/N-sulfotransferase, respectively – presented a tracheal migratory phenotype, similar to the FGFR homolog mutants, *heartless* and *breathless*, during development (Figure 1-15A) (Lin *et al*., 1999). Investigating further, the group detected a

reduction in the activity of the FGF pathway using an antibody specific to the di-phosphorylated, active form of MAPK (Figure 1-15B). The *Ndst1* gene encodes the enzyme, N-deacetylase/N-sulfotransferase, required for initiating the modification process by replacing the acetyl group of GlcNAc for a sulphate. Pan *et al*. (2006), using *Ndst1* knockout mice, displayed the importance of these HS modifications for FGF signalling during lens development. They saw less developed lenses in the majority of mutants, but also a lack of FGF2 binding when added exogenously to frozen slices of *Ndst1*-knockouts. Finally, they saw a reduction in the phosphorylation state of a crucial pathway transducer, ERK-1, and also the loss of an FGF target gene, *erm*, in lens epithelium.

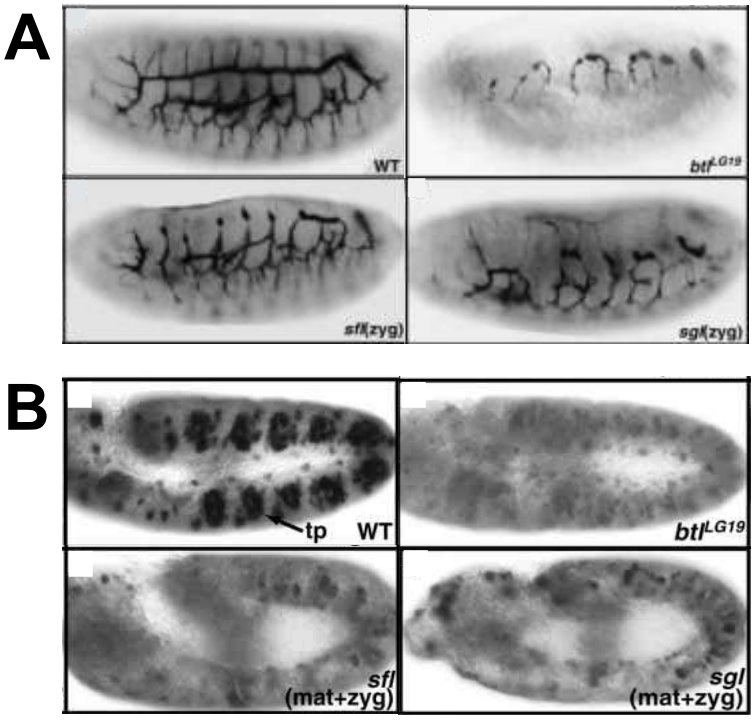

Figure 1-15. HS interacts with the FGF pathway during *drosophila* development. (A) The enzymes involved during HS chain synthesis, *sfl* and *sgl,* are required for tracheal cell migration. Embryos shown are of intermediate severity.
(B) Loss of maternal and zygotic *sfl* and *sgl* leads to a significant reduction in the detection of the active diphospho-MAPK in stage 11 *drosophila*.
Figure adapted from: (Lin *et al*., 1999).

The use of biochemical techniques and genetic analysis have provided overwhelming evidence for the interaction of HS chains with the FGF pathway during development. This could occur by GAG-ligand or GAG-ligand-receptor complex formation,

allowing for the stable activation of the pathway. The smallest alteration to the HS chain could enhance or diminish the signal activity, as seen by the positive correlation between the level of 6-O-sulphation in exogenous HS and the proliferative response of cells exposed to FGF2. It is clear from the evidence above that the FGF pathway can be influenced by the presence of HS chains across various developmental contexts.

1.3.3.2. HS chains can interact with the Wnt pathway

The majority of studies identifying interactions between HS and the Wnt pathway also utilise mutants involved with its synthesis; to see what effect reducing the presence of HS has on Wnt ligand distribution and pathway activity during development. In fruit flies the homolog of vertebrate Wnt-1 is encoded by *wingless* (*wg*), and has a role as a morphogen during segment polarity and subsequent naked cuticle formation, but is also an important signalling molecule within the wing imaginal disc. *Wg* can act at long- and short-ranges to regulate the expression of various genes. Disrupting the levels of HS using the mutant *drosophila* strains *tout velu, sister of tout velu*, or *brother of tout velu*, which are *drosophila* homologs for mammalian *Ext1*, *Ext2*, and *Extl3*, respectively, has profound effects on the *wg* pathway (Han *et al.,* 2004; Bornemann *et al.,* 2004). Han *et al*. (2004) showed that *ttv, sotv* and *botv* mutants disrupted the expression of the long range Wg target, *distal-less*, but to varying degrees: *botv* affected levels in all mutant cells; *ttv* and *sotv* mutants only saw drops further from the origin of the *wg* ligand at the dorsoventral border of the imaginal disc. Bornemann *et al*. (2004) saw that cells within the wing imaginal disc harbouring mutations in *ttv* or *sotv*, or both, not only resulted in the disruption of extracellular movement of the wingless ligands but also caused the loss of its downstream target, *achaete*, during development (Figure 1-16).

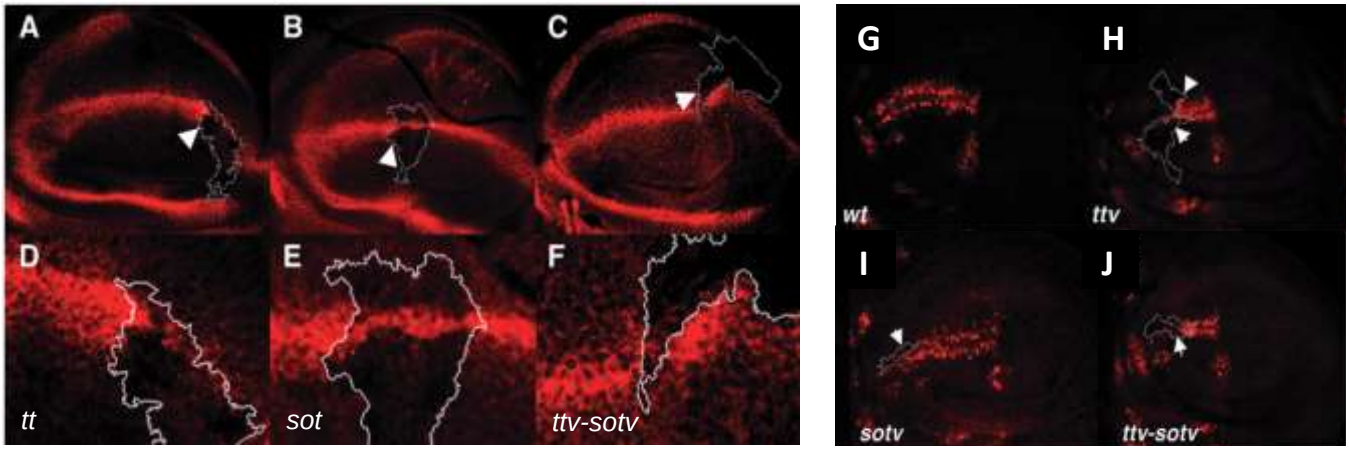

Figure 1-16. The Wnt-1 homolog, Wg, gradient is disrupted and signal activity reduced in the wing imaginal disc of glycosyltransferase mutants.
(A-F) Extracellular Wg detection in the wing imaginal disc with (A, D) *ttv*, (B, E) *sotv*, or (C, F) *ttv-sotv* mutant clones.
(G-J) Identification of wingless signal activity through detection of *achaete* in (G) wild-type wing imaginal discs with (H) *ttv*, (I) *sotv*, or (J) *ttv-sotv* mutant clones.
All images are oriented with the anterior to the left and posterior to the right. White boundaries highlight areas containing mutant clones
Figure adapted from: (Bornemann *et al.*, 2004).

As GAG chains, such as HS, are normally bound covalently to a core protein during their synthesis, it is interesting to see if Wnt signalling is disrupted in the absence of proteoglycans and not just their individual side-chains. It has been shown that cells cultured in serum-free medium will dose-dependently respond to HSPGs in the presence of a constant level of Wnt3a (Fuerer *et al.*, 2010), and this response cannot be recapitulated upon addition of HS chains alone. Two glypicans have been identified in the fruit fly, dally and dally-like (Nakato *et al.*, 1995). Wing imaginal discs carrying mutant clones in *dally*, *dally- like*, or both genes has provided evidence for the requirement of HSPGs to maintain the *wingless* gradient in *drosophila* (Han *et al.*, 2005). The same group provided early evidence for the ability of *notum*, a secreted protein with a role in Wg inhibition, to modulate both dally and/or dally-like core proteins and thus wingless activity. Further support for the ability of core proteins to modulate signalling alone has been provided using glypican-3 knockout mice. Song *et al.* (2005) saw an increase in Wnt canonical pathway activity

but also a decrease in the Wnt/JNK, non-canonical, pathway in mice lacking GPC3. This effect was deemed to be due to the loss of a core protein and not the subsequent elimination of its associated HS chains, as cells expressing GPC3 without HS chains were able to elicit a response upon addition of Wnt5a.

The evidence presented here points, not only, towards HS chains, but also their core proteins, as modulators of Wnt ligands, and subsequent pathway activity. Not only can HS assist in the activation or inhibition of the Wnt canonical pathway in different contexts, HSPGs can alter the non-canonical branch *in vivo* – shown by the GPC3 knockout mice. This means HSPGs are crucial modulators of the Wnt pathway and could therefore be utilised in a regenerative capacity.

1.3.3.3. HS chains can interact with the Hh pathway

Interactions between HS and the Hedgehog ligand, sonic hedgehog, have been well documented at a biochemical level (see Chapter 6 – 6.1. Introduction), and there is also overwhelming *in vivo* evidence, using molecular genetics, for the interaction and modulation of the Hedgehog pathway by HSPGs and their HS sidechains. This section will provide evidence using the latter to highlight the important role played by HS during Hedgehog signalling in a developmental context.

Developing fruit fly embryos form bands of denticles with naked regions between, however, RNAi silencing of the glypican genes, *dally* or *dally-like*, causes a segment polarity phenotype akin to the lawn of denticles formed after the loss of the Hedgehog ligand (Desbordes and Sanson. (2003). This phenotype is incredibly similar to the *wg* mutant due to the normal induction of Hedgehog via Wg, across the parasegment groove. Therefore, using the Gal4-UAS expression system, Desbordes and Sanson, 2003) were able to uncouple the Wg and Hh pathways through heterologous expression. Preventing the translation of *dally* or *dally-like*, using targeted

dsRNA, did not alter ectopic expression of the Wg target, *en,* in Gal4-UAS embryos, but silencing the glypican genes inhibited the expression of the Hedgehog target, *wg.* This study highlighted the ability of various HSPGs to show specificity in regulating signal pathways during development.

The wing imaginal disc requires the expression of the Hedgehog ligand in the posterior compartment during its development. Hedgehog then signals to the anterior side – visualised through the stabilisation of cubitus interruptus (Ci) - leading to transcription of target genes. Han *et al*. (2004), using wing imaginal discs carrying mutant clones for enzymes involved during HS synthesis, *sotv* and *botv*, saw a reduction in the range of Hedgehog signalling. The same mutant clones also presented a reduction in the movement of the Hedgehog ligand from its source - at the wing imaginal disc DV boundary. Consistent with changes to the activity of the Hedgehog pathway after disrupting HS synthesis, Bornemann *et al*. (2004) presented similar results using *ttv* mutant wing imaginal discs. However, pathway disruption was most pronounced in *ttv-sotv* clones (Figure 1-17). Using the EXT1 gene trap mutant in mice, Koziel *et al*. (2004) concluded that HS was instrumental in controlling the range of an important mammalian Hedgehog ligand, IHH, during endochondral ossification of long bones, causing delayed hypertrophy, which leads to irregular bone formation.

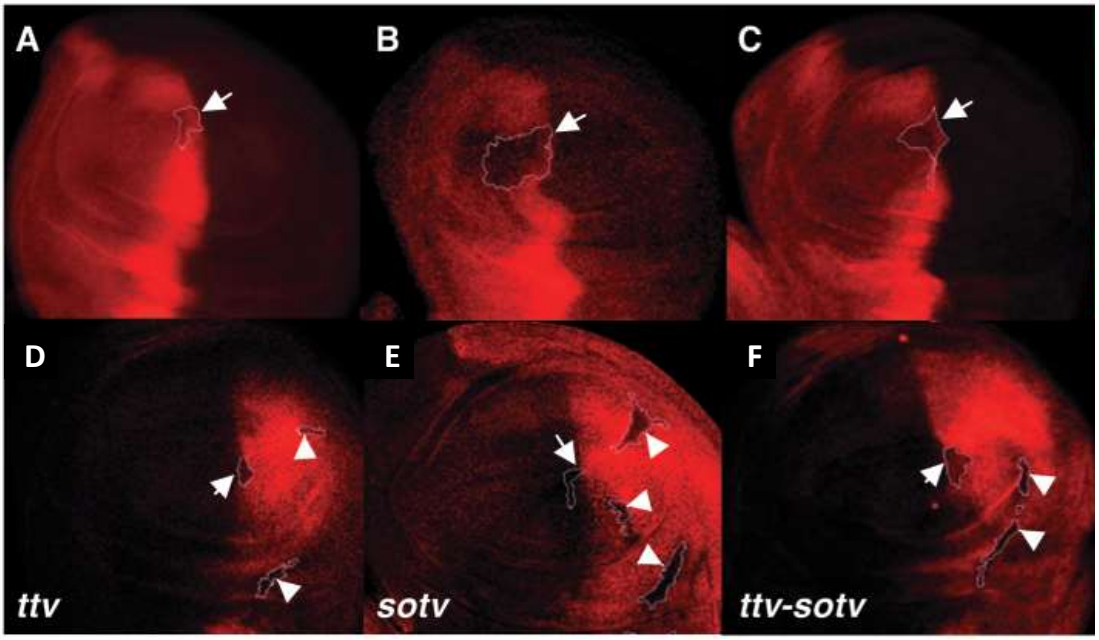

Figure 1-17. The distribution of the Hedgehog ligand is disrupted, and signal activity reduced in the wing imaginal disc of glycosyltransferase mutants.
(A-C) Hedgehog signal activity through the detection of stable Ci in the anterior wing imaginal discs of (A) *ttv*, (B) *sotv*, and (C) *ttv-sotv* mutants.
(D-F) Extracellular Hh ligand distribution in the posterior wing imaginal discs of (D) *ttv*, (E) *sotv*, and (F) *ttv-sotv* mutants.
White borders highlight mutant clones of the respective mutants, at the anteroposterior boundary (arrows), and those posterior to the AP boundary (arrowheads).
Figure adapted from: (Bornemann *et al*., 2004)

It is clear, from published literature, that HSPGs and their side chains have the ability to not only control the distribution of Hedgehog ligands, but also modulate their activity during development; from fruit flies to mammalian models, therefore implicating that HSPGs could also show themselves to be, at the very least, crucial during zebrafish development. However, a group have identified normal Hedgehog pathway activity during *ext2* null embryo development (Fischer *et al.*, 2011). This could mean *ext2* was redundant in that context, therefore further testing is required. Also, analysing signalling events after amputation of *dackel/ext2* tails could provide evidence for HSPG-dependent activation of the Hedgehog pathway in a different context.

1.3.4. Heparan sulphate is involved during tissue repair

The extracellular matrix (ECM) is a diverse and dynamic environment composed broadly of proteins, proteoglycans, and glycoproteins, supporting cells under a variety of circumstances – most notably during development or when disrupted after injury (Hynes., 2009). The proteins of the ECM are all subject to degradation, which could present various cues to receptive cells. A major group of enzymes involved in the degradation of extracellular components is the matrixmetalloprotease (MMP) family (Page-McCaw *et al.,* 2007). These enzymes have been linked with many diseases, such as rheumatoid arthritis and cancer, which suggests an important role in maintaining the homeostatic environment – most likely through their regulation of communication between cells. The HSPG core protein syndecan-1 has the ability to be cleaved by MMP-1, leading to an increase in cell migration (Endo *et al.,* 2003). A second group of enzymes involved in cleaving proteins of the extracellular matrix belongs to the 'a disintegrin and metalloproteinase' (ADAM) family. There is experimental evidence that one ADAM, ADAM17, can be regulated by HS chains during the shedding of Shh ligands from the cell surface (Dierker *et al.,* 2009).

The increase in expression of *Ext2* mRNA was detected, using RT-PCR, within 5-hours post-injury in mouse hypoglossal motor neurons (Figure 1-18A) (Murakami *et al.,* 2006). This translated to an increase in HS detection, through immunohistochemistry, after neurons recovered for 7 days after their resection. After various peripheral nerve injuries, including sciatic nerve transection, the mRNA and protein levels of glypican-1 were upregulated in the dorsal root ganglion neurons (Bloechlinger *et al.,* 2004). Beyond the nervous system, after inducing skeletal muscle injury through the application of barium chloride, there was small change in HS levels but

a dramatic change in their distribution (Casar *et al.*, 2003). Furthermore, syndecan-3 was identified as the core protein most significantly up regulated during muscle repair (Figure 1-18B).

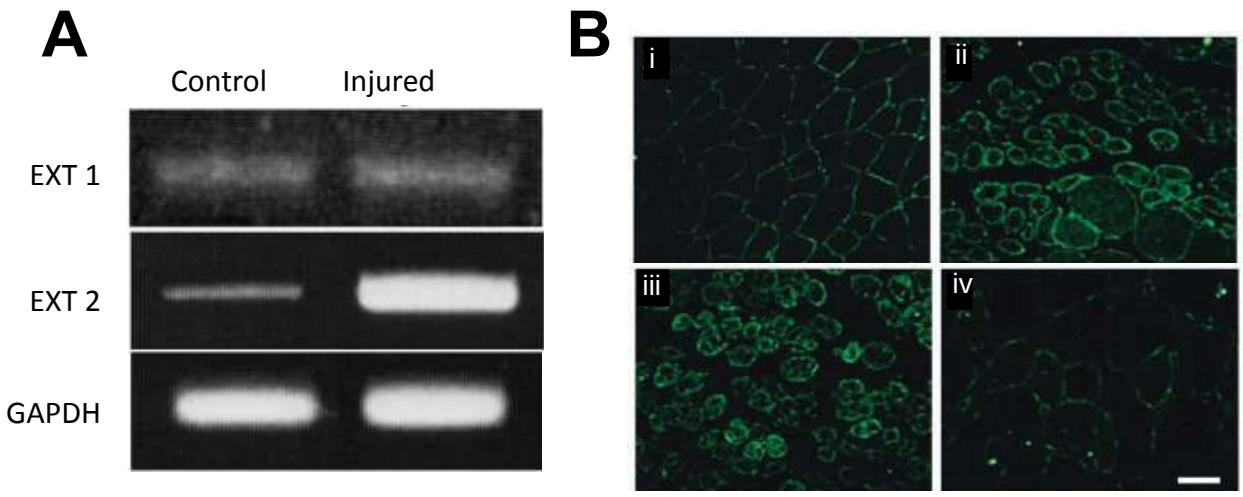

Figure 1-18. There is an up increase in HS synthesis and HSPG presence after various tissue injury.
(A) EXT1 and EXT2 mRNA detection by RT-PCR in uninjured hypoglossal nuclei and 7 days after resection.
(B) Immunofluorescence detection of syndecan-3 after skeletal muscle injury in mice. (Bi) Control, (Bii) 4, (Biii) 5, and (Biv) 15 days after barium chloride injection.
Figure adapted from: (A) (Murakami *et al.*, 2006). (B) (Casar *et al.*, 2003).

From the modulation of HSPG shedding by MMPs, to the increased activity of ADAM-dependent cleavage of the potent morphogen, Shh, it is evident that HSPGs are powerful modulators of the extracellular environment. They also exhibit changes in expression in response to tissue injury. As an extracellular macromolecule HSPGs are evidently very important regulators of signals instrumental in coordinating a multitude of responses, from differentiation, proliferation, and cell migration. Therefore, HSPGs are strong candidates for modulating cellular responses during epimorphic regeneration.

1.4. Aims and Objectives

The ability of lower vertebrates to regenerate has been exploited over recent decades, however, some have been studied more intensively than others, mainly the urodele amphibians - newts and salamanders - and the anuran amphibians, for example *Xenopus laevis*. Many of the studies to identify the pathways that are active, and whether they can interact with one another, during regeneration make use of the adult zebrafish. However, this is time consuming and restricts experiment sample size. Regeneration studies within larval zebrafish have focused on the caudal fin fold. This means the majority of the tissue lost is epithelial and therefore less representative of the loss of a limb - where several tissue types are damaged. Therefore, I will amputate larval tails within the pigment gap, which will cause traumatic loss of developing ectoderm as well as mesenchymal tissues such as skeletal muscle, and developing neurons.

The larval zebrafish, as a highly genetically tractable model organism, represents an exciting model for use during high-throughput screens. Their ability to form stable transgenic lines allows them to be used as simple models for complex mammalian diseases. Also, an ability to develop rapidly and transparently, outside the mother, in small volumes of water, makes visualising their development very easy. Finally, application of chemicals to water maintaining fish can provide us with a lot of information, especially when combined with techniques such as *in situ* hybridisation and immunohistochemistry. Using chemicals, I will attempt to identify any interactions between the pathways active during larval tail regeneration.

Recently, *dackel/ext2* zebrafish were identified to be unable to regenerate their tails after amputation within the pigment gap before 5-days old. As the mutation is in one of the glycosyltransferases important for HS chain synthesis, it would be interesting to see which pathways are disrupted during its regeneration. As this project was setup in collaboration with a

lab in Singapore to study the ability of HS chains to assist in the regeneration of damaged tissue; it allowed me to utilise their expertise and equipment to work towards isolating a HS chain that could target the earliest signal pathway identified during zebrafish tail regeneration.

To this end, these are the specific aims of this study:

1. Identify signal pathways activate during caudal fin regeneration, and whether they can interact with one another.
    1a. More specifically the Hedgehog, Fibroblast Growth Factor and Wnt pathways.
    1.b Attempt to identify the earliest pathway induced.
2. To determine the consequences of disrupted HS chain synthesis on these pathways during regeneration.
    2.a Use the *dackel* mutant to identify any previously unidentified mutant zebrafish that may also lack the ability to fully regenerate their tails.
3. Isolate a HS chain that can target the earliest pathway active during larval tail regeneration.
4. Attempt to reverse the regenerative phenotype of *dackel* mutants through the application of a newly isolated HS fraction.

2 Materials and Methods

2.1. Zebrafish maintenance and amputation.

Zebrafish were raised under standard conditions at 28.5^{o}C. Embryos were incubated in fish water (1X E3 with methylene blue) and staged according to specific morphology (Kimmel *et al.,* 1995).

Fish for *in situ* hybridisation experiments were first anaesthetised at 3-days post fertilisation through exposure to 5 % Tricaine for 2 min. Larvae were transferred to a strip of masking tape in a petri-dish lid and cut within the pigment gap of the caudal fin using a surgical blade. Fish were then allowed to recover in fish water at 28.5^{o}C for an allotted time before fixing in 4 % PFA overnight at 4^{o}C, followed by methanol series to 100 % and stored at -20^{o}C.

To determine the difference in regenerative capacity between strains, zebrafish larvae were amputated at 2-days old within the pigment gap and allowed to recover for 3 days at 28.5^{o}C and then fixed in 4 % PFA before imaging.

2.2. Wholemount *in situ* hybridisation.

2.2.1. Probe synthesis.

Production of the template for probe synthesis was carried out by first amplifying a region of a stock plasmid containing the gene, or using primers, designed using primer3, from IDT (Table 1) to amplify zebrafish cDNA. Templates were then transcribed using their respective RNA polymerase. The PCR program was run for 35 cycles, each consisting of 45 seconds at 94^{o}C; 30 seconds at 58^{o}C; 120 seconds at 72^{o}C.

Probe	Primers	RNA Polymerase
fgf10a	F1: TGCTTCTGTTCCTGTGTTCG R1: CACGATAGGAATGGGGAGAA F2: GTTCCTGTGTTCGGCTCTG R2-T3:GGATCCATTAACCCTCACTAAAGGGAAGGGAGAAAGTGTGTGGCTGT	T3
wnt10a	F1: TTTTGGTTCAAAGGGCAGAC R1: TCCCTGGCTGGTCTTGTTAC F2: CTTTGACCCCATCCTCAATG R2-T3: GGATCCATTAACCCTCACTAAAGGGAATGTTACAGATCCGGCCTTG	T3

Table 2.1. Primers for anti-sense probe synthesis from cDNA

Template production using PCR

For templates from cDNA an initial PCR reaction using the F1/R1 primers was setup:

2.5 µL 10X PCR Buffer

1 µL of a 1:3 NTP mix

0.5 µL TAQ DNA Polymerase

1 µL of 2.5 µM F1 and R1 primers

1 µL cDNA

18 µL MilliQ H_2O

Templates from plasmid used the PCR reaction below only. After the first – nested – PCR the amplification product was carried over:

20 ng plasmid / 1 µL nested PCR amplification in 85 µL H_2O

10 µL 10X PCR Buffer

1 µL NTP mix

2 µL TAQ DNA polymerase

1 µL of primer F2 and R2-T3/7 at 25 µM

The PCR products were purified using centrifugal filter units (Millipore: UFC505024) according to manufacturer's instruction. Finally, DNA was quantified using a spectrophotometer.

Transcription:

1 µg DNA template in 21 µL H_2O

3 µL Transcription buffer 10X (NEB)

3 µL Digoxigenin-RNA labelling mix (Roche)

1.5 µL RNase Inhibitor, murine (NEB: M0314)

T3/T7 RNA polymerase

The reaction mixture was incubated for 2 h at 37^{o}C after which 2 uL RNase-free DNase I (NEB, M0303) plus 18 µL depc treated H_2O was added for 30 min at 37^{o}C. Transcription mix was filtered through Sigmaspin™ sequencing reaction clean-up columns (Sigma-Aldrich, S5059), according to manufacturer's instructions, into 14 µL RNA later (Sigma, R0901). Anti-sense probe was run on a 1% agarose gel to validate its presence.

2.2.2. In situ hybridisation.

Embryos/larvae were fixed at required stages in 4 % PFA overnight at 4^{o}C, dehydrated in methanol series (30%, 60%, 100%) and stored at -20^{o}C.

First day

After re-hydration and washes in PBST (Phosphate Buffer Saline + 0.1% tween-20) samples were permeabilised with proteinase K (Sigma, 10 ug/mL) for 10 min. They were then exposed to 4 % PFA for 20 min at room temperature to stop further permeabilisation, rinsed in PBST and incubated in hybridisation buffer (25 mL formamide, 125 mg RNA (Roche), 12.5 mL 20X SSC, 250 uL 20 % Tween-20, 50 uL heparin, 50 mL H_2O) at 70^{o}C for 2 h. Hybridisation buffer was replaced by probes diluted in hybridisation buffer and incubated overnight at 70^{o}C.

Second day

Embryos/larvae were washed in (25 – 75 %) PBST/ (75 – 25 %) Hyb- solution series to end in 2X SSC, followed by a series of washes at room temperature with (25 – 75 %) PBST/ (75 – 25 %) 0.2X SSCT solutions until samples were in PBST, followed by blocking buffer (2% sheep serum; 100 mg Bovine serum powder in PBST) for 2 – 3 hours. Blocking buffer was removed and replaced with AP-conjugated anti-DIG antibody at 1:10,000 in blocking buffer overnight at 4^{o}C with agitation.

Third day

Embryos/larvae were washed thoroughly with PBST and detected using NBT/BCIP substrate (Sigma) in staining buffer (10 % 1M Tris pH9.5, 5 %1M $MgCl_2$, 3.3 % NaCl in MilliQ H_2O + 0.1 % tween-20).

Within this thesis, only fish younger than 3-days old and the detection of *dlx5a* expression across all samples were done using this protocol. All other *in situ*s were carried out using the TSA *in situ* method (see below – 2.2.3).

2.2.3 Tyramide signal amplification (TSA) in situ hybridisation and validation.

In situ hybridisation using the TSA kit (Perkin Elmer) – according to the manufacturer's instructions - was incorporated into the wholemount *in situ* hybridisation protocol - as outlined above.

On day 2 of the *in situ*, after 0.2X SSC/PBST washes at room temperature, samples were washed briefly with maleic acid buffer (150 mM maleic acid, 100 mM NaCl, 250 mM NaOH, pH 7.5 + 0.1 % tween-20), followed by incubation for 3 hours in maleic block (2 % Blocking Reagent (Roche, 11096176001) in maleic acid buffer + 0.1 % tween-20). Larvae were then incubated with horseradish peroxidase-conjugated anti-DIG at 1:2000 in maleic block overnight at 4^{o}C with agitation. On the third day samples were washed with PBST, and incubated in tyramide amplification reagent (1:100 DNP substrate in amplification buffer) for

30 min; agitating gently every 10 min. Samples were washed thoroughly with PBST, blocked in maleic block for 2 h then incubated overnight at 4°C in 1:500 alkaline phosphatase-conjugated anti-DNP antibody in maleic block. Detection was carried out using the NBT/BCIP substrate in staining buffer.

After carrying out the amplification *in situ* using the TSA kit reagents at various concentrations it was important to validate the method. As there was a high level of staining within the fin fold of uncut caudal fins using the *pea3* probe it was necessary to determine whether this was true staining or an artefact of the TSA kit. When 3-day old zebrafish were treated for 4 h with 10 uM SU5402, staining was absent, and applying a sense probe for pea3 lacked any staining (Figure 2-1).

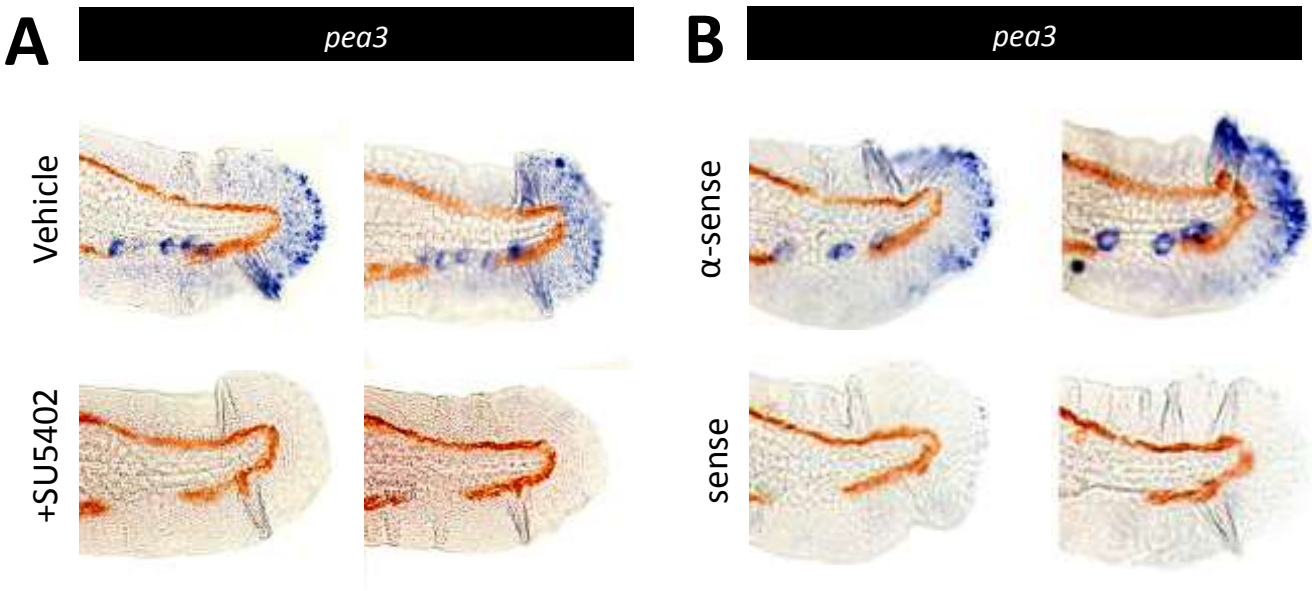

Figure 2-1. Validation of *in situ* hybridisation using the Tyramide Signal Amplification (TSA) kit.

In situ hybridisation using the Tyramide Signal Amplification (TSA) to detect *pea3* after zebrafish caudal fins were treated with SU5402 for 4 hours before fixing (A). Anti-sense or sense probe for *pea3* on 3-day old zebrafish caudal fins (B).

2.3. Chemical treatment of zebrafish.

After fish were amputated they were administered with 50, 10, or 10 µM of cyclopamine (Sigma, C4116), SU5402 (Calbiochem, 572630), or GSK-3 inhibitor XV (Calbiochem, 361558) in fish water, respectively. For short-term – pulse – treatments, amputated larvae were exposed to chemicals for the following times: cyclopamine, 8 h; SU5402, 4 h; GSK-3 inhibitor XV, 6 h, prior to being fixed in 4 % PFA overnight at 4ºC. For continuous treatment with cyclopamine, fish were immediately exposed to 50 uM cyclopamine in fish water after amputation and fixed at the defined time point. Control fish were incubated in the relevant vehicle at the same final concentration as their respective chemical.

2.4. Wholemount fluorescent antibody stain.

Zebrafish larvae were fixed at the required stage overnight in 4% PFA at 4ºC and dehydrated in 100% methanol.

First Day

After re-hydration and washes to PBST (phosphate buffer saline + 0.1% Tween-20), samples were permeabilised with 10 µg/mL proteinase K (Sigma) in PBST for 10 min. They were then post-fixed in 4% PFA for 20 min at room temperature, rinsed in PBST and blocked in 10% new born calf serum (NBCS) in PBST. Primary antibodies were added and incubated overnight at 4ºC in 10% NBCS at the following concentrations: p63 (SantaCruz, sc-8431), 1:400; anti-phospho-histone H3, 1:200 (Invitrogen).

Second Day

Embryos were washed in PBST, and blocked in 10% NBCS for 2 hours. Samples were incubated at 4ºC overnight with the secondary antibody goat-anti mouse Alex488 at 1:200 for

p63 detection, or goat anti-rabbit at 1:200 for detection of phospho-histone H3, in 10% NBCS-PBST (Molecular Probes).

Third Day

Samples were washed in PBST, and fixed in 4% PFA at room temperature for 20 min. Embryos were washed in PBST and stored in Vectashield® with DAPI (Vector Laboratories) at 4°C. Images were taken using the Olympus FV1000 confocal on a BX61 upright microscope.

2.4.1. Quantification of anti-phospho-histone-3 (H3P) staining.

The Perkin Elmer Volocity software was used to analyse the number of H3P-positive cells of Z-stacked images of zebrafish tail regenerates. Briefly, a region of interest 500 um from the wound site, and all dots below 50 μm^2 were excluded from the count (Figure 2).

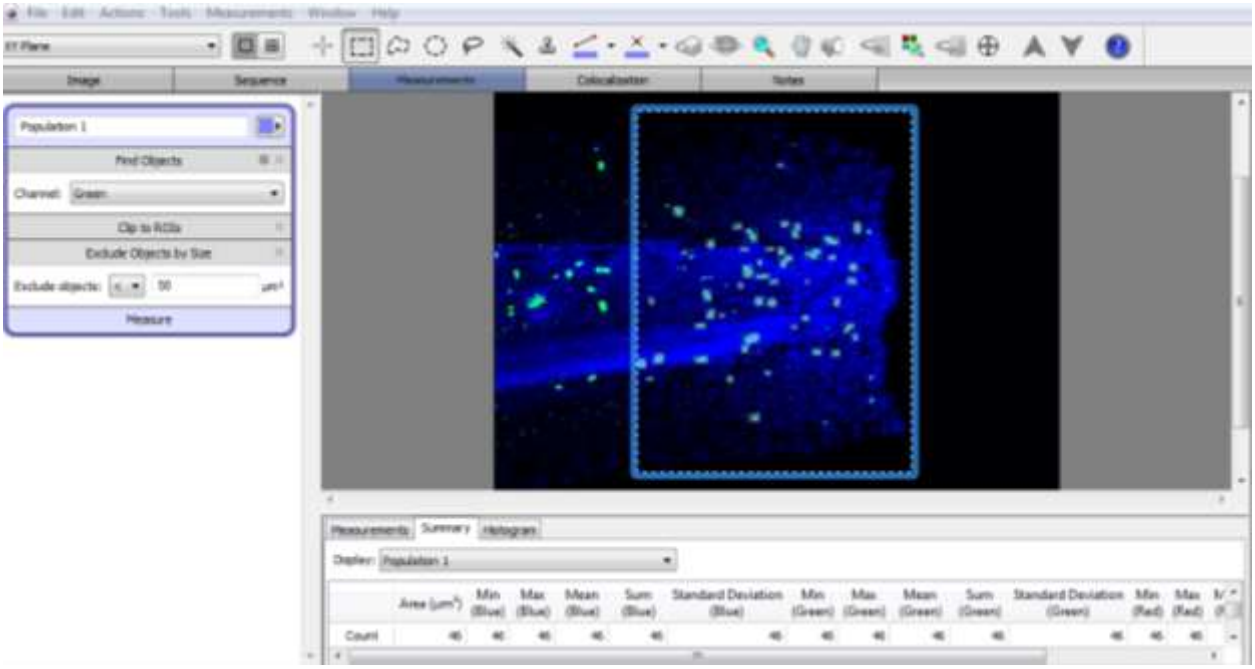

Figure 2-2. A sample image of the Volocity software analysis of H3P-positive cells.
A region of interest (box) was drawn and green dots smaller than 50 μm^2 were excluded.

2.5. Construction of a transgenic fish line to express a photo-convertible fluorescent protein, kaede.

2.5.1. Gateway clonase for the production of a ubi-kaede expression vector.

Using the gateway clonase technology, three components of the construct – p5e-ubiquitin promotor, pMe-Kaede (kindly supplied by Rob Wilkinson, Van Eeden lab), and p3e-PolyA – were inserted into the destination vector. Briefly, the correct amount of the three entry vectors were calculated and mixed in TE buffer, and added to the destination vector. Finally, the clonase enzyme (Invitrogen, 12538120) was added to the reaction mix and incubated for 16 hours at 25ºC to synthesise the final construct (Figure 2-3.). To end the reaction 1 uL ProK was added to the mix for 10 min at 37 ºC.

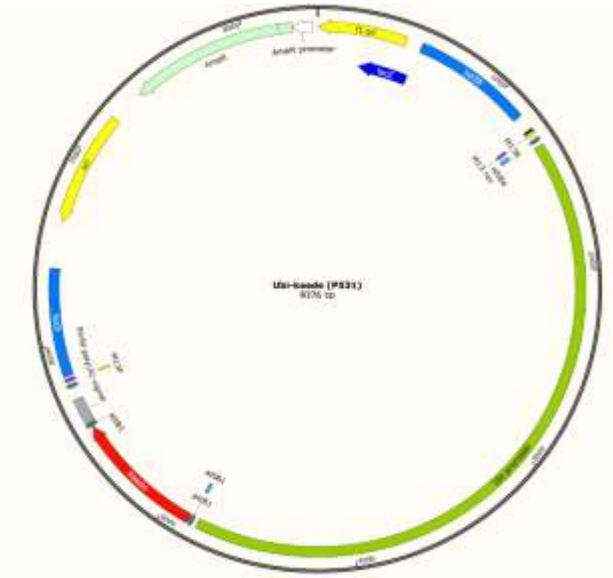

Figure 2-3. A schematic showing the Ubi-kaede construct after the gateway clonase reaction.

The ubiquitin promotor (green) drives the photo-convertible kaede (red) expression, which includes a polyA tail (grey) for faithful translation of RNA to protein. The final expression clone was 8376 bp.

2.5.2. Transformation of the ubi-kaede expression vector

The construct was then amplified using high efficiency 5-α E. coli (NEB, C2987) so that there were sufficient amounts for injection. Briefly, 2.5 µL ubi-kaede DNA construct was

mixed with 2.5 µL bacteria and left on ice for 30 min, heat-shocked for 30 seconds, and rested on ice for 5 min. Next, 400 µL SOC growth medium was added to samples and incubated at 37ºC with agitation for 1 hour. Bacteria were then spread using a sterile spreader onto an ampicillin growth plate and incubated at 37ºC overnight.

The next day, colonies were picked using a toothpick and placed in LB containing 50 µg/mL kanamycin and incubated with agitation for 18 hours at 37ºC. Samples were then spun down to obtain a pellet, supernatant removed, and resuspended in 200 µL P1 buffer. 200 µL P2 was added and mixed, leaving to stand for 5 min at room temperature. 200 µL P3 buffer was then added and samples were inverted several times, spun at 14,000 rpm for 3 min and supernatant transferred to a fresh Eppendorf containing 600 µL isopropanol. Tubes were spun at 16,000 rpm for 20 min at 4ºC, PE buffer was added to samples and inverted. Buffer was removed and samples were left to air dry and then 50 µL TE was added.

2.5.3. Injection and screening for stable ubi-kaede transgenic lines

The ubi-kaede construct was injected into AB wild-type zebrafish at the one-cell stage to reduce the likelihood of mosaic expression in founder fish and their offspring. The DNA construct was mixed with RNA coding for the tol2 transposase - to increase the chance of DNA integration – so that the final concentration of both was 25 ng/µL. All injections were carried out using a micro injector (World Precision Instrument, USA) viewed under a dissecting scope (Leica Microsystem GmbH, Wetzler, Germany). Embryos were kept in place using an agarose gel plate containing grooves, and injected directly into the cell using pulled glass capillary needles (Kwik-Fil Borosiliocate Glass Capillaries, World Precision Instruments Inc, USA).

Once injected, embryos were sent to be raised in the University of Sheffield aquarium facility until sexually mature; 3-months postfertilization. Next, F0 ubi-kaede-injected adult fish were each out-crossed with a wild-type – AB strain - fish. The offspring of each pair-mate was then screened for the presence of green fluorescence. F1 fish expressing kaede throughout the

whole body were sent to be raised for future experiments, and assigned a unique allele number: ubi-kaede^{sh343}.

For the conversion of the kaede protein in live fish the laser power and number of cycles was determined using a previously published journal (Dixon *et al.*, 2012). *Ubi-kaede*^{sh343} or *dackel;ubi-kaede*^{sh343} fish were mounted in 1% low melt agarose containing 2% tricaine on glass slides with a cover slip pressed gently on top. Using 405 nm laser at 50% power and 60 cycles on a precise region the kaede protein was converted from green to red. Converted fish were incubated in the dark at 28.5ºC. To determine the longevity of converted kaede, images were taken at 24 and 48 hours post-conversion (Figure 2-4). Detection of green and red was done using 488 nm and 560 nm excitation wavelengths, respectively. Once a line had been established, ub-kaede^{sh343} fish were out-crossed with *dackel* mutants to establish the *dackel;ubi-kaede*^{sh343} line. The subsequent crosses were then screened by crossing with *dackel* fish and selecting for the pectoral phenotype and detection of GFP expression.

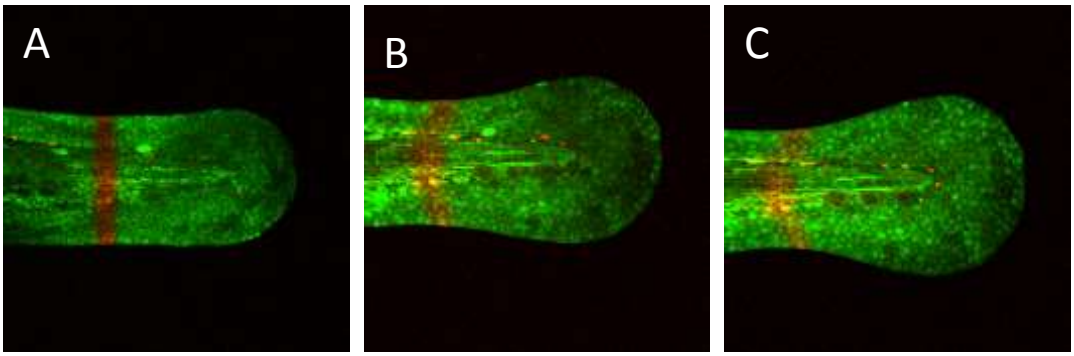

Figure 2-4. Converted kaede is visible 48 hours post conversion in larval tails
(A-C) An uncut caudal fin of a wild-type ubi-kaede^{sh343} with a UV-converted strip of kaede (red) at (A) 48 hours postfertilisation (hpf). (B) 72 and (C) 96 hours post-fertiliasation which were 24 and 48 hours post-conversion, respectively, at these time points. Red dots are autofluorescence. Images taken on an Olympus confocal microscope with a 20X objective. All images represent one sample.

2.6. Identification of *daedalus*/*fgf10* mutants

To genotype *Daedalus/fgf10* mutant embryos and their siblings, DNA was first extracted using the HotSHOT protocol (Meeker *et al.*, 2007). Briefly, larvae were placed in separate PCR tubes in 50 mM NaOH and heated to 95ºC for 10 min. 1M Tris-pH8 was added at 10 % (v/v). Samples were spun down at 1000 *g* for 2 min. The protocol for genotyping mutants and siblings has been taken from already published work (Norton *et al.*, 2005). Briefly, genomic DNA was amplified with the PCR primers GCTCTTCCCAGTTTTCCGAGCTCCAGGACAATGTGCAAATCG (forward) and TCCGTTCTTATCGATCCTGAG (reverse), followed by digestion with Taq1. Digested DNA was run on a 2 % gel. Mutant, *Daedalus*, embryos created a band of 300 bp, whereas the wild-type generated a band of 260 bp. The heterozygous siblings had two bands: 260 bp and 300 bp (Figure 2-5).

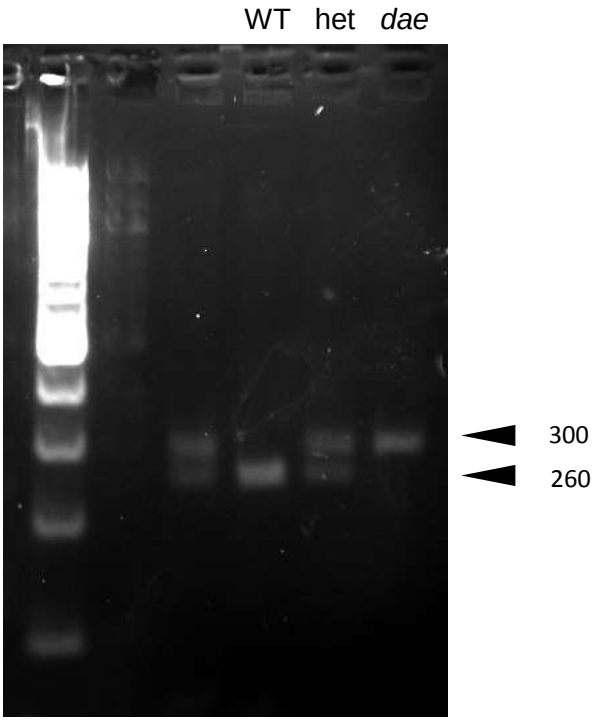

Figure 2-5. A sample gel showing the bands of digested *daedalus* and sibling DNA

2.7. Sonic hedgehog HS-binding sequence validation using tritiated heparin

An 18-amino acid peptide sequence corresponding to the herpin/HS-binding domain of human Shh ligand (Rubin *et al.*, 2002) was synthesised and linked with a biotin either on the carboxyl- or amino-terminus via a 6-aminohexanoic acid (AHX), termed ISP1 or ISP2. Both ISP-1 and ISP-2 were applied to nitrocellulose at 0.1 mg/µL and air dried for 1 hour at room temperature, then 80^{o}C at -10psi for 45 min. Next, 0.1 uCi tritiated heparin in 300 µL of PBS/4 % BSA was applied to the filter paper and incubated with agitation overnight at room temperature. Filter paper was washed with PBS and placed in a scintillation vial. 2 mL Ultima Gold Scintillation fluid was added and each vial measured twice using the 1450 Microbeta Trilux counter (Perkin Elmer).

2.8. Isolation of HS fractions using High performance Liquid Chromatography (HPLC)

After the ISP-1 peptide sequence was determined to interact stronger than ISP-2 with heparin/HS (see: shh heparin-binding sequence validation), 5 mg of the peptide was coupled to a streptavidin column (1 mL, GE Healthcare) according to the manufacturer's guidelines. After the column was equilibrated with low salt buffer (20 mM PBS, 0.15 M NaCl, pH 7.2), 5 mg of HS from porcine mucosa (HS^{pm}) was applied. Isocratic flow (1 mL/min) was monitored by UV detection at 232 nm. An unbound fraction ($HS23^{-ve}$) was collected as flow-through; bound fractions of HS ($HS23^{+ve}$) were eluted with high salt buffer (20 mM PBS, 1.5 M NaCl, pH 7.2), lyophilised for 72 hr, and then run over a HiPrep Desalting Column (GE Healthcare) according to manufacturer's instructions. Desalted samples were lyophilised, weighed and stored in a desiccator at room temperature. Figure 4 is a schematic depicting the process of HPLC.

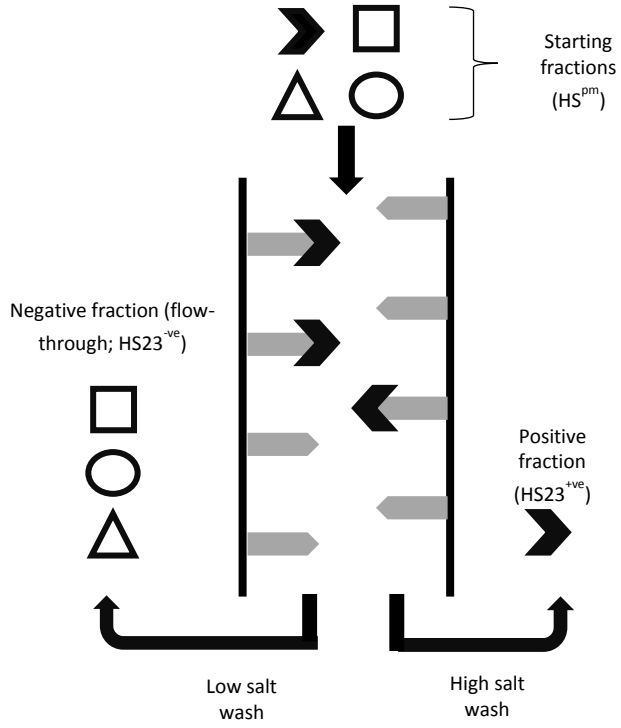

Figure 2-6. Schematic for the isolation of HS23 fractions using HPLC

2.9. Disaccharide analysis of HS fractions using HPLC-SEC-RI

The disaccharide composition of each heparan sulphate fraction was carried out by IRL (New Zealand). Heparan sulphate (starting material) (Celsus Laboratories Inc., HO-3105), HS23^{+ve} and HS23^{-ve} were sent for analysis. Briefly, HS samples were digested to di- and oligosaccharides using 5 mIU heparitinase I, II, and III (Ibex Technologies, Canada) at 37^{o}C. Digestion was terminated by heating to 100^{o}C for 5 min.

The HPLC-SEC chromatograms were obtained using two Superdex™ Peptide 10/300 GL columns (300 x 10 mm, GE Healthcare, Buckinghamshire, UK) in series, on a Waters 2690 Alliance system with a Waters 2410 refractive index detector (range 64). The dn/dc for quantification from the RI was set at 0.129. Samples (2 mg/mL) were injected and eluted with 50 mM ammonium acetate (0.5 mL/min) at room temperature. Heparin oligosaccharide and disaccharide standards (Iduron Ltd, Manchester, UK and Dextra Laboratories Ltd, Reading,

UK), previously run under the same conditions, were used for identification purposes. Data was collected and analysed using DAWN Astra software (Version 4.73.04, Wyatt Technology Corp., Santa Barbara, CA, USA).

2.10. Protein binding assay.

GAG-binding plates (Iduron) were first incubated overnight at room temperature with 5 µg/mL with HS^{+ve}, HS^{-ve}, or HS^{pm} in standard assay buffer (SAB: 100 mM Sodium Chloride, 50 mM Sodium Acetate, 0.2 % v/v Tween 20, pH 7.2); SAB was used in blank wells. Plates were then washed with SAB three times, incubated with blocking solution (0.4 % w/v fish gelatin in SAB) for 1 h at 37°C. Next, 3.75, 7.5, and 15 nM of recombinant human SHH (rh-SHH; R&D System: 1314-SH) or BMP-2 (rh-BMP2; R&D System: 355-BM), or 100, 200, and 400 ng/mL of ISP-1, were dissolved in blocking solution. The plates were washed three times with SAB and each dilution of recombinant protein (200 µL) or biotin-conjugated ISP-1 peptide were added into triplicate wells and incubated for 2 h at 37°C, followed by SAB washes. To assess SHH/BMP-2-binding ability, 200 µL of 1000 ng/mL anti-His tag biotinylated antibody (R&D System: BAM050), or 250 ng/mL anti-BMP-2 biotin conjugated antibody, in blocking solution was added and incubated for 1 h at 37°C then washed off. Detecting protein/peptide bound 200 µL of 220 ng/mL ExtrAvidin AP in blocking solution was added, incubated for 30 min at 37°C, and then rinsed with SAB. Finally, 200 µL development reagent (SigmaFAST p-Nitrophenyl phosphate) was added, incubated at room temperature for 40 min and read using a 405 nm laser (Hidex sense microplate reader).

2.11. Surface Plasmon Resonance (SPR)-based measurement of competition for Shh between heparan sulphate (HS) fractions and heparin.

2.11.1. Principles of Surface plasmon resonance (SPR).

Surface plasmon resonance (SPR) is an incredibly powerful, natural phenomenon able to be exploited to monitor a range of biomolecular interactions in a label-free environment. It exploits the optical phenomenon brought about by surface plasmon polaritons (SPP). SPPs form when free electrons within the conducting band of a metal are excited by the interactive electromagnetic field at the metal-dielectric interface (in this case gold with glass); these charged oscillations are known as SPPs, which form evanescent electrical fields that are highly sensitive to a change in the refractive index of the sensing medium, for example, gold. Therefore, when the analyte – sonic hedgehog protein - binds to a surface-bound ligand – heparin – on a gold sensor chip (e.g. streptavidin (SA) chip), altering its refractive index, this leads to a change in the reflected angle of polarized incident light (Figure 2-7). It is the change in the angle of reflected light that is proportional to the mass of material bound.

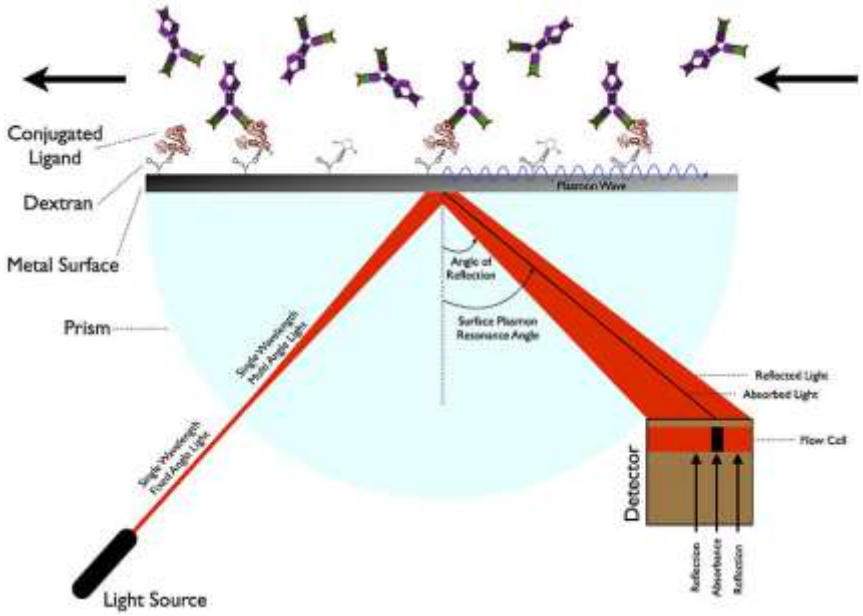

Figure 2-7. A schematic depicting the change in SPR angle during a binding event on a sensor chip

2.11.2. SPR competition assay

To determine the binding ability of Shh to heparin, a biacore streptavidin (SA) sensor chip (GE healthcare) was first coated with 38 response units (RU) of biotinylated-heparin, according to the manufacturer's instructions. Next, 12.5 – 200 nM rh-SHH (rh-SHH; R&D System: 1314-SH) was injected over the chip using the BIAcore T100 surface plasmon-resonance instrument, according to the manufacturer's instructions (GE Healthcare). Once the optimum concentration of ligand (50 uM) was determined, rh-SHH was pre-mixed with each HS fraction at 5 or 10 µg/mL and incubated on ice for 10 min. Solutions were injected over the heparin-coated SA chip. Readings were collected using the BIAcore T100 software; graphs representing the relative rh-SHH bound were plotted using GraphPad.

2.12. Cell culture

The MC3T3-E1 pre-osteoblast cell line was obtained from ATCC (CRL-2593) and cultured in maintenance medium (Alpha MEM (Sigma: M0894) supplemented with 10% FCS; 100 U/mL Penicillin, 100 µg/mL Streptomycin (Gibco); 2 mM L-glutamine (Gibco); 1 mM Sodium pyruvate (Gibco)). Cells were incubated at 37ºC with 5 % CO_2. All experiments were carried out using cells before reaching passage 10.

2.13. Cell treatments

Cells were first seeded at 1.58 x 10^4 cells/cm^2 and incubated overnight in maintenance media. Media was then removed and replaced with treatment media: maintenance medium containing rh-SHH (R&D System: 1314-sh) at concentrations stated. For glycosaminoglycan (HS^{+ve}, HS^{-ve}, or HS^{pm}) treatments, HS fractions were first incubated with rh-SHH for 10 min on ice before being added to maintenance media, and then cells for a predetermined incubation time. Cyclopamine (Sigma, Cat no: C4116) was dissolved in DMSO and aliquoted for storage at -20ºC. Prior to treatment of cells, cyclopamine was heated to 50 ºC for 10 mins and added to the appropriate treatment media at 5 µM. DMSO was used as a vehicle control.

2.14. Real-time polymerase chain reaction (RT-PCR).

For RT-PCR, cells were maintained and treated with media containing only 2 % FCS, as this reduced background gene expression to its minimum (Page 52, Figure 2-8).

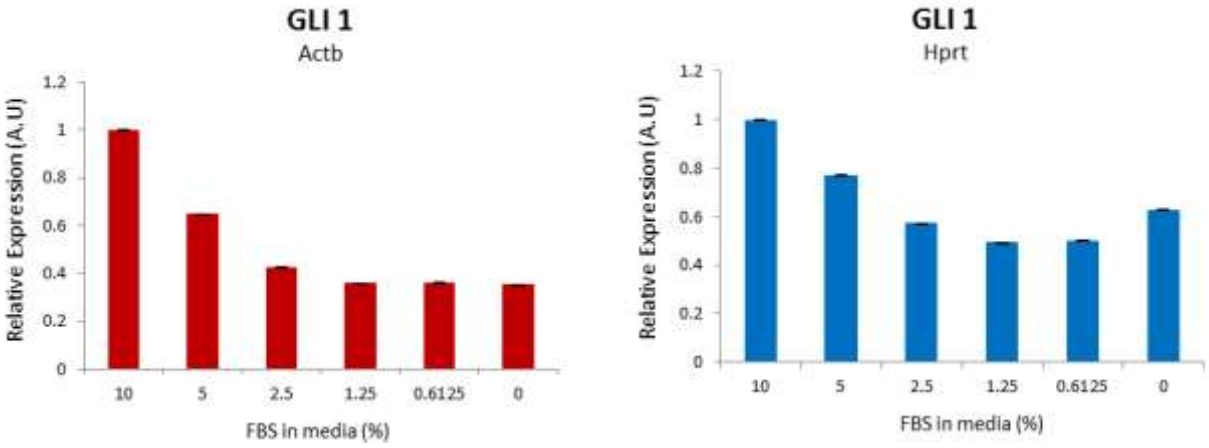

Figure 2-8. FBS in maintenance medium dose-dependently regulates GLI1 expression in MC3T3-E1 cells

GLI1 expression in MC3T3-E1 after incubation for 24 hours in 0 – 10% FBS media. Data presented as mean ± SEM.

Cellular RNA was isolated using TRIzol® (Life Technologies) according to the manufacturer's protocol. Reverse transcription, using SuperScript VILO cDNA synthesis kit (Invitrogen), was carried out on equal amounts of RNA following the manufacturer's instructions. Quantitative PCR was performed using the following TaqMan Gene Expression Assay primers from Life Technologies: Gli1 (Mm00494654_m1), Patch1 (Mm00436026_m1), Actb (Mm00607939_s1), or Hprt (Mm00446968_m1) in a 20 µL reaction with 2X TaqMan Fast Universal PCR Master Mix (Applied Biosystems) and nuclease-free water, with 30 ng cDNA. The QuantStudio 6 Flex System was set up with an initial 95ºC for 20 seconds, followed by 45 cycles of 95ºC for 1 second and 60ºC for 20 seconds. Results were analysed using the comparative Ct method.

2.15. Alkaline phosphatase (ALP) assay

2.15.1. MC3T3-E1 pre-osteoblast cells increase ALP activity in response to Shh and BMP2.

To test the ability of the heparan sulphate fractions to augment SHH activation, another bioassay was used – alkaline phosphatase (ALP) activity of preosteoblast MC3T3-E1 cells. The mouse preosteoblasts have been reported to increase ALP activity in response to exogenous Shh in a dose-dependent manner (Yuasa *et al.,* 2002).

2.15.2. ALP detection in MC3T3 cells

MC3T3-E1 cells were first seeded at 3 x 10^4 cells/well in 24-well plates and incubated overnight in maintenance media. Culture media was removed, and cells were incubated in treatment media (maintenance medium with or without rh-SHH in the presence or absence of GAG fractions at defined concentrations) for 3 or 6 days; treatment media was replaced either every other day or every three days, after which ALP activity was determined. The following steps were all carried out on ice. Cells were washed twice with chilled PBS and lysed in RIPA buffer (50 mM Tris-HCl pH 7.4, 1 % NP-40, 150 mM NaCl, 0.25 % Deoxychlorate) containing proteinase inhibitors (Calbiochem), scraped with a cell lifter, and retrieved in Eppendorf tubes. The protein content was determined using the BCA protein assay kit (Pierce Chemical) according to the manufacturer's instructions. ALP activity was measured by adding *p*-nitrophenyl phosphate (Invitrogen, #00-2212) to 7 ug protein, and incubated for 1 hour at 37^{o}C. Absorbance was read at 405 nm (Hidex sense microplate reader), and relative ALP activity was calculated.

2.16. Heparan sulphate toxicity screen and treatments

2.16.1. Heparan sulphate toxicity

One-cell stage zebrafish eggs were placed in individual wells of a 96-well plate. Increasing concentrations of porcine mucosal heparan sulphate (HS^{pm}; Celsus) was added at 100 µL to each well. Zebrafish chorions were then pierced with a 25-gauge needle and incubated under normal conditions for 5 days. Percentage survival was then calculated.

2.16.2. Exogenous application of HS to early stage zebrafish

10 or 50 µM HS^{pm}, and 10 µM of $HS23^{+ve}$ or $HS23^{-ve}$ were added to the fish water of 10-hours post fertilisation (hpf) larvae and incubated for 14 hours, fixed in 4 % PFA overnight and dehydrated in methanol series to 100 % before carrying out *in situ* hybridisation on samples.

2.16.3. Exogenous application of HS to rescue dackel regeneration

Dackel mutant and sibling zebrafish were anaesthetised with tricaine and amputated using a surgical blade within the caudal fin pigment gap. Larvae were transferred to 10 µM of HS^{pm}, $HS23^{+ve}$, $HS23^{-ve}$, or water alone in fish water for three days, fixed in 4 % PFA and then imaged.

2.17. Zebrafish regenerate length measurement using the anus-caudal axis

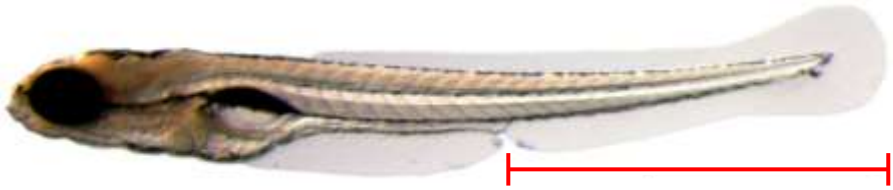

Figure 2-9. Measuring the tail length of zebrafish larvae using the anus-caudal axis. Images of zebrafish bodies were taken using a light microscope-mounted camera and the length between the anus and caudal tip of the intact, or regenerating, tail was measured (red line).

The length of Zebrafish regenerates was measured using the anus-caudal axis (Figure 2-9). Using Photoshop, I determined the length between the anus and caudal-most tip of the tail in pixels, which I then converted to µm. This was my method of choice because it utilised a point of reference that would be relatively stationary, whilst the larvae developed, up to three days after the initial resection. Due to the dynamic nature of the amputation point during regeneration it would have been difficult to identify the original amputation plane beyond one day postamputation., therefore I believe the anus-caudal axis was the best way to obtain consistent measurements. Uncut control tails were measured in the same way.

2.18. Scoring Zebrafish tail regeneration after exposure to Cyclopamine

The tails of 2 days postfertilisation larvae were amputated within the pigment gap and allowed to regenerate for 72 hours in the presence, or absence, of 50 uM cyclopamine after which samples were fixed in 4% PFA. Images were taken using a camera attached to a light microscope. Each image had its experimental condition noted and given a corresponding random number. Viewing the images in a random order I gave their overall regenerative morphology a score between 0 and 10. With 10 being the ability to replace the fin fold and 0 was given to tails lacking a regenerating fin fold with a notochord protrusion - present immediately after tail amputation - was still discernible at the caudal-most tip.

3 The Hh, Wnt, and FGF pathways are upregulated during larval tail regeneration

3.1. Introduction

The mechanisms responsible for the coordination of a regenerative response in zebrafish, after caudal fin amputation, are becoming more and more well-defined in the adult model. Many of the pathways active during early development are shown to be upregulated during regeneration. These include, but are not limited to: BMP, Hedgehog, Wnt and FGF pathways. Studies looking at the possible interactions between these pathways during regeneration focus primarily on their modulation of well-established regeneration markers - *aldh1a2* (raldh2) and some *msx* genes. However, our understanding of whether these activated pathways can interact with one another is lacking. Therefore, the first part of this study was to first establish a time course for the activation of developmental signals, focusing on the Hedgehog, Wnt and FGF pathways, and also determine the appearance of the wound epidermis and blastema during larval tail regeneration. This will hopefully support the evidence provided by Kawakami *et al*. (2004): there are many similarities between larval caudal fin fold amputation and adult zebrafish caudal fin regeneration.

Kawakami *et al*. (2004) only looked at regeneration within the fin folds - composed predominantly from epithelial cells - of 48-hour old zebrafish. Compared to complete limb regeneration, amputation of the fin fold lacks major tissue groups, such as muscle, nervous and notochord. To reach a compromise in larval zebrafish I have moved the amputation plane more proximal - within the pigment gap. Besides the ectoderm-derived epithelium of the skin, tissues derived from the mesoderm, such as skeletal muscle, and spinal cord will be damaged. Another interesting tissue that will be affected is that of the notochord – an important organising centre

for the muscles and neural tissue. Whether this could be a signal centre for subsequent tissue regrowth in zebrafish has yet to be determined.

To this end, in this chapter I have used larval zebrafish, amputated within their pigment gap, as a model to understand the molecular activity during caudal fin regeneration. I have used chemicals to determine any interactions between pathways but also how, if at all, they affect the the wound epidermis and blastema. In the context of amputation within the pigment gap, from here on, the zebrafish larval caudal fin will be referred to as their tail.

3.2. Results

3.2.1. The wound epidermis and blastema are both present during larval tail regeneration

To first demonstrate that the zebrafish strain - AB - was able to regenerate, 2-day post-fertilisation larval tails (n = 6) were removed using a surgical blade within the pigment gap (Figure 3-1A) and allowed to recover for three days. After this time, the majority of the original tissue had been replaced (Figure 3-1C), however their gross morphology could be distinguished easily from the 5-days post fertilisation, uncut, tails (Figure 3-1D).

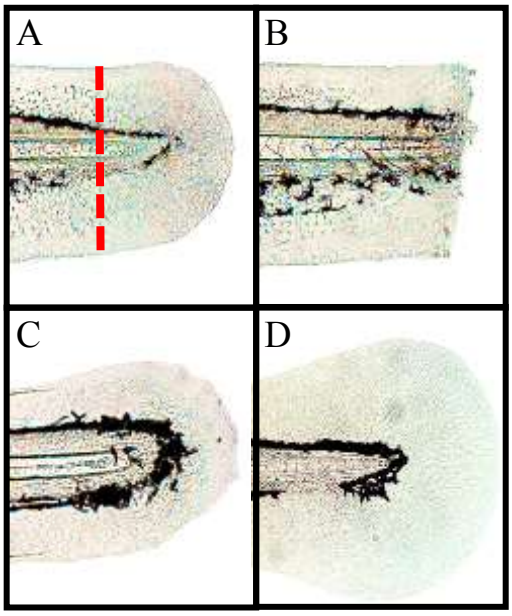

Figure 3-1. Wild-type zebrafish regenerate the majority of their tail after 3 days.
(A-C) Representative samples of a single zebrafish imaged at 2 dpf, prior to amputation (A), immediately after tail amputation (B) and then 3 days postamputation (C). Red dashed line highlights the amputation plane.
(D) The caudal fin of a 5 dpf zebrafish larva.
All images are lateral views oriented with rostral to the left and caudal to the right. (n = 6).

In situ hybridisation was used to identify key markers, *dlx5a* and *raldh2*, for wound epidermis and blastema formation, respectively (Figure 3-2). Larval tails were amputated, allowed to recover for 12, 18, 24, or 30 hours, and fixed for the detection of transcripts. After 18 hours the regenerates strongly expressed *dlx5a* in two distinct dorsal and ventral domains that gradually extended their expression, meeting at the most distal point by 30-hours post amputation (hpa). The blastema marker, *raldh2*, was not expressed until 24 hpa, in the presumptive mesenchyme, in regions similar, but more proximal, to the staining of *dlx5a* as seen at 18 hpa. These domains became larger and more intense by 30 hpa. There was no detection of the wound epidermis or blastema marker in the caudal fins of uncut control tails.

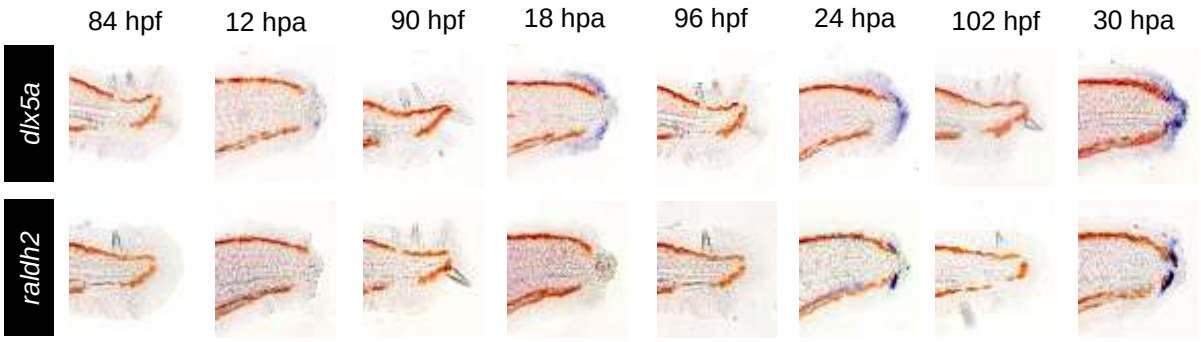

Figure 3-2. The wound epidermis and blastema form during zebrafish caudal fin regeneration. Expression of the wound epidermis (*dlx5a*) and blastema (*raldh2*) markers between 12 and 30 hours postamputation (hpa) in wild-type zebrafish tails. Control, uncut tails (hpf), are shown to the left of their respective amputated tails. Expression detected by *in situ* hybridization. n = 10 per gene per time point.

3.2.2. Early developmental pathways are active during epimorphic regeneration

As they have been shown to be expressed in response to the activation of their respective pathways, the following probes were used: *ptc1*, *axin2*, and *pea3*, to detect any increase in activity of the Hedgehog, Wnt and FGF pathways, respectively (Roehl and Nüsslein-Volhard, 2001; Jho *et al.*, 2002; Pearse *et al.*, 2001). Other probes were used to detect the ligands - *ihhb*, *wnt10a*, and *fgf10a* – for the three developmental pathways. The WNT10A and FGF10 ligands

have been heavily linked with having roles during epimorphic regeneration (Stoick-Cooper *et al.*, 2006; Yokoyama *et al.*, 2000). An even more interesting find was that FGF10-soaked beads returned the regenerative capacity, and induced the expression of genes, when implanted into limb stumps of *Xenopus* in their non-regenerative - refractory – periods (Yokoyama *et al.*, 2001). As there was less literature reporting on Hedgehog ligand expression, besides that of Shh, the *ihhb* probe was used in an attempt to identify a novel ligand upregulated during regeneration. Larval zebrafish tails were amputated and allowed to recover for 12, 18, 24, or 30 hours, after which *in situ* hybridisation was carried out.

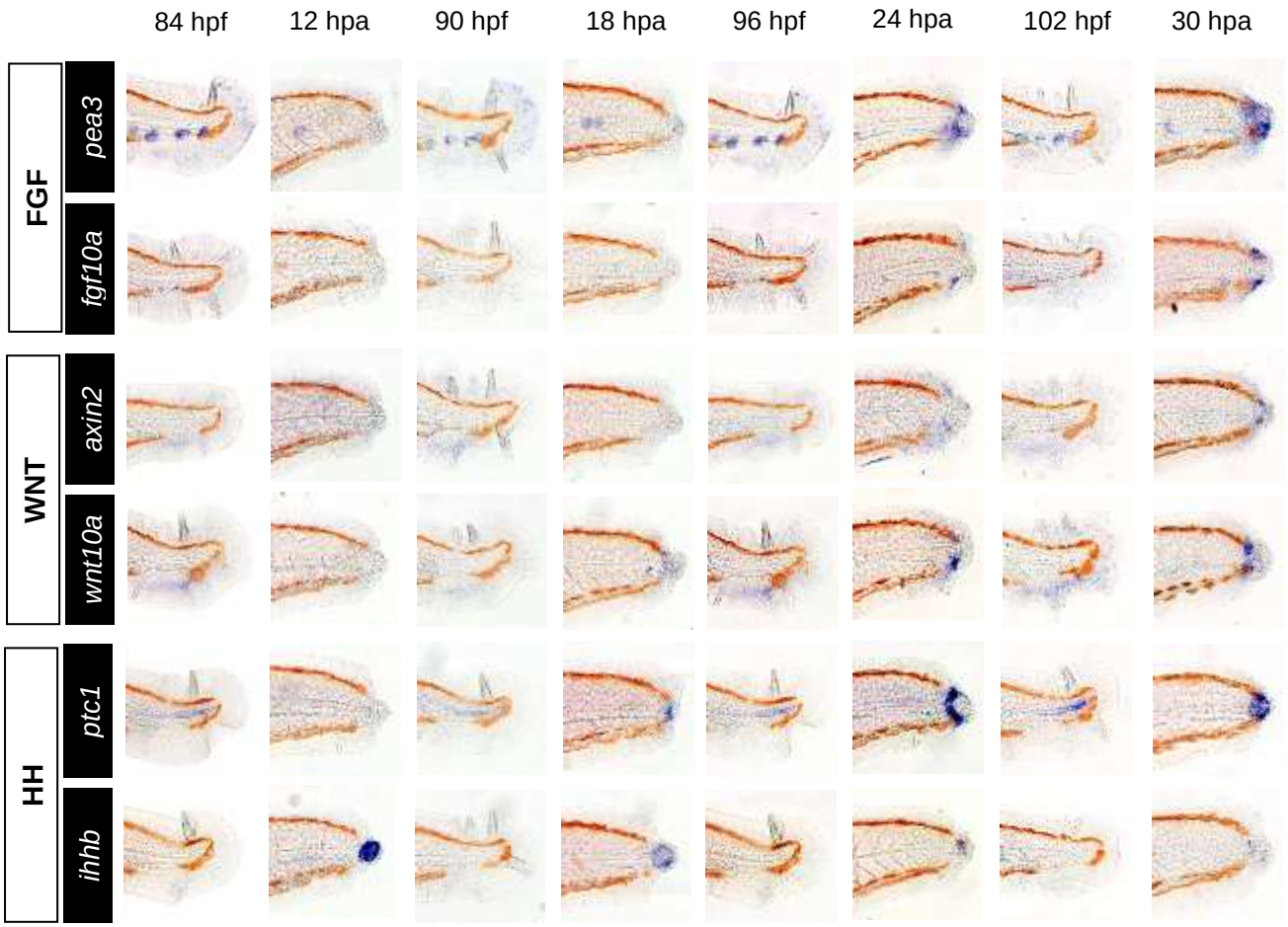

Figure 3-3. Developmental pathways are active during wild-type epimorphic regeneration. Expression of the transcripts for ligands involved during development (*fgf10a, wnt10a* and *ihhb*) between 12 and 30 hours postamputation (hpa), including their corresponding uncut control tails (hpf). *In situ* hybridization of gene transcripts for the activation of the Wnt, Hh, and Fgf pathways: *axin2, ptc1,* and *pea3*, respectively, in cut (hpa) and uncut (hpf) larval tails. n = 10 per gene per time point.

All the genes probed for were upregulated during the regenerative process; *axin2* and *pea3* transcripts were present at 24 hpa – the latter exhibited a deeper and broader stain. However, *ptc1* was the earliest read-out to be expressed, at 18hpa, and all transcripts were detected up to 30 hpa (Figure 3-3). The ligand transcripts for each pathway were all also expressed, and at similar times to their respective read-out gene. The most notable expression was that of *ihhb*, seen to be expressed in a very precise bead-like structure within the distal-most tip of cells at 12 hpa (Figure 3-3), earlier than that of *fgf10a* or *wnt10a*: first expressed after 18 hpa and 24 hpa, respectively. Ligand expression persisted until 30 hpa, however *ihhb* was weak to non-existent by this time.

Uncut – control – 5-day old larval tails had detectable levels of all genes, apart from *ihhb*. The pigment gap was stained with *axin2* and *wnt10a* in 4-day old larvae, whereas the neuromasts of the developing lateral line were stained with the FGF transcripts, *pea3* and *fgf10a*. *Ptc1* was detected in cells around the distal tip of the notochord in uncut control tails.

3.2.3. The Hedgehog pathway has an early role during larval tail regeneration

As *ihhb* was the earliest transcript to be detected out of all others screened, a second *in situ* hybridisation screen for other Hedgehog ligands was carried on amputated tails immediately after, or 3 hpa (Figure 3-4). The zebrafish have five Hedgehog genes: *shha/b, ihha/b*, and *desert hedgehog* (*dhh*) (Jackman *et al.*, 2010); this study probed for four of these.

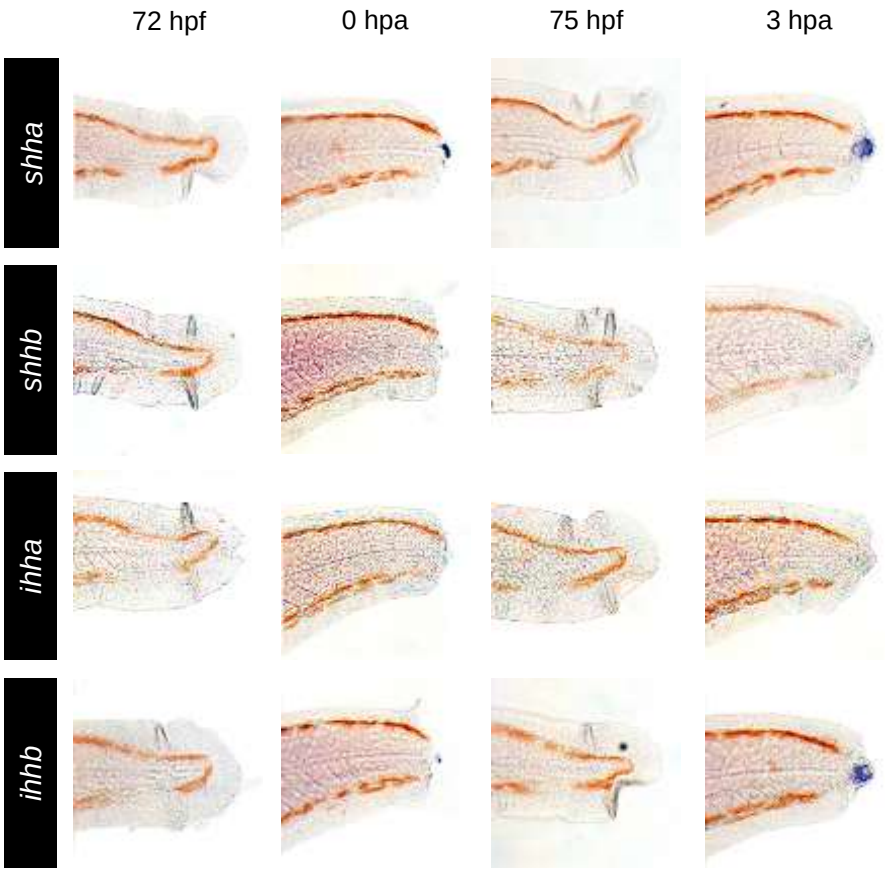

Figure 3-4. The genes encoding Hedgehog ligands are expressed early during wild-type tail regeneration.
In situ hybridization of hedgehog ligand transcripts immediately after amputation (0 hpa) and 3 hpa in wild-type larvae. Uncut controls (hpf) are to the left of their corresponding amputated tails. n = 10 per time point per gene.

Furthermore, to highlight the need for Hedgehog signalling during regeneration, 2 dpf larval zebrafish tails were amputated and immediately exposed to 50 µM cyclopamine for the entire duration of their 72-hour recovery period (Figure 3-5). Firstly, all cyclopamine treated fish were unable to regenerate their tails when compared to untreated controls or those exposed to 0.5% ethanol. Furthermore, *in situ* hybridisation revealed the presence of not only *ihhb* but also *shha* in the distal most tip of the regenerate. *Shha* was seen in fish fixed immediately after amputation (Figure 3-4B, red arrowhead) and at 3 hpa, whereas *ihhb* was first seen at 3 hpa. There was no detection of *ihha* or *shhb* at either of the time points.

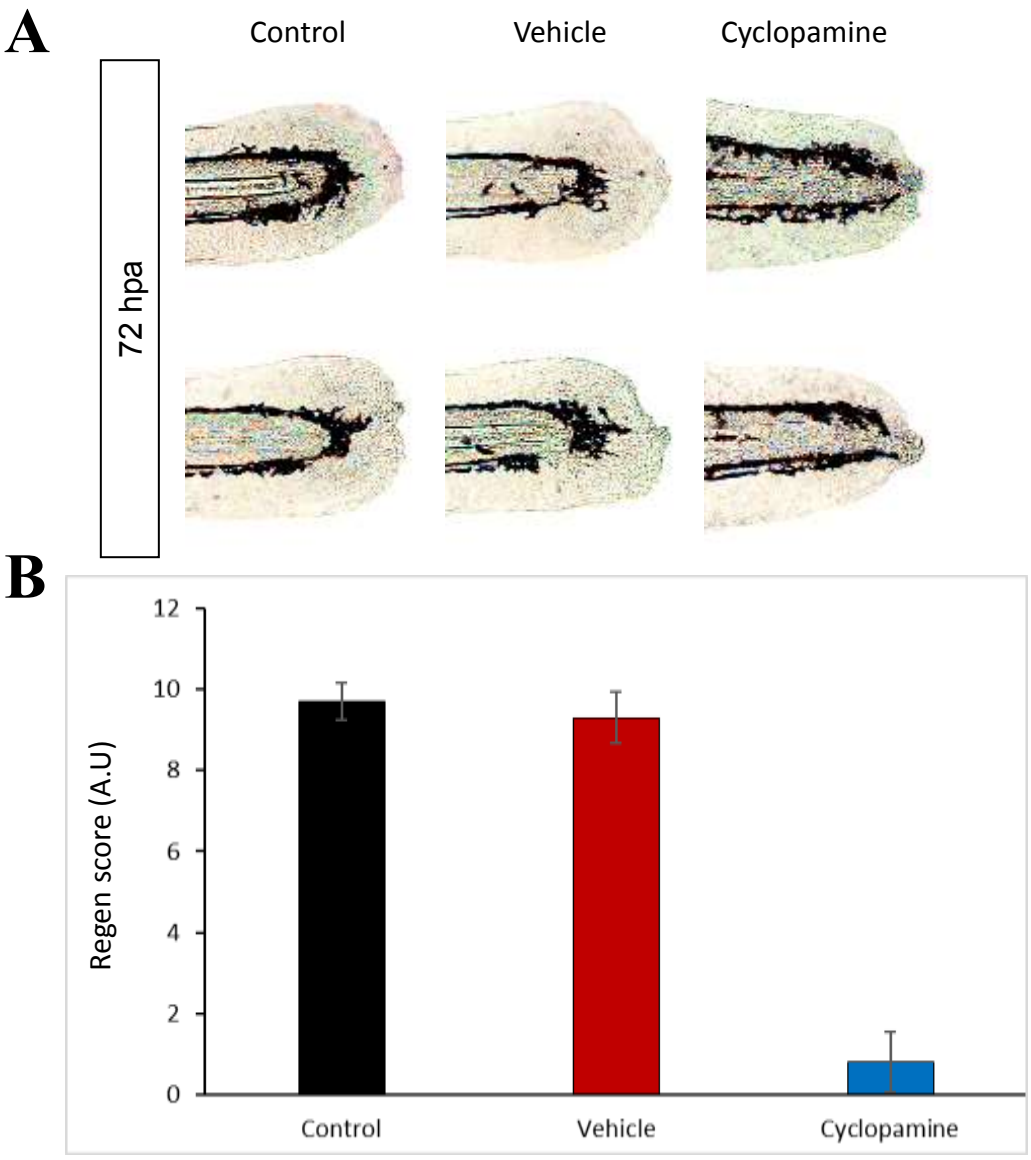

Figure 3-5. The genes encoding Hedgehog ligands are expressed early during wild-type tail regeneration.
(A) Zebrafish larvae maintained in: fish water (i), 0.5 % Ethanol vehicle (ii), or 50 uM cyclopamine (iii) continuously for 72 hours immediately after amputation of the caudal fin. Images are representative results from one experiment (n = 10). (B) A graph to show the average regeneration score of regenerating zebrafish tails exposed to 0.5% ethanol (vehicle) or 50 uM cyclopamine for 72 hours postamputation. n = 10 for all samples; data presented as mean ± SEM.

To determine whether the Hedgehog pathway could regulate the initiation and maintenance of key structures during epimorphic regeneration, zebrafish larval tails were amputated and immediately treated with 50 µM cyclopamine, fixed after 30 hours, and stained,

using *in situ* hybridisation, for *dlx5a* and *raldh2* detection (Figure 3-6). The wound epidermis (*dlx5a*) was severely disrupted after continuous Hedgehog inhibition. This was also the case for the blastema (*raldh2*), which was absent after exposure to cyclopamine, but not 0.5% ethanol alone.

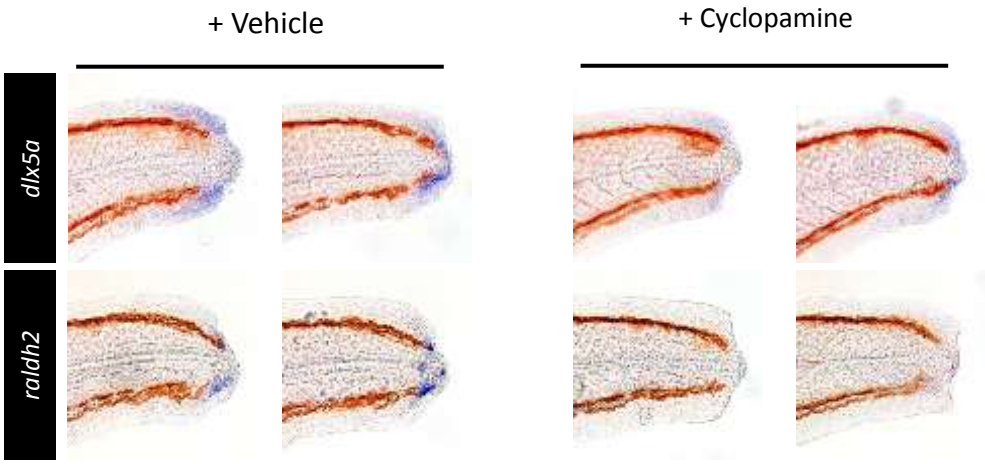

Figure 3-6. Blocking Hedgehog signaling prevents the formation of the wound epidermis and blastemal during tail regeneration.
Wound epidermis (*dlx5a*) and blastema (raldh2) detection, using *in situ* hybridization, after fish were exposed, immediately after tail resection, to 50 µM cyclopamine or vehicle (0.5 % ethanol) in fish water for 30 hours immediately after tail amputation. Images represent an individual experimental sample; n = 10 per treatment per gene.

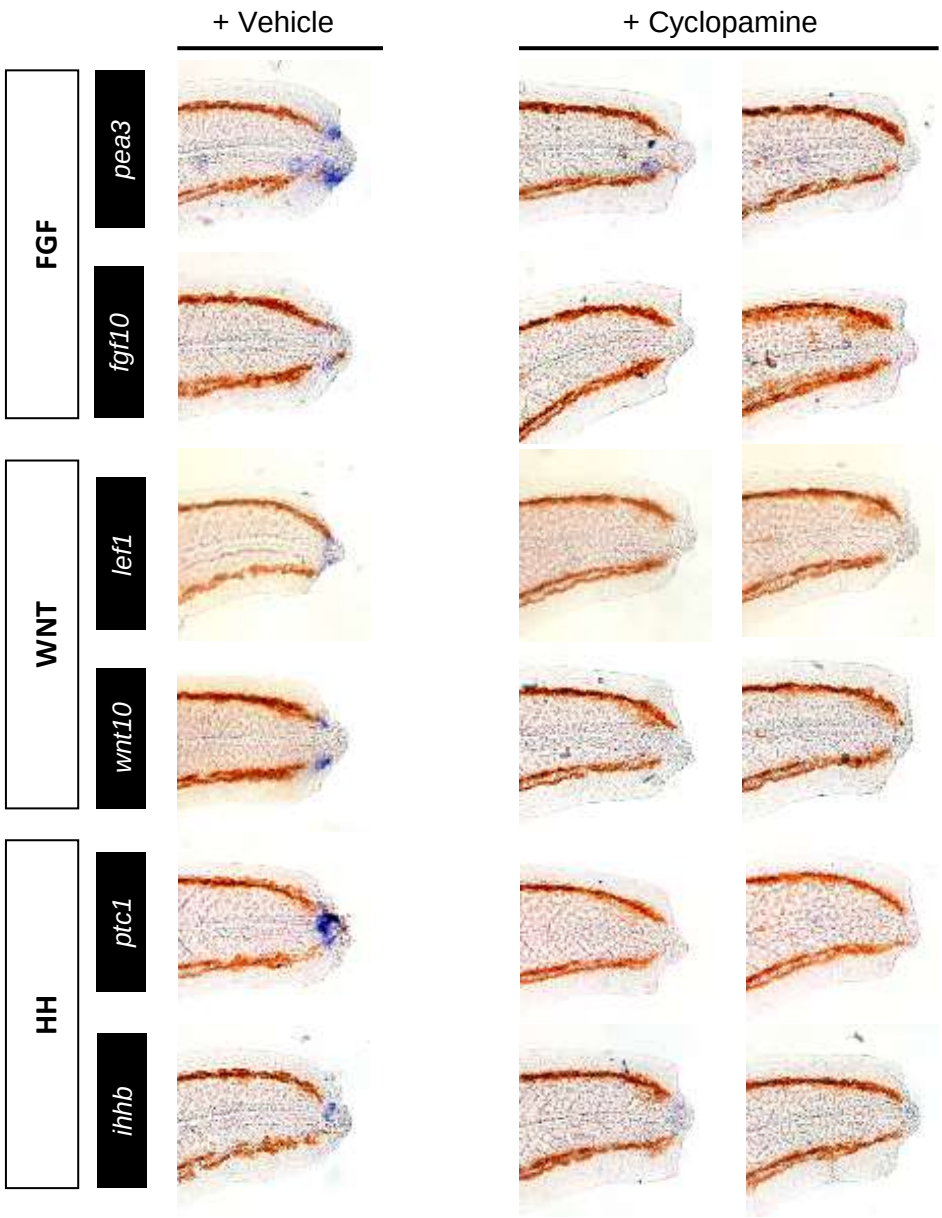

Figure 3-7. Inhibition of the Hedgehog pathway during larval tail regeneration blocks signal pathway activation.

In situ hybridization to detect the expression of ligands (*fgf10, wnt10,* and *ihhb*) and pathway read-outs (FGF, *pea3;* Wnt, *axin2;* Hedgehog, *ptc1*) after caudal fins were exposed to 50 µM cyclopamine or vehicle (0.5 % ethanol) immediately after tail amputation and fixed at 30 hours post amputation. Two samples are shown per gene for Cyclopamine treated fish. n = 10 per

Finally, the result of continuous hedgehog inhibition on the Wnt, FGF and Hedgehog genes was that of a complete loss in expression (Figure 3-7). There was no staining in zebrafish larval tails at 30 hpa after continuous exposure to 50 µM cyclopamine.

3.2.4. Signal pathways interact during larval tail regeneration

The final stage of this chapter was dedicated to providing evidence for any interactions between developmental pathways during larval tail regeneration. This was carried out using 3-day old larvae and chemicals that can modulate well-known targets of the Hedgehog, Wnt and FGF pathways: cyclopamine, GSK3-inhibitor, and SU5402, respectively. Determination of pathway interaction was carried out by administrating chemicals to amputated tails for short periods of time, followed by *in situ* hybridisation for ligands (*fgf10a, wnt10a*, and *ihhb*) and pathway read-outs (*pea3, axin2/lef1*, and *ptc1*). The predetermined treatment times for cyclopamine, GSK3-inhibitor and SU5402 were 8, 6 and 4 hours prior to fixing samples (Figure 3-8A, 3-9A, 3-10A), and concentrations were reported to be optimum at 50, 10 and 10 µM, respectively; these were tested again throughout the experiment. This showed that cyclopamine, GSK3-inhibitor, and SU5402 all altered the expression of their target genes as expected (Figure 3-8B, 3-9B, 3-10B). All samples were fixed after 30 hpa, regardless of the chemical used.

3.2.4.1. Inhibition of the Hedgehog pathway abrogates FGF and Wnt signal activity

Pulse treatment of regenerating larval tails with the Hedgehog inhibitor cyclopamine provided some interesting results. Firstly, tails did not exhibit any detectable alterations in the development of their wound epidermis (*dlx5a*) or blastema (*raldh2*) by 30 hpa. Vehicle controls also showed normal development of the same regeneration structures. However, both the Wnt and FGF genes exhibited reduced intensities in the presence of cyclopamine, to varying degrees (Figure 3-8B).

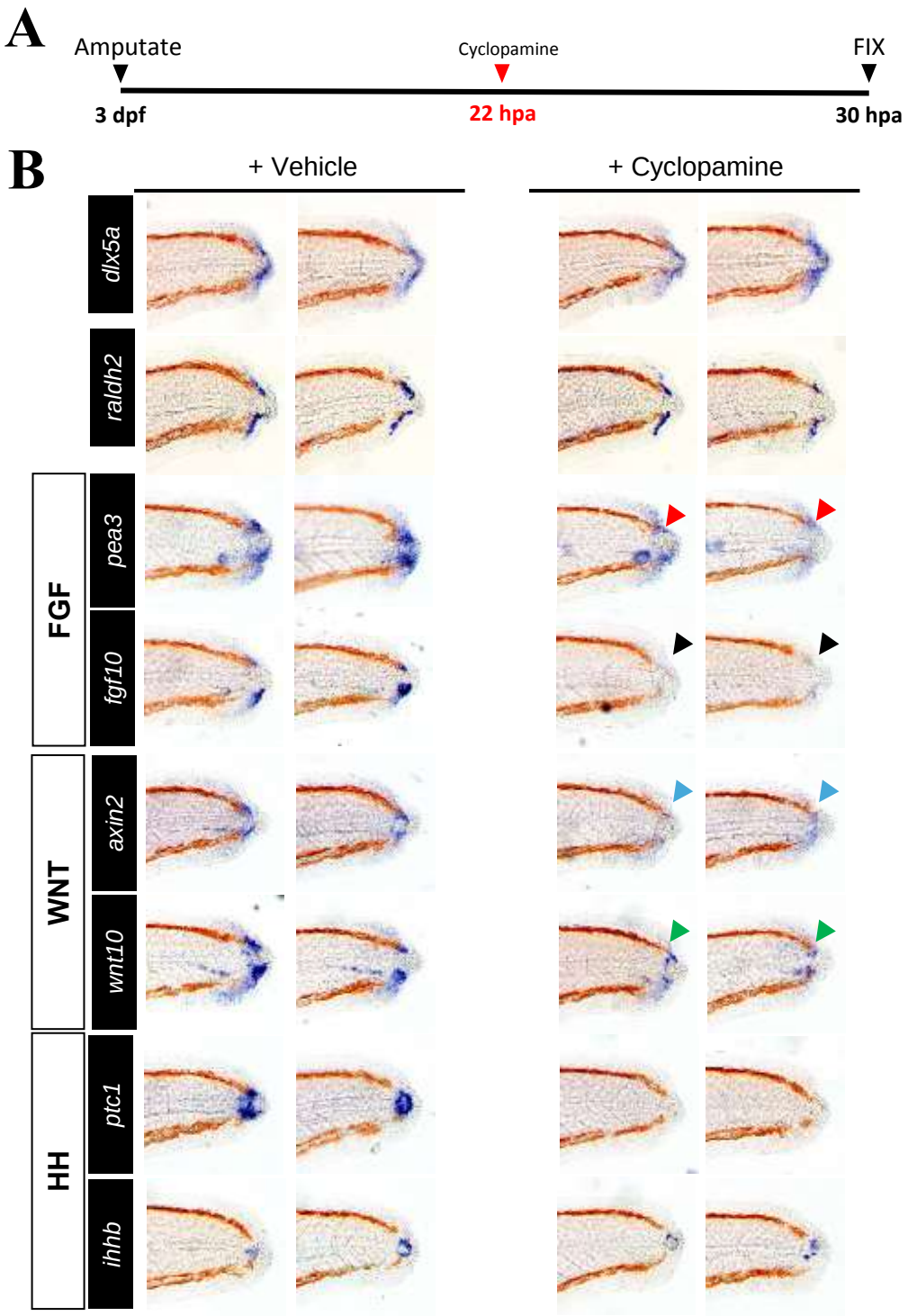

Figure 3-8. The hedgehog pathway mediates the activity of Fgf and Wnt pathways during caudal fin regeneration.

(A) A diagram to show the pulse treatment timecourse of cyclopamine exposure to regenerating caudal fins. (B) *In situ* hybridization of regenerate structures (*dlx5a* and *raldh2*) and developmental pathway activities (Fgf: *pea3*, *fgf10*; Wnt: *axin2*, *wnt10*; Hedgehog: *ptc1*, *ihhb*) after 8 hours exposure to 50 uM cyclopamine before fixing at 30 hours postamputation (hpa). Two representative samples are shown per gene per experimental treatment. Arrowheads demarcate regions of reduced gene expression following exposure to cyclopamine. n = 10 per experimental treatment per gene.

Axin2 (Figure 3-8B, blue arrowheads) was downregulated more so than *pea3* in cyclopamine treated tails (Figure 3-8B, red arrowheads); both genes were unchanged after exposure to vehicle alone. Ligand expression was also variably altered: *fgf10a* was almost completely lost after the short treatment with cyclopamine (Figure 3-8B, black arrowheads), whereas the intensity of *wnt10a* expression was greatly reduced (Figure 3-8B, green arrowheads). *Ptc1* was used as a positive control, and was undetectable after pulse treatment with the Hedgehog inhibitor. It was interesting to observe that the *ihhb* transcript was still present. Short-term vehicle exposure did not significantly alter the gene expression in regenerating larval tails.

3.2.4.2. The Wnt pathway modulates wound epidermis and blastema formation, and also regulates FGF signal activity.

The Wnt pathway was augmented using a GSK3-inhibitor. Through its inhibition of its target, GSK3, there is a reduction in β-catenin phosphorylation and degradation, causing an increase in nuclear localisation of β-catenin which activates downstream transcription. The GSK3-inhibitor was applied at 10 μM to larval tails for 6 hours before fixing at 30 hpa.

After short-term activation of the Wnt signalling pathway there was a dramatic difference in the expression of *dlx5a* within the wound epidermis (Figure 3-9B, red arrowheads). There was still the presence of the regular, distal-most stain, however there was a spreading towards proximal regions. The *raldh2* expression profile changed from having two individual domains to an almost continuous one, breaching the midline, which was also complemented with an increase in intensity, after Wnt pathway induction in regenerates (Figure 3-9B, green arrowheads).

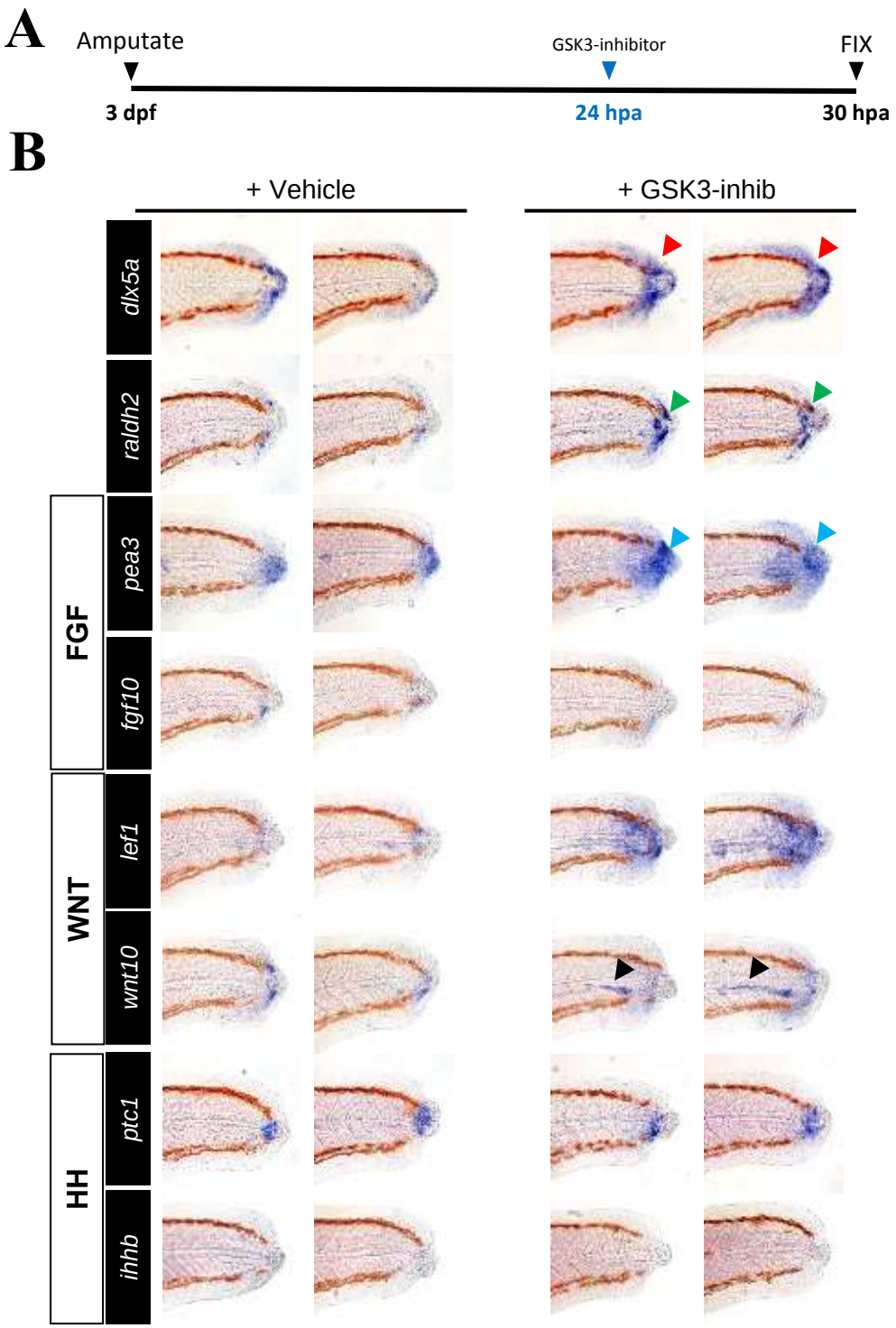

Figure 3-9. The Wnt pathway modulates regenerate structures, and can interact with the FGF pathway.

(A) A diagram to show the timecourse of 10 uM GSK-3-inhibitor exposure to caudal fin regenerates during a pulse treatment. (B) *In situ* hybridization of caudal fin regenerate structures (*dlx5a* and *raldh2*) and development pathway activity (Fgf: *pea3, fgf10*; Wnt: *axin2, wnt10*; Hedgehog: *ptc1, ihhb*) after 6 hours exposure to 10 uM GSK-3-inhibitor before fixing at 30 hours postamputation (hpa). Two representative samples are shown per gene per experimental treatment. Arrowheads demarcate altered gene expression following exposure to the GSK3-inhibitor. n = 10 per experimental treatment.

Furthermore, after GSK3-inhibitor treatment there were changes in the expression levels of the FGF read-out, *pea3* (Figure 3-9B, blue arrowheads). There was a significant expansion in the *pea3* domain of 30 hpa tails following the brief activation of the Wnt pathway. Interestingly, *wnt10a* exhibited ectopic expression around the midline of regenerating larval tails after exposure to GSK3-inhibitor (Figure 3-9B, black arrowheads), however, there was no detectable change in intensity. This change was not seen when only vehicle was added to fish water. Finally, short-term activation of the Wnt pathway had no effect on the expression of *ptc1*. *Lef1* served as a positive control to indicate faithful upregulation of the Wnt pathway after chemical inhibition of GSK3. Vehicle alone did not alter the expression of *lef1*.

3.2.4.3. *Inhibition of the FGF pathway during larval tail regeneration reduces Wnt activity.*

To inhibit the FGF pathway in larval zebrafish I treated them for 4 hours with 10 µM of SU5402 - a broad spectrum FGFR inhibitor - prior to fixing at 30 hpa. There were no appreciable changes to wound epidermis or blastema formation: SU5402 treated fish had the same *dlx5a* and *raldh2* expression patterns as vehicle controls (Figure 3-10B).

Analysis of gene expression after downregulation of the FGF pathway highlighted only one change: *Axin2* staining became very weak, even after inhibition of the FGF pathway for a short period of time (Figure 3-10B, black arrowheads). Regenerating tails exposed to vehicle alone showed no changes in *axin2* expression. The expression levels and location of the read-out for the Hedgehog pathway, *ptc1*, during tail regeneration did not show any differences after exposing them to SU5402, or vehicle alone. Interestingly, no changes in *fgf10a* expression were seen after short term exposure to SU5402.

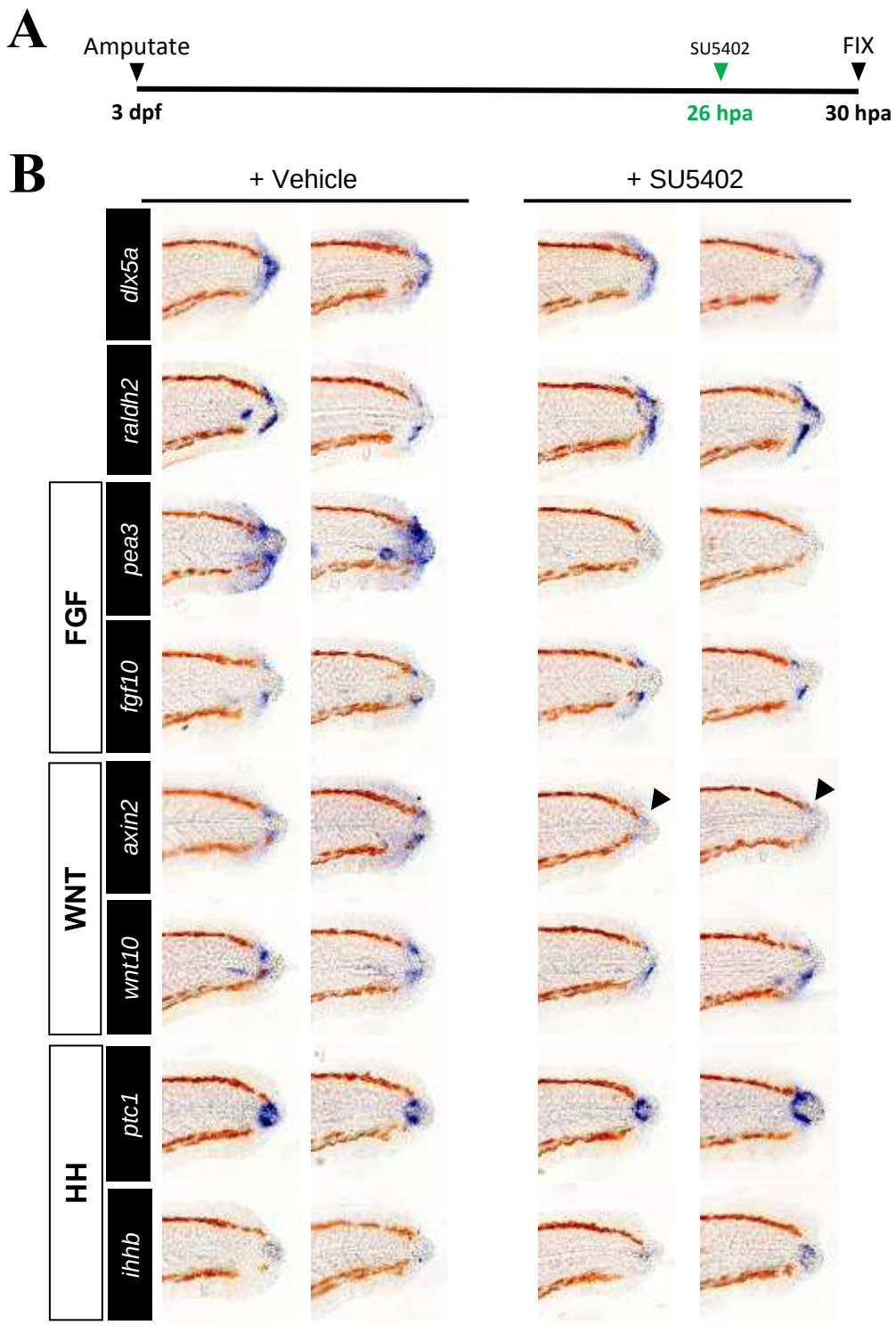

Figure 3-10. The Fgf pathway can modulate the Wnt pathway during caudal fin regeneration. (A) A diagram to show the timecourse of 10 uM SU5402 exposure to caudal fin regenerates during a pulse treatment. (B) *In situ* hybridization of regenerate structures (*dlx5a* and *raldh2*) and development pathway activity (Fgf: *pea3, fgf10*; Wnt: *axin2, wnt10*; Hedgehog: *ptc1, ihhb*) after 4 hours exposure to 10 uM SU5402 before fixing at 30 hours postamputation (hpa). Two representative samples are shown per gene per experimental treatment. The black arrowheads demarcate reduced *axin2* expression following exposure to SU5402. n = 10 per experimental treatment per gene.

3.3. Discussion

Amputation of the larval zebrafish tail induces a complex mechanism, involving a plethora of molecular prompts in order to replace the lost tissue, known as epimorphic regeneration. At a molecular level this chapter highlighted many similarities, and some differences, between epimorphic regeneration of larval and adult zebrafish, but also other species able to regenerate, such as *xenopus laevis* and the urodele amphibians. I showed that the wound epidermis (WE) and blastema could be demarcated, at specific time points after amputation, using *in situ* hybridisation to stain for their previously identified gene markers (*dlx5a* and *raldh2 – aldh1a2*). Also, the presumptive blastema contained the read-out transcripts – *pea3, axin2/lef1*, and *ptc1* – for the crucial signalling cues during development - Hedgehog, Fibroblast growth factor, and Wnt. This highlights the importance for the upregulation of these pathways during epimorphic regeneration of larval zebrafish tails. Furthermore, using pharmacological studies to target these pathways, I provided evidence for interactions between them.

It is difficult to make direct comparisons between larval tail regrowth and that of complete limb regeneration, as the tissues involved differ greatly. However, to identify genetic similarities and differences during the regeneration of various organs and/or appendages could help us to understand the roles of various molecular cues. And highlighting any genetically conserved functionality across species could help uncover essential regulators of epimorphic regeneration, independent of context, i.e. limb or fin regeneration.

A common molecular marker for the WE is *dlx5a*, which has been identified in the basal layer of the wound epidermis during larval fin fold and adult zebrafish caudal fin regeneration (Yoshinari *et al.*, 2009). Dlx5a is a homeodomain transcription factor, expressed during paired – pectoral – and unpaired – median fin fold – fin development (Heude *et al.*, 2014). I was unable to detect *dlx5a* in the median fin fold of 4-day post fertilisation (dpf) tails, but was able

to visualise a distal structure in the larval tails at 30 hpa. At 18 and 24 hpa *dlx5a* was seen in dorsal and ventral aspects of the regenerating tail, eventually meeting at 30 hpa. This suggests, much like the early stages of adult regeneration, the WE forms by lateral migration of epithelial cells in larval tails after amputation. However, further studies, using a more accurate method of cell tracking in larval tails undergoing regeneration would be required to confirm this hypothesis.

The blastema, another crucial landmark during the early stages of the regeneration landscape, is thought to house cells that have dedifferentiated to become more plastic for their role in contributing to new tissue formation. A strong marker for this structure, in both adult and larval caudal fins, is the retinoic acid (RA) synthesising enzyme retinaldehyde dehydrogenase, *raldh2/aldh1a2* (Mathew *et al.*, 2009). In the same study, Mathew *et al.* (2009), through *in situ* hybridisation, saw *raldh2* expression as early as 4 and 72 hpa in larval and adult regeneration, respectively. The present study first identifies upregulation of the same gene at 24 hpa (Figure 3-2). However, Mathew *et al.* (2009), carried out experiments on the median fin folds of larval zebrafish; this study focuses on surgical removal of tails within the pigment gap, proximal to the fin fold, which includes developing muscle, spinal cord, and notochord. The time taken for the wound to close and a WE to form – preceding blastema formation – could be one reason for the disparity between initial *raldh2* expressions. RA has been identified as an important signal during limb development, but also for the analogous fish structure, the pectoral fins (Gibert *et al.*, 2006). Interestingly, RA signalling has not been identified in the tail bud during the early stages of zebrafish caudal fin development (Figure 3-11 – red arrowhead). Therefore, it seems *raldh2* expression, followed by RA synthesis, is unique to larval tail regeneration. However, this does not seem to be the case during axolotl limb regeneration. Using a transgenic axolotl with a retinoic acid response element (RARE) fused with EGFP (RARE-EGFP), Monaghan. J and Maden (2012), were able to visualise cells

receiving RA signals. After amputation of transgenic limbs, they saw expression of EGFP in the wound epidermis. The same group also identified *raldh2* in the mesenchyme of developing limbs, with EGFP expressed in the ectoderm. This could mean that RA signals from mesenchymal cells to the distal wound epidermis during regeneration. Similar studies using zebrafish are lacking, therefore it would be of great interest to see if the same mesenchyme-to-ectoderm RA signal also applies.

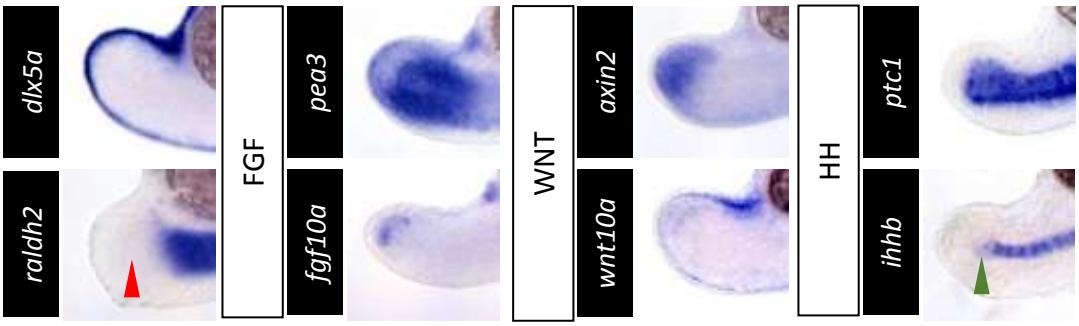

Figure 3-11. Gene expression during zebrafish tail bud development.
In situ hybridisation, of 18 hours postfertilization (hpf) embryos, to detect gene expression during the crucial stages of tail bud development. Red and green arrowheads highlight interesting expression patterns of *raldh2* and *ihhb*, respectively.

The involvement of various development factors, including, but not limited to, Hh, Wnt and FGF, have been well documented during epimorphic regeneration in various model organisms. Using *in situ* hybridisation to detect target gene expression of these aforementioned pathways I was able to identify the activity of all three in close proximity to where the blastema would eventually form (Figure 3-3). The earliest pathway to be activated in our regeneration model was Hedgehog, because *ptc1* RNA was expressed at 18 hpa – 6 hours before *axin2* and *pea3* – peripheral to the distal-most region of the notochord. This contradicts much of the adult zebrafish literature studying the early activation of signal pathways during caudal fin regenerationMany experiments have identified the Wnt/β-catenin pathway as the major upstream regulator during regeneration. *Lef1*, a gene induced by canonical Wnt activation, was seen at 12 hpa, and was still present at 96 hpa in the basal layer of the wound epidermis of adult

caudal fins (Poss *et al.*, 2000b). Furthermore, Wehner *et al*. (2014) identified, using the transgenic zebrafish reporter lines TCF-dGFP and TCF:mCherry, a discrete domain of cells within the presumptive blastema were receptive to Wnt signalling. The same group provided evidence that suggested Wnt/β-catenin was able to control the re-activation of genes known to be involved during early development. On the other hand, within the wound epidermis, Lee *et al*. (2009) identified FGF signalling as an upstream modulator of not only the Wnt pathway, but also a regulator of *shh* expression within newly forming scleroblasts. However, the same group did not induce the canonical Wnt/β-catenin pathway to determine if Wnt signalling could induce the FGF pathway. In the present study, pharmacological upregulation of the Wnt pathway, using the GSK-3-inhibitor, during larval zebrafish regeneration, suggested there was a direct interaction between the Wnt and FGF pathways. Addition of 10 µM GSK3-inhibitor to fish water for 6 hours caused an increase in the expression of *pea3*. As such a short pulse of activation could alter levels of a gene normally expressed through the activation of the FGF pathway, I could postulate that, in this context, the Wnt pathway could directly modulate FGF pathway activity. Furthermore, genes involved during WE and blastema formation, *dlx5a* and *raldh2*, respectively, were altered after activation of the Wnt pathway (Figure 3-8). These findings are supported by an experiment carried out by Stoick-Cooper *et al*. (2006) using the heat-shock inducible Wnt inhibitor, Dkk-1. After down regulation of the Wnt pathway, *msxb* – another genetic marker for the blastema – expression was downregulated, and also a reduction in the expression of the FGF read-out gene and ligand, *sprouty4* and *fgf20a*, respectively. This suggests that there could be a direct role for the Wnt pathway in maintaining crucial features during epimorphic regeneration of zebrafish larval tails.

In this study, Wnt-dependent regulation of the WE and blastema genes did not seem to be due to its ability to regulate the FGF pathway, because there were no changes in *dlx5a* and *raldh2* gene expression after larval tails were exposed for 4 hours to 10 µM SU5402.

Interestingly, after the same treatment, 30 hpa tails exhibited a reduction in *axin2* expression (Figure 3-9); a gene usually expressed after Wnt activation. This suggests a feed-back-loop could exist between the FGF and Wnt pathways during this relatively late stage of regeneration in the larval tail. This is in line with the results of an epistasis experiment carried out during tadpole tail regeneration (Lin *et al*., 2008). FGF signalling was shown to be downstream of the Wnt pathway, and also the transcripts for the Wnt ligands, *wnt3a* and *wnt5a,* were downregulated after SU5402 treatment. As their model also shares many key features - a developing notochord, spinal cord and muscles - with larval zebrafish tails, suggests a Wnt-FGF feedback loop could be conserved during epimorphic regeneration in animals still in their early stages of development.

These results provide evidence for the initiation of a feedback loop between the Wnt and FGF pathways during larval tail regeneration, in both fish and the *Xenopus.* And the Wnt pathway is involved during the formation and/or maintenance of the WE and blastema. In support of a conserved role for Wnt signalling during larval animal regeneration, Yokoyama *et al*. (2011) showed that early-stage tadpoles relied on the upregulation of the Wnt pathway more so than the more mature froglings – hinting at the presence of trophic factors released by axons damaged after amputation. Downregulation of FGF signalling did not alter the gene expression of the WE or blastemal markers, but could modulate the Wnt read-out, *axin2*. However, the proposed role for the FGF pathway during adult caudal fin regeneration is as a regulator of position-dependent growth rate: a proximal amputation plane induces a higher proliferative index than a more distal one (Lee *et al.,* 2005).

Through *in situ* hybridisation to detect *ptc1* gene transcript expression, and using a pharmacological approach to identify changes in gene expression after short- and long-term downregulation of the Hedgehog pathway, I was able to determine the Hedgehog pathway to be the earliest - of the three pathways analysed - regulator of epimorphic regeneration in the

larval tail model. After *in situ* hybridisation of larval tails following their amputation I was able to detect an increase in *ptc1* expression at 18 hpa – earlier than the FGF and Wnt read-out genes – and an up regulation of *ihhb* at 12 hpa - earlier than the FGF and Wnt ligands (Figure 3-3). Further probing for Hedgehog ligands that could be responsible for this early *ptc1* upregulation identified *shha* and *ihhb* at 3 hpa within, what I presume to be, the notochord (Figure 3-4B). Using the *Xenopus* as a model, and *in situ* hybridisation, Taniguchi *et al*. (2014) detected *shh* RNA within the notochord and *ptc1* in the spinal cord, suggesting the Hedgehog ligand signalled from the notochord to the spinal cord during regeneration. In our model the pattern of *ptc1* expression indicates the only cells receptive to Hedgehog signals are presumptive mesenchymal cells. More evidence for expression of *shh* and *ihh* ligands during regeneration comes in the form of qPCR detection within 21-days post amputation newt limbs (Singh *et al.*, 2012). The same group used an activator-inhibitor approach to identify any interactions between Hh and Wnt signalling. After inhibition of the Hh pathway and activation of the Wnt pathway limb regeneration was able to proceed as normal. This supported the results of this study; positioning Hedgehog upstream of the Wnt pathway. After downregulation of Hedgehog signalling, using 50 µM cyclopamine for 8 hours, 30 hpa tails exhibited reduced expression of *fgf10a, wnt10a, axin2* and *pea3* (Figure 3-7). This suggested that Hedgehog signalling could directly influence the activity of both the Wnt and FGF pathways. It would be interesting to identify if the *shha* and *ihhb* ligands have differing roles during regeneration. However, I was unable to breed *shha/syu* mutant zebrafish from the University of Sheffield facility, and in the case of Ihhb, I was unable to source a stable mutant line from the Sanger Institute. In the end, time did not permit me to establish these zebrafish mutants for analysis.

The requirement for Hedgehog signalling early during larval zebrafish epimorphic regeneration was further highlighted when tails were unable to regenerate after exposure to cyclopamine for 3 days, immediately after amputation. (Figure 3-4A). Furthermore, tails

treated, immediately after amputation, with 50 µM cyclopamine, followed by *in situ* hybridisation, exhibited a downregulation of genes normally expressed at the same time point – 30 hpa - in untreated tails (Figure 3-5 and 3-6). One reason for this lack of regeneration could be due to a reduction in proliferation within the blastema (Taniguchi *et al*., 2014). Further chemical treatments and staining of proliferating cells would be needed in order to determine whether Hh, or the FGF and/or Wnt pathways could modulate proliferation during regeneration. Schnapp *et al*. (2005) carried out experiments that provide evidence for the role of Hedgehog signalling in dorsoventral patterning during regeneration of the axolotl tail. They reported a reduction in Pax7-positive cells within cyclopamine treated tails, suggesting Hh signals could regulate differentiation – at least for muscle cells – during regeneration. However, as the experiments continuously administered cyclopamine to regenerating tails the effects were most likely due to indirect inhibition, or upregulation, of down-stream effectors of the Hedgehog pathway, i.e. Hh acted via the FGF and/or Wnt pathway to modulate muscle differentiation during regeneration.

Finally, the expression patterns of *ihhb* and *ptc1*, during zebrafish tail bud development, differ slightly to those seen during larval tail regeneration. *Ptc1* is expressed from within the tail bud towards the head of the zebrafish (Figure 3-11), however in regenerating tails I saw a very defined population – adjacent to the notochord - of cells expressing *ptc1*. In the case of *ihhb*: it is expressed strong within the notochord up to a certain point, after which it is very faint at the caudal tip (Figure 3-11 – green arrowhead). These comparisons of gene expression, between early-development and regenerating zebrafish tails, provides evidence for their upregulation being triggered for the purpose of regeneration and not simply relying on the persistence of the same coordinated expression of developmental signalling pathway genes.

3.4. Conclusion

It is clear from these results that developmental pathways, such as Hh, Wnt and FGF, are all re-expressed during larval tail regeneration. Through pharmacological techniques I have uncovered potential interactions between these pathways, but also identified the Wnt pathway's ability to modulate WE and blastema formation (Figure 3-11).

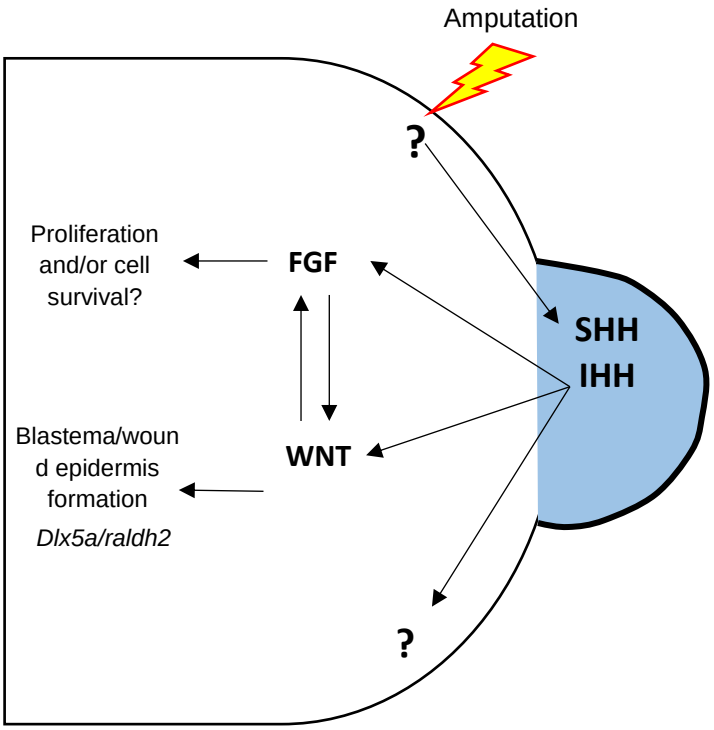

Figure 3-11. A model for the cell signalling events controlling larval tail regeneration.
Through chemical exposure and *in situ* hybridisation, experiments thus far highlight an early expression of Hedgehog ligand genes (*shha* and *ihhb*) within the distal region - presumed to be the notochord (blue area) – of tail regenerates. Hedgehog signalling is able to regulate expression levels of some Wnt and FGF genes, but also the Wnt and FGF pathways seemed to regulate one another. Wnt activation can also increase genes associated with the maturation of the crucial wound epidermis and blastema structures (*dlx5a* and *raldh2*).

Through an unknown mechanism the Hedgehog ligands, *shha* and *ihhb*, are expressed within a defined domain that appears to include the distal notochord, which becomes exposed to the external environment after amputation. Next, the Hedgehog pathway is activated in cells in a proximolateral domain in the presumptive mesenchymal cells, which in turn can induce Wnt and FGF pathways, which then appears to establish a feedback loop. Furthermore, I was able to provide evidence for Wnt signalling having a direct role during the maturation of the WE, because the Wnt read-out, *axin2*, was expressed after the WE marker, *dlx5a*. Therefore, the Wnt pathway might not have such an early role during WE formation. However, the Wnt

pathway could be involved in the induction of the blastema, because *axin2* had an overlapping temporospatial expression profile with *raldh2*, and upregulating the Wnt pathway increased *raldh2* staining. Further experiments to determine a potential role for the FGF pathway during regeneration are required. The present study has uncovered an early requirement for Hedgehog signalling during epimorphic regeneration, and the presence of pathway interactions; however, future epistasis experiments would help to decipher the true hierarchy of the FGF and Wnt pathways.

4 The Glycosaminoglycan, Heparan Sulphate, is important for Zebrafish larval tail regeneration.

4.1 Introduction

Thanks to the use of various animal models, from the hydra to amphibians, our knowledge regarding molecular cues, and their roles played during epimorphic regeneration is expanding all the time. In Chapter 3 I was able to identify genes upregulated during larval tail regeneration, including the detection of several ligands. However, our understanding of the roles played by extracellular components during this process is lacking. During a small screen to identify zebrafish with a non-regenerative phenotype, it was the *dackel/ext2* mutant which exhibited the strongest loss in regenerative ability (Figure 4-1). As we now know, the *dackel/ext2* mutant lacks a crucial glycosyltransferase required during the polymerisation step of HS chain synthesis. There are four recognised *dackel* alleles: *to273b, tw25e, tf205,* and *to79c* (Van Eeden *et al.,* 1996). This present study used the *to273b* and *tw25e dackel* mutants and, due to both mutations resulting in the translation of truncated Ext2 proteins, from here on I will not specify which mutant has been used in each experiment.

Previous experiments, analysing the effects of disrupting HS synthesis has on signalling pathways during development, have provided strong evidence that these glycosaminoglycan (GAG) chains can interact with and regulate the distribution of many proteins, but could also affect their binding to specific receptors. Very few studies have been published regarding signal pathway disruption in the context of zebrafish development. One experiment used the *dackel* zebrafish, and found that FGF10 signalling required the synthesis of HS chains, through Ext2 and Extl3 activity, for the development of their pectoral fins. However, after ten days *dackel* mutants die; mainly due to their inability to feed independently of a yolk sac and the lack of an inflated swim bladder - restricting us to the larval zebrafish as a model.

It was highlighted earlier (Chapter 1 – Section 1.1.) that the wound epidermis is an integral structure for the progress of epimorphic regeneration to the next stage – blastema formation. The early stages of this require the proximal-to-distal migration of epithelial cells from non-wounded regions, which eventually thickens to form the wound epidermis. Therefore, as the *dackel* larval tail showed no sign of a regenerative response after surgical removal, it is possible that HS chains provide the molecular cues and/or extracellular attachment sites for epithelial migration. If the WE is able to develop then the inability to mount a regenerative response could be due to a lack of cell communication in the absence of cell-surface, or extracellular, HS chains.

This chapter aims to use the *dackel* mutant to identify possible reasons behind its inability to regenerate following tail resection. The first part focuses primarily on validating the presence of a wound epidermis and blastema during *dackel* tail regeneration, and also the detection of genes identified during wild-type regeneration, using *in situ* hybridisation. The second section uses the *dak;ubi-kaede*^{sh373} transgenic line to identify any irregular migration during epimorphic regeneration in the *dackel*.

4.2. Results

4.2.1. The *dackel/ext2* mutants fail to regenerate their tails.

I first had to provide evidence that the *dackel/ext2* phenotype was due to the requirement of the gene during regeneration and not because of an underlying developmental defect of the larval tail. To this end, the development of 21-somite embryos and, after being allowed to develop further, the same zebrafish, at 5-days post fertilisation (dpf) caudal fins were documented. *Dackel* mutants, as expected, accounted for 6 of the 20 embryos analysed.

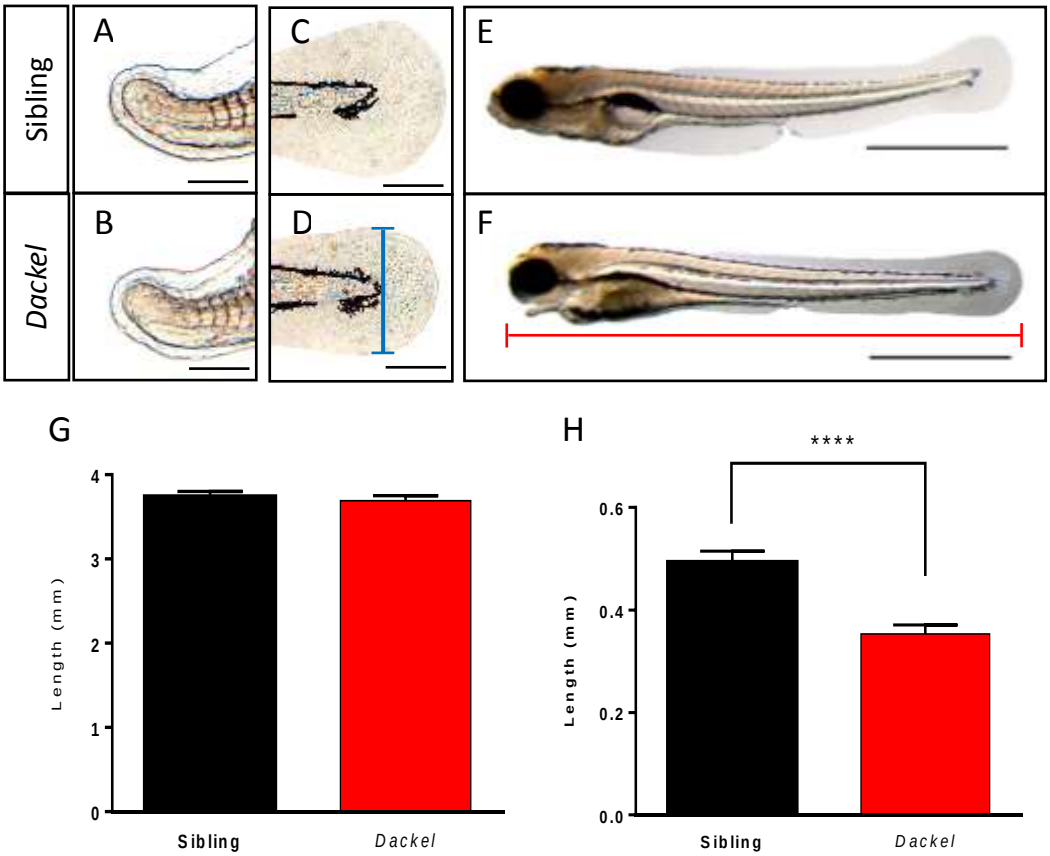

Figure 4-1. The *dackel/ext2* mutant develops a smaller caudal fin compared to its sibling.
The caudal fin of 21-somite (A) sibling and (B) *dackel/ext2* zebrafish. (C) Lateral view of 5-days postfertilisation (C) sibling and (D) *dackel* mutant caudal fin: 10 X objective. (A-D) Scale Bars represent 0.25 mm. Wholemount lateral view of 5 dpf (E) sibling and (F) *dackel* zebrafish: 1.6 X objective. Scale bars represent 1 mm. (G) A graph comparing the average body length of the sibling (n = 14) and *dackel* (n = 6) zebrafish, measurements taken as shown in F (red line). (H) A graph comparing the width of the sibling (n = 14) and *dackel* (n = 6) zebrafish caudal fin; measurements taken perpendicular to the caudal-most point of the pigment cells (D, blue line). (G, H) Data presented as mean ± SEM. H: statistical analysis carried out using Student's t-test, ****$p < 0.0001$.

Of all mutant tail buds visualised at the 21-somite stage (6/6), there were no noticeable defects when compared to their siblings (Figure 4-1). There were, however, noticeable differences in caudal fin fold size between sibling and mutants at 5 dpf (Figure 4-1C, D). *Dackel* caudal fins had significantly narrower caudal fins. These results were further highlighted when capturing images of the whole zebrafish (Figure 4-1E, F). Homozygous mutant *dackels* had smaller features – most notably the head - and a narrower fin fold, which was most evident around the anus, at 5 dpf.

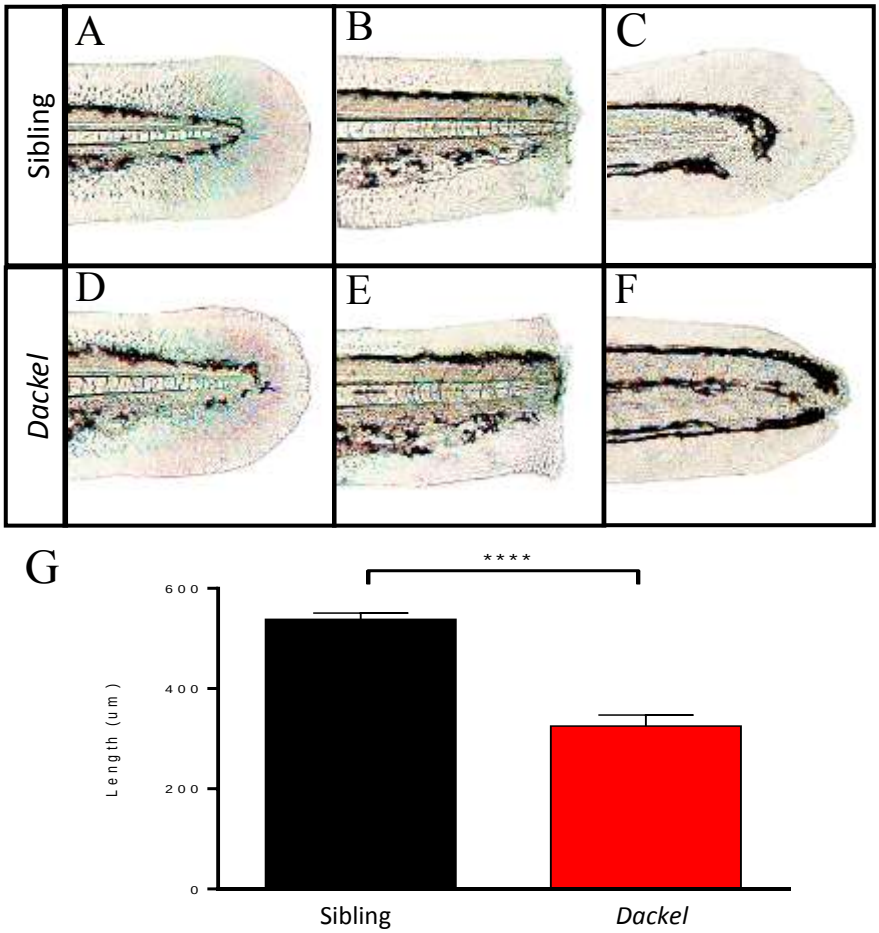

Figure 4-2. The *ext2* mutant, *dackel*, fails to regenerate after tail amputation. Amputation of (A-C) sibling and (D-F) *dackel/ext2* caudal fins. 2 days postfertilization (dpf) (A) Sibling and (D) *dackel* caudal fins. Sibling (B) and *dackel* (E) zebrafish tails immediately after amputation. (C) Sibling and (F) dackel caudal fins 3 days postamputation. (G) A graph to show regenerate length 3 days of amputation (n = 20); data shown as mean ± SEM; statistical analysis carried out using the Student's t-test, ****$p < 0.0001$.

After 2-day old sibling and *dackel* embryos were amputated in the pigment gap, fish recovered for three days, and regeneration length measured. For the purpose of this experiment a proximal point, relatively stationary over the three days, had to be chosen to measure to the posterior most tip of the tail. The structure appointed was the anus; dubbed the anus-caudal axis (Figure 4-1F, red bar). It was evident, at 3-days postamputation (dpa), that the *dackel* was unable to regenerate, and formed a stump at the original amputation plane (Figure 4-2). Sibling larvae were able to regenerate the majority of their lost tissue. Regeneration length was then quantified using the anus-caudal axis of 3 dpa sibling and mutants (Figure 4-2G). There was a significant difference ($p < 0.0001$) between the average length of regeneration in sibling (538 µm) and *dackel* (325 µm) larvae.

4.2.2. Heparan sulphate is required for proper wound epidermis and blastema formation.

To fully understand at which point the *dackel* mutant stops regenerating I started by detecting the most important structures formed during normal epimorphic regeneration: the wound epidermis and blastema. Carrying out *in situ* hybridisation to identify the key gene markers, *dlx5a* and *raldh2*, and also immunohistochemistry to label epithelial cells through the application of a monoclonal antibody to stain p63-expressing cells, I was able to detect defects in the formation of both.

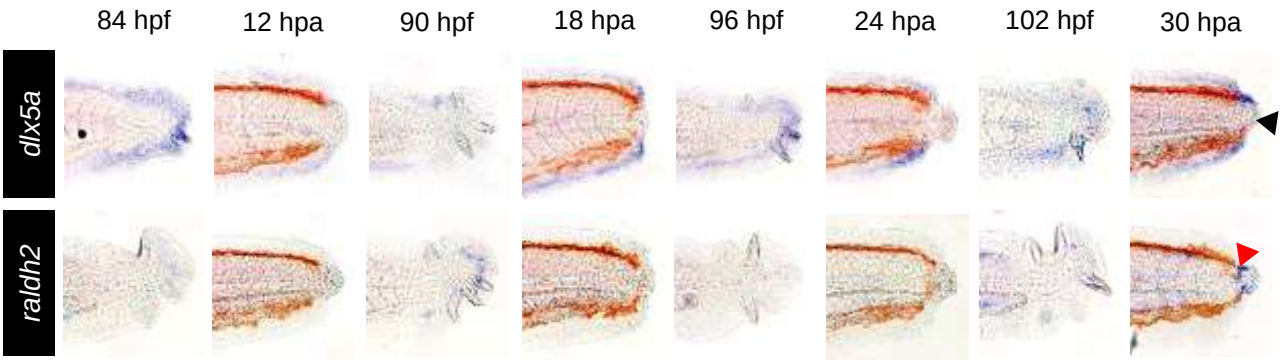

Figure 4-3. *Dackel* mutants heal, but fail to form complete regenerate structures.
In situ hybridization of *dlx5a* and *raldh2* to show key regenerate structures in *dackel* mutants after caudal fin amputation between 12 and 30 hours postamputation (hpa). Uncut, same age, controls are shown to the left of their respective amputated tails. *Dlx5a* and *Raldh2* demarcate the wound epidermis and blastema, respectively. n = 10 per time point per gene.

3 dpf *dackel* tails were amputated and fixed between 12 and 30 hpa for *in situ* hybridisation of *dlx5a* and *raldh2* (Figure 4-3). The expression profiles of both transcripts during *dackel* regeneration differed to those seen during wild-type regeneration. Detection of the first wound epidermis cells was at 12 hpa, becoming progressively more intense towards 30 hpa. By this time the expression domain of *dlx5a* was incomplete compared to that seen in wild-types; the most distal region of the regenerate did not contain any *dlx5a*-expressing wound epidermis cells (Figure 4-3, black arrowhead). The earliest expression of *raldh2* was only seen after 30 hpa in *dackel* tails, and only included a small population of cells concentrated close to the distal-most point, but still proximal to the wound epidermis (Figure 4-3, red arrowhead). *Dlx5a* was shown to be expressed within a distal region of the *dackel* caudal fin fold in uncut control tails (9/10 across all time points), however the area of expression would have been removed within amputated *dackel* tails and so I judged that its upregulation was the direct consequence of tail resection. *Radlh2* only presented some expression in a few uncut (6/10) - 90 hpf – *dackel* caudal fin folds, and was absent in uncut controls across all remaining – 84, 96 and 102 hpf - time points.

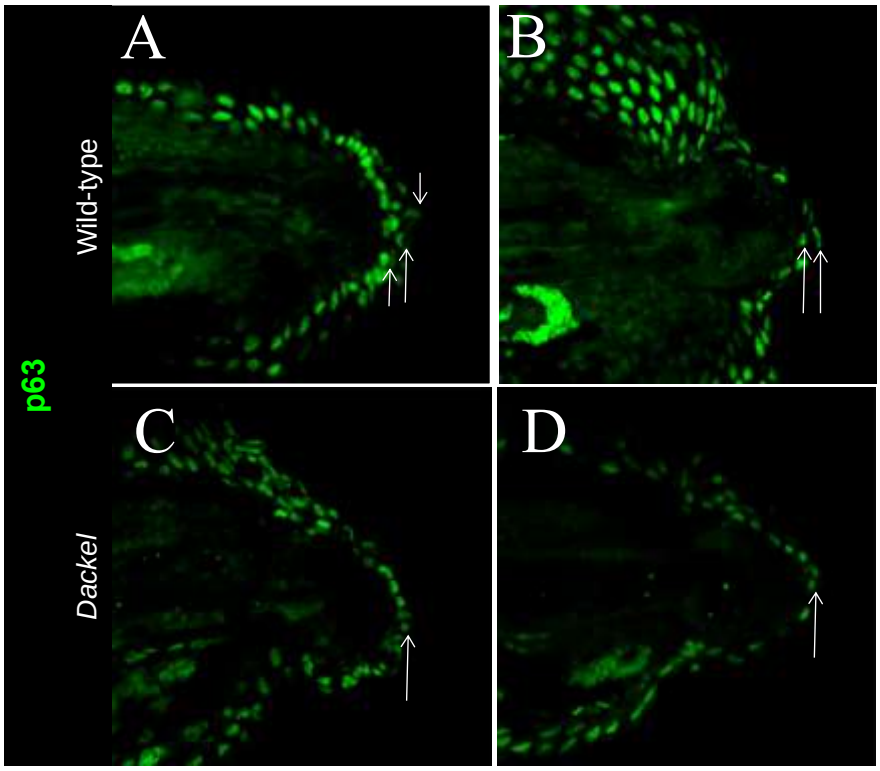

Figure 4-4. *Dackel* mutants heal, but fail to show signs of a mature wound epidermis.
(A-D) Fluorescent immunohistochemistry for P63 at 30 hpa (A, B) wild-type (n = 10) and (C, D) *dackel* (n = 10) caudal fins. Each white arrow indicates a separate layer of the wound epidermis. Each image represents the middle layer of a Z-stack, of different samples, using a 20 X objective.

Beyond the expression of *dlx5a* in the wound epidermis during regeneration, it is also possible to identify a thickening of the same structure using immunohistochemistry to detect p63-expressing cells. The p63 gene is homolog of the p53 transcription factor, and is required for limb development and stratification of the epidermis (Mills *et al.*, 1999). Imaging zebrafish using the p63 antibody in conjunction with confocal microscopy allowed for several layers to be built into a z-stack. Analysis of p63-positive cells during regeneration in the wild-type, and *dackel* mutants showed differences in thickness between their wound epidermis structures. Whereas the *dackel* mutant could heal, and form a monolayer of epidermal cells at 30 hpa (10/10), wild-type fish formed a stratified wound epidermis comprising at least two layers, up to a maximum of three (10/10) (Figure 4-4, white arrows).

4.2.3. Signal pathway activity is perturbed during *dackel* tail regeneration.

After highlighting a failure of the *dackel* to form a blastema or wound epidermis through the loss, or reduction, of their gene markers, and exhibiting a wound epidermis lacking layers using immunohistochemistry, the next step was to identify the consequences of reduced HS synthesis on signal pathway activity during epimorphic regeneration.

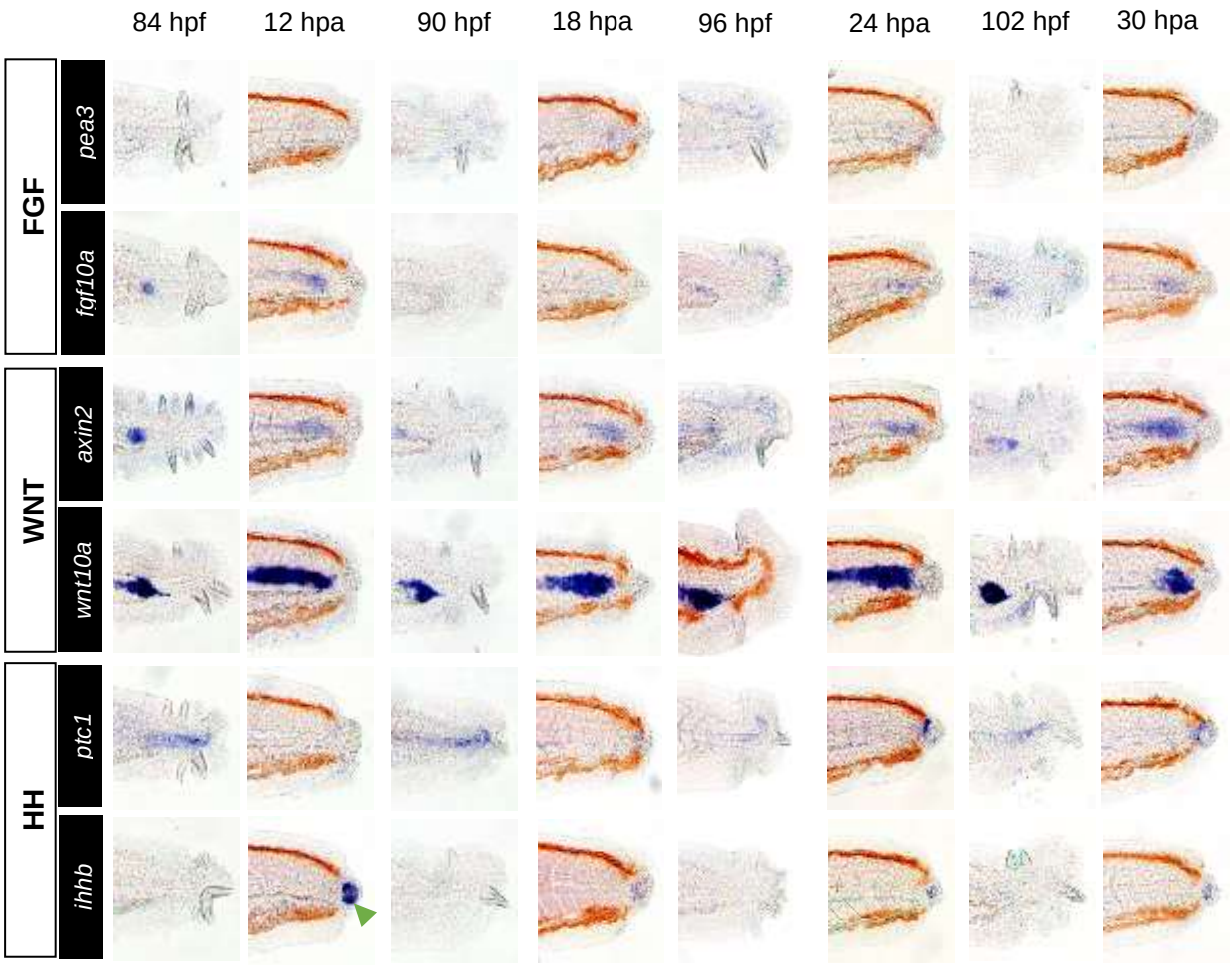

Figure 4-5. Activity of developmental pathways, FGF, Wnt and Hedgehog, are abrogated during *dackel/ext2* mutant regeneration.
In situ hybridization for the expression of FGF, Wnt and Hh gene pathway markers during epimorphic regeneration of *dackel* mutant tails. The following probes were used for each of the pathways: Fgf - *pea3, fgf10a*; Hedgehog -*ptc1, ihhb*; Wnt - *axin2, wnt10a*. Uncut, same age, controls are shown to the left of their respective amputated tails. n = 10 per gene per time point.

In situ hybridisation, to detect transcripts shown to be upregulated during wild-type regeneration, was carried out to identify any changes in gene expression during *dackel* epimorphic regeneration (Figure 4-5). Between 12 and 30 hpa the expression of *pea3* or *axin2* was absent, however *axin2* exhibited ectopic expression in the midline, which was also present in the same region of uncut control tails. *Ptc1* was first evident at 24 hpa, and remained at 30 hpa, but stained a much smaller region compared to that of their wild-type counterparts. The transcripts of *fgf10a*, *wnt10a*, and *ihhb* were variably affected. *Fgf10a* was completely absent - except for some midline staining - in the region previously identified in wild-types. *Wnt10a* stained strongly within the same expression domain as *axin2*. Like *axin2*, *wnt10a* was also seen in a similar region in 4-day old uncut caudal fins. The induction of *ihhb* expression in *dackel* mutants was detectable at 12 hpa, and in the same region – a bead-like distal structure – as that identified during wild-type tail regeneration (Figure 4-5, green arrowhead).

As the expression profile of *ihhb*, during *dackel* regeneration, was identical to that of the wild-type, it was of interest to see if I could identify, by staining at earlier time points, any delays to the induction of Hedgehog ligands in *dackel* tails (Figure 4-6).

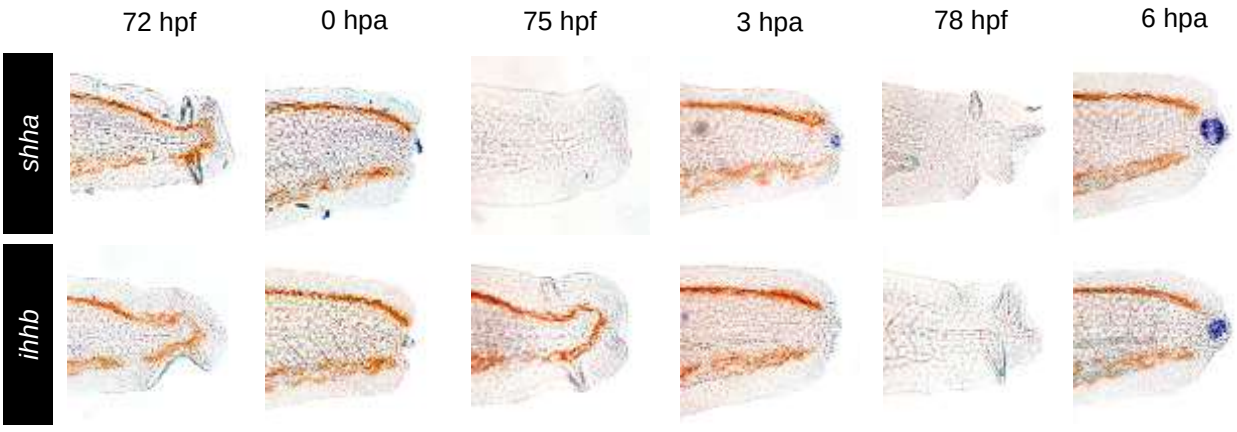

Figure 4-6. Hedgehog ligand genes are expressed early during *dackel* tail epimorphic regeneration. *In situ* hybridization of *shha* and *ihhb* immediately after caudal fin amputation (0 hpa), 3 and 6 hours postamputation (hpa) in *dackel* mutant zebrafish. Uncut, same age, control *in situ*s are shown to the left of their respective amputated tails. n = 10 per gene per time point.

Tails of 3 dpf *dackel* were amputated, fixed immediately after amputation, or at 3 and 6 hpa, then, using *in situ* hybridisation, stained for the presence of *shha* and *ihhb* transcripts. The *dackel* took longer to reach similar expression levels to those seen in wild-types. At 3 hpa *Shha* was weakly expressed, and *ihhb* undetectable – a time point when both were seen to be expressed strongly in wild-type regenerates. However, both Hedgehog ligands seemed to recover by 6 hpa. Also, the region that *shha* and *ihhb* were detected in the *dackel* mutant was identical to that seen during wild-type regeneration (Figure 3-4).

4.2.4. Cell migration during epimorphic regeneration does not require the presence of heparan sulphate.

In light of earlier evidence highlighting the absence of a multi-layered wound epidermis during *dackel* regeneration (Figure 4-4), I was curious to see whether this was due to inadequate migration of lateral epithelial cells. To help answer this question an *in vivo* system was created, whereby a population of cells could be selectively labelled to be a different colour to surrounding cells. This was made possible thanks to a special sub-set of fluorescent proteins: photoactivatable fluorescent proteins (PAFPs). Included in this family is the PAFP found naturally in coral, kaede; which is able to convert from green to red when exposed to ultraviolet light (Stark and Kulesa, 2007). Photo-conversion of the kaede protein was shown to be reliable and exhibited a slower rate of photobleaching compared to its closest rival in KikGR. To this end, I constructed an expression vector consisting of the ubiquitin promotor, kaede protein, and polyA tail for injection into one-cell stage embryos. The fish were raised and screened for highly uniform expression of the kaede protein in its GFP conformation. F1 generation wild-type and *dackel* fish with the *ubi-kaede*^{sh343} gene were used during this experiment.

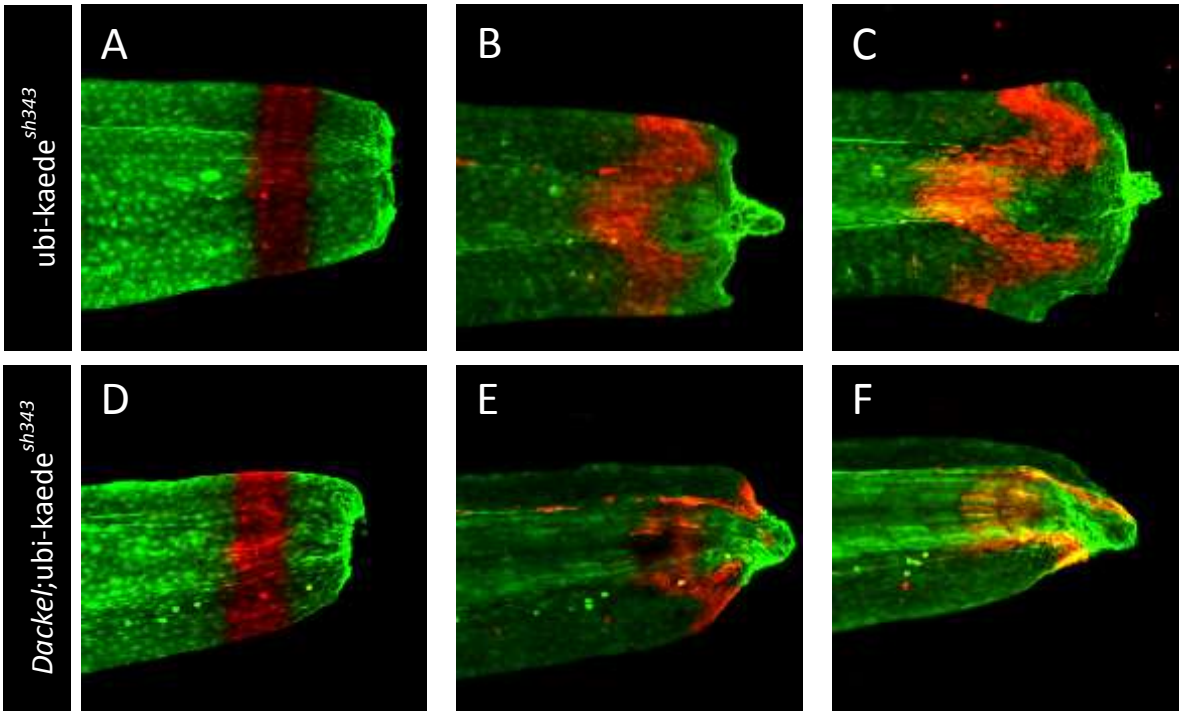

Figure 4-7. Heparan sulphate is not required for cell migration during tail regeneration.
(A-C) Wild-type ubi-kaede^{sh343} larval tails and (D-F) *dackel*;ubi-kaede^{sh343} larval tails. UV-conversion of a predetermined region (red) of (A) ubi-kaede^{sh343} and (D) *dackel;*ubi-kaede tails immediately after amputation. UV-converted ubi-kaede^{sh343} larval tails (B, E) 24 hours and (C, F) 48 hours post-conversion and amputation. A-C and D-F represent a single wild-type;ubi-kaede and *dackel*;ubi-kaede tail, respectively, tracked over two days. UV-converted cells are visible 2 days post-conversion in both wild-type and *dackel* strains, however there are differences in the morphology of migrating cells between tails after (B, E) 24 and (C, F) 48 hours postamputation.

After a strip of kaede-expressing cells was photo-converted, proximal to the amputation plane in both wild-type and *dackel* ubi-kaede^{sh343} strains, and their progress was tracked over 48 hours. It is clear that cells of both zebrafish strains were capable of migrating in response to tail amputation (Figure 4-7). At 24 hpa two populations of wild-type cells began to migrate in dorsal and ventral regions, adjacent to the midline (Figure 4-7B), and *dackel* mutant cells of the same region and further from the midline had approached the distal most region of the regenerating tail (Figure 4-7E). By 48 hpa, wild-type cells had continued moving as a group towards the wound epidermis, and were occupying a region similar to that of the blastema. In

dackel tails at 48 hpa the migrating cells had grouped in the distal-most region of the regenerate. In contrast, cells in the region of the midline showed negligible movement after 48 hours of regeneration in both wild-type;kaede^{sh343} and *dackel*;kaede^{sh343}. There are noticeable differences in general morphology between UV-converted migrating cells of wild-type and *dackel* kaede^{sh343} strains. Wild-type;kaede^{sh343} regenerating tails present a broadly spread group of cells that have yet to reach the distal tip of the regenerate, whereas those of the *dackel*;kaede^{sh343} are more narrow and already present at the distal-most point of the amputated tail.

4.3. Discussion

Epimorphic regeneration is a complex process involving cell migration, proliferation and re-differentiation, using various molecular cues, all of which have the potential to be modulated by extracellular macromolecules. One such candidate is the cell-surface/extracellular matrix heparan sulphate proteoglycan (HSPG), as it has been identified to be able to interact with the ligands of signalling pathways involved during the development of various anatomical structures. Transcripts for the same proteins were re-expressed during the regenerative process in our larval zebrafish model (Chapter 3). This chapter provided evidence for the requirement of HS chains during epimorphic regeneration, using the *dackel/ext2* zebrafish – lacking a functional glycosyltransferase, Ext2, required for HS polymerisation. Using *in situ* hybridisation to detect the upregulation of several genes, associated with Hh, FGF, and Wnt pathway activation, identified their disruption during *dackel* tail regeneration. Also, the expression of gene transcripts for the FGF and Wnt ligands identified in wild-type tail regenerates were completely absent after the disruption of HS synthesis in *dackel* mutants. Furthermore, the WE failed to thicken, however, cell migration occurred in line with what was seen during wild-type regeneration.

The wound epidermis (WE) and blastema are both important structures involved in the regenerative process - the latter containing cells that contribute towards new tissue growth. And the wound epidermis is vital for the progress of epimorphic regeneration beyond the wound healing phase. It has also been described as a diverse signalling centre for the maintenance of the blastema (Lee *et al.,* 2009). To analyse the maturity of the WE I utilised an antibody to detect a marker - p63 - of epithelial cells. At 30 hpa in wild-type zebrafish tails up to three separate layers of epithelial cells could be seen, but in the *dackel* it was still only one-cell thick – this was also backed up by the lack of *dlx5a* expression in the distal-most region of their regenerating tails (Figure 4-3). This could point towards a lack of migration in the initial stages of regeneration, however, the wound still heals, which requires the migration of epithelial cells. Also, our results gained from tracking cells of the *dak;ubi-kaede*^{sh343} line suggested migration was similar to that seen during wild-type regeneration (Figure 4-7). Perhaps, in larval zebrafish, the prerequisite of a functional WE is thickening of the structure through proliferation. As Hh signalling has been implicated in proliferation during regeneration (Schnapp *et al.,* 2005; Taniguchi *et al.,* 2014), and in regenerating *dackel* tails the same pathway is downregulated early (Figure 4-5 and 4-6), this suggests HS chains could be involved during WE thickening in a Hh-dependent manner. Analysis of proliferation was done, alongside the *daedalus/fgf10* mutant, in Chapter 5 (Figure 5-5). There was a significant reduction in proliferating cells within *dackel* tails during regeneration, however the distribution of H3P-positive cells in the *dackel* tail did not deviate from the normal distribution, which appeared to be proximal to the WE. Therefore, there could be other HS-dependent pathways responsible for WE maturation.

The transcripts for the Shha and Ihhb ligands within regenerating *dackel* tails exhibited normal spatial distribution, but were delayed in their expression. However, *ptc1* upregulation was reduced heavily in regions proximolateral to the Hedgehog ligand-expressing domain. This

suggested that HS might interact with these Hedgehog ligands to regulate interactions with their receptors. One possible mechanism for the HS chains in this context is that of ligand cleavage. Shh is modified by the addition of cholesterol and palmitate moieties at the C- and N-terminus of the protein, respectively, and is also cell-surface bound until it is cleaved by an evolutionarily conserved membrane-associated protein, dispatched (Nusse, 2003; Burke *et al.*, 1999). HSPGs have been linked with the ability to modulate a disintegrin and metalloprotease (ADAM) family member - ADAM17 – involved in the cleavage of newly synthesised SHH ligands (Dierker *et al.*, 2009). A second possible mechanism for HS-dependent Hh signalling is through the cleavage of a ligand-bound HSPG: for example, syndecan-1 can be cleaved by membrane type matrix metalloprotease 1 (MT1-MMP) in cell culture (Endo *et al.*, 2003). Furthermore, *mt1-mmp* upregulation has been seen in the basal wound epidermis, and blastema, of regenerating zebrafish caudal fins (Bai *et al.*, 2005). This data suggests that the syndecans of hedgehog-expressing cells of the regenerating tails could be cleaved to allow for ligands to migrate to cells receptive to the signal. In *dackel* mutants, perhaps the only cells able to induce *ptc1* expression are those close enough for Shha/Ihhb to be able to interact with their receptors, using any residual Ext-1 synthesised HS chains, or without requiring the assistance of GAG chains at all. The weak activation of the Hedgehog pathway seemed sub-optimal for the subsequent induction of potential down-stream FGF and Wnt pathway induction (Figure 4-5). Finally, the HS could be on the cell surface of receiving cells, allowing for a stable ligand-receptor interaction, i.e. the more established role for HSPGs during development. It is also possible that these aforementioned mechanisms could be working simultaneously or at various overlapping times during regeneration (Figure 4-8).

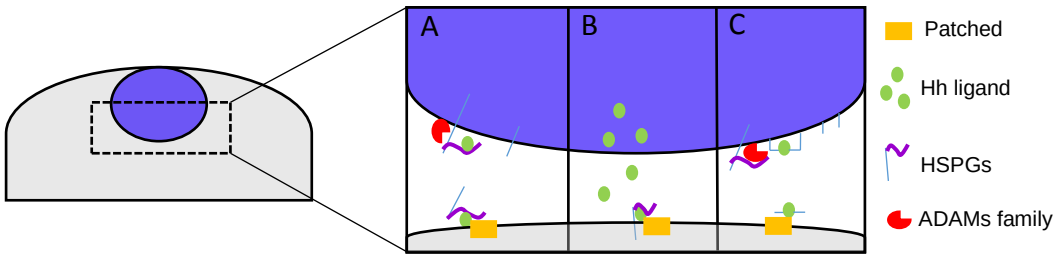

Figure 4-8. Possible models for the interactions of HS chains with the Hedgehog ligands during zebrafish larval tail regeneration.
(A) HS chains on the surface of Hh-synthesising cells could be cleaved through proteolysis of the HSPG core protein; releasing HS-bound Hedgehog ligands.
(B) HS chains of receiving cells could interact with Hedgehog ligands released from the source to allow for a more stable interaction with their receptor, patched.
(C) Hedgehog synthesised within the presumptive notochord could be released through HS-dependent activation of a disintegrin and metalloprotease (ADAM) family of proteins.

In the previous chapter (Chapter 3: 3.3. Discussion) I provided evidence for the Hedgehog pathway acting upstream of the Wnt and FGF pathways, and its ability to directly regulate the expression of their downstream target genes during larval zebrafish tail regeneration. This chapter provided results consistent with these previous findings: zebrafish tails lacking HS chains present a reduction in Hh pathway activity, and also lacked the FGF and Wnt read-outs, and their ligands, during epimorphic regeneration. However, the loss of Wnt and FGF genes is greater in the *dackel* than wild-type regenerating tails treated for 8 hours with cyclopamine. This could be a consequence of timing: persistent reduction in HS synthesis causes a more dramatic disruption compared with exposure to a chemical for a short time, or the Hh signal of regenerating *dackel* tails did not induce sufficient Wnt or FGF ligand expression and in the absence of HS chains any ligand produced was unable to interact properly with their respective receptors, further reducing the downstream gene expression of those pathways (Figure 4-9).

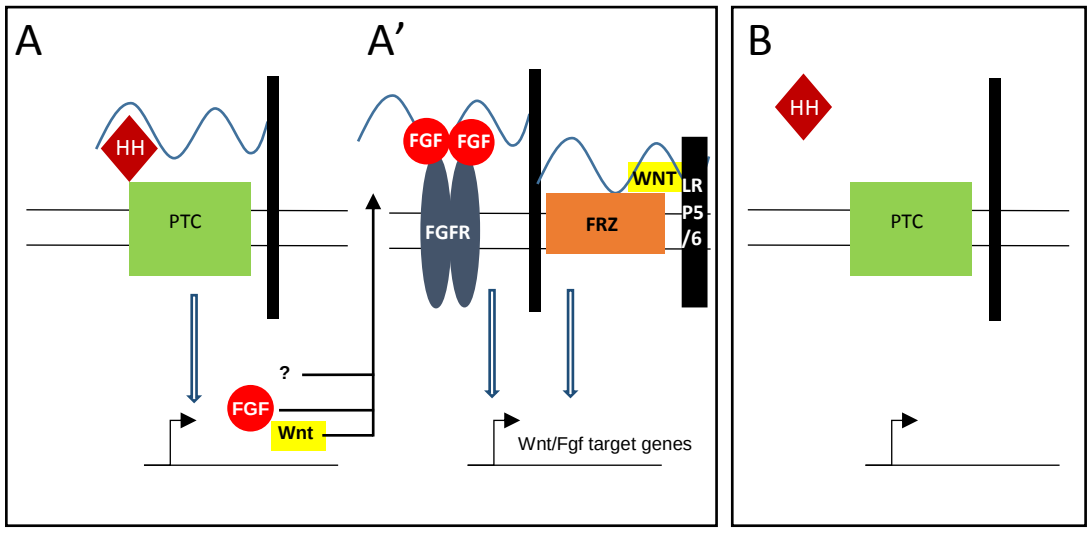

Figure 4-9. A lack of HS synthesis leads to changes in downstream signal effectors of the Hh pathway

(A) Hedgehog ligands are expressed during tail regeneration and, presumably, they interact with HS chains of receiving cells to induce gene expression, which then go on to signal via HSPG-dependent pathways (A').

(B) In the absence of HS synthesis the Hedgehog pathway is not activated and thus gene expression reduced, which prevents FGF and Wnt signalling in an auto- or paracrine manner.

Investigations into the role of HSPGs during regeneration are lacking. Further to this study, it would have been beneficial to construct a Cre:Lox zebrafish line to enable the conditional knock out the *ext2* gene during adult caudal fin regeneration. This would have given more insight into the role of HS chains in a more dynamic environment, uncovering more functions unidentifiable during larval tail regeneration, i.e. new bone formation. Furthermore, I could have used the same line to determine whether HS already present were required for regeneration, or if it was the responsibility of newly synthesised chains. As early Hedgehog ligand expression was unaffected during *dackel* regeneration, it would have been interesting to identify the HS-independent mechanisms responsible for their induction, and possibly uncover the earliest signal required to initiate epimorphic regeneration, one such candidate being reactive oxygen species (ROS). These are chemically reactive molecules containing oxygen, including oxygen ions and hydrogen peroxide. They are also by-products of biological

metabolism, and have been indicated to be crucial during some signalling events (González-Rubio *et al.,* 1996). Furthermore, these ROS have been identified almost immediately after amputation in the tails of *Xenopus* tadpoles and zebrafish, prior to the expression of *shha*/*ihhb* in zebrafish larval tails (Love *et al.*, 2013; Yoo *et al.*, 2012). It has also been shown, in the Roehl Lab, that inhibition of ROS synthesis, using a chemical inhibitor of dual oxidase (duox), early Hedgehog ligand transcripts of *ihhb* were downregulated (Unpublished data). Furthermore, preliminary data suggests *ihhb* does not require the transcription of new proteins (Roehl Lab, unpublished data), therefore ROS could be directly interacting with a protein already present within these Hedgehog-expressing cells – most likely a kinase that could be regulated by various ROS molecules.

4.4. Conclusion

Zebrafish transgenic lines are usually established to study the potential causes behind the manifestations of a disease. In this case, *dackel/ext2* mutants were utilised to understand the mechanisms causing tumours within patients suffering from hereditary multiple exostoses (HME), also known as multiple osteochondroma. However, in the present study, it was used to identify the roles played by HS during the complex process of epimorphic regeneration – as a previous screen identified this mutant to be unable to induce tail regeneration. Questions included whether signalling pathways were affected, and whether the early migration of cells had been disrupted.

Using this zebrafish lacking a functional gene crucial during HS chain synthesis, *ext2*, this chapter suggested HSPGs are a key regulator of signalling events during epimorphic regeneration. *In situ* hybridisation provided evidence for its role as a modulator of the developmental pathways re-expressed following tail amputation. However, the residual HS chains being synthesised by Ext1, or unaffected proteoglycans, such as chondroitin sulphate,

could have been sufficient to allow for the migration of cells, identified using the *ubi-kaede*^{sh343} stable transgenic line, during regeneration. On the other hand, it is more likely that cell migration does not rely heavily upon HS chains but the core proteins still present in *dackel/ext2* mutants, or other proteins unrelated to the GAG family.

This chapter highlighted the potential of zebrafish, not only as a model for its initially intended purpose, but as a tool for enhancing our knowledge of a process not fully understand: epimorphic regeneration. The *dackel* mutant has put a spotlight on avenues yet to be explored in the field of zebrafish regeneration, one such example being a study into the role of *fgf10* during epimorphic regeneration in larval tails.

5 FGF10 acts as a Mitogen during Epimorphic Regeneration.

5.1. Introduction

As previously highlighted in Chapter 1: FGF signalling has an important role during epimorphic regeneration. Thus, it was interesting when I was able to see a visible reduction in the expression of FGF pathway-associated gene markers, *fgf10a* and *pea3* (Figure 4-5), but also altered blastema and wound epidermis gene marker expression, using *in situ* hybridisation, in regenerating *dackel* tails (Figure 4-3). The abrogated FGF signalling in *dackel* prompted me to explore further the role of *fgf10* gene expression during larval zebrafish tail regeneration.

During development, *fgf10* expression is vital for proper mammalian limb and lung formation (Sekine *et al.*, 1999), and initiation of the chick limb bud depends on FGF10 signalling from mesoderm to ectoderm (Ohuchi *et al.,* 1997). The *daedalus/fgf10* and *dackel* mutants both lack their pectoral fins (Figure 5-1A), and it has also been shown that FGF10 signalling relies on HSPG synthesis by the zebrafish Ext2 and Extl3 glycosyltransferases (Norton *et al.,* 2005). Results earlier within our study suggest HS synthesis might also be required for FGF10 signalling during zebrafish larval tail regeneration. As *fgf10* gene expression has been seen during *Xenopus* limb regeneration, and when applied exogenously, can rescue their regenerative response during their non-regenerative – refractory - period (Yokoyama *et al.,* 2000; Yokoyama *et al.*, 2001), it would be interesting to characterise the role of FGF10 during larval zebrafish epimorphic regeneration.

The strain used in the following chapter was the *fgf10*^{tbvbo} mutant, *daedalus*, which has a lysine-to-stop change at amino acid 5 which leads to the translation of a truncated, null,

protein. To this end, utilising the *daedalus/fgf10* mutant, alongside *in situ* hybridisation to detect changes in gene expression and immunohistochemistry to identify the mitogenic marker, phosphorylated histone H3, I attempted to identify the role, or roles, of *fgf10* expression during zebrafish larval tail regeneration.

5.2. Results

5.2.1. The *daedalus/fgf10* mutant shows normal caudal fin development.

As the pectoral fins failed to develop in *daedalus/fgf10* mutants, it was necessary to determine whether these zebrafish could develop their caudal fins normally before carrying out analysis of their regenerative capacity.

Caudal fins of the mutant were comparable to those of wild-types, besides the lack of pigmentation due to the *daedalus* line having a *nacre* background (Figure 5-1A). To determine whether a phenotype was present at an earlier stage but recovered, I chose to document their morphology just after tail bud formation. The tail bud begins forming at 11 hpf, however it is not until around 18 hpf that the tail becomes more pronounced. At this latter stage *daedalus* tail bud development appeared normal when compared to wild-type and siblings (Figure 5-1B-D, black arrowheads). The normal development did not seem to rely heavily, if at all, on the expression of *fgf10* as it is seen late during caudal fin development in 35 hpf wild-type embryos (Figure 5-1E, red arrowhead). Therefore, any regeneration phenotype that occurs in the *daedalus* zebrafish should be due to the FGF10 ligand being required during that particular stage of larval tail regeneration.

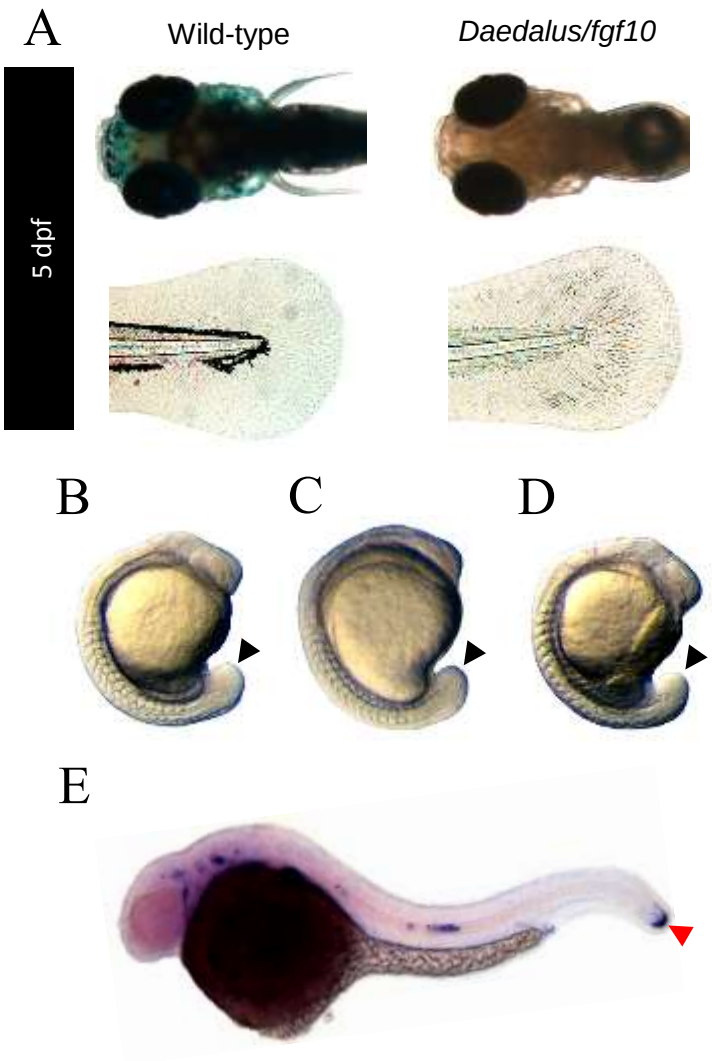

Figure 5-1. *Fgf10* is genetically redundant during caudal fin development
(A) The dorsal aspects of 5-days post-fertilisation (dpf) wild-type and *daedalus* zebrafish heads. 5X objective. (B-D) 18 hpf embryos. (B) wild-type, (C) *daedalus* sibling, and (D) *Daedalus.* Black arrowheads highlight tail buds of the respective zebrafish strains. (E) *In situ* hybridization to detect expression of *fgf10a* (red arrowhead) in 35 hpf wild-type zebrafish.

5.2.2. *Daedalus/fgf10* have a reduced regenerative capacity.

At 2 dpf, wild-type, *daedalus/fgf10* mutants and their siblings were allowed to recover for 3 days after tail amputation, and differences in their regenerative capacities were evident (Figure 5-2A). The tails of 3 dpa *daedalus* zebrafish showed some progression through

the epimorphic regeneration, however it looked to have stalled prior to regenerative outgrowth – leaving the new tail more truncated when compared to siblings and wild-types.

After quantifying the regeneration length of zebrafish strains, using the anus-caudal axis, there was evidently a difference in regenerative ability between control (wild-type, 538 µm, (n=20); sibling, 519 µm, (n=10) and *daedalus*, 428.5 µm, (n=20)) zebrafish. Furthermore, one-way ANOVA analysis of the data determined that there was a statistically significant difference ($p < 0.0001$) in regenerative ability between zebrafish strains (Figure 5-2B).

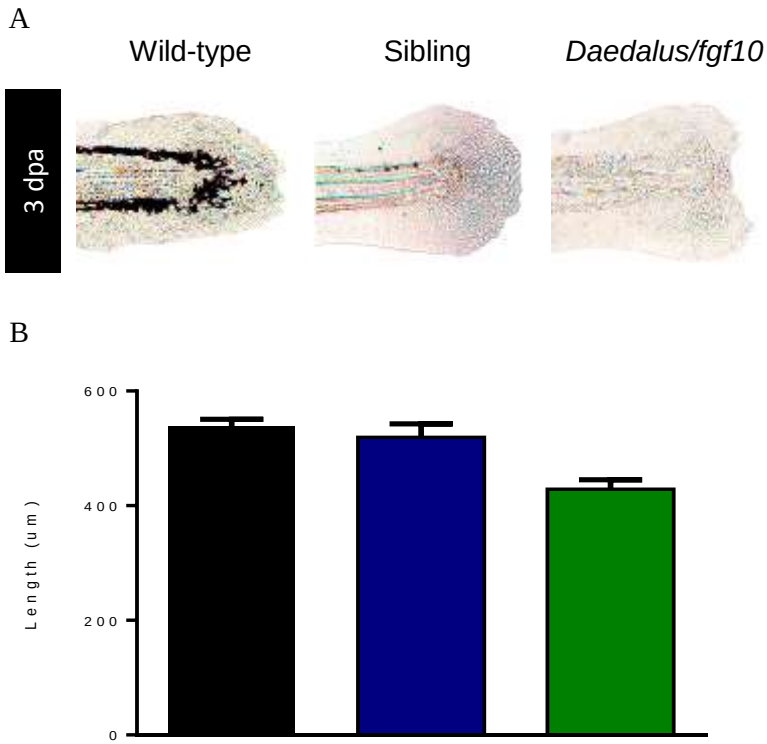

Figure 5-2. The *fgf10* mutant, *daedalus*, presents a reduced regenerative capacity.
(A) Lateral view comparing *daedalus* larval tail regenerates after 3-days postamputation (dpa) to wild-type and sibling. (B) Quantification of regenerate length, measuring from anus to caudal tip, at 3 dpa. Wild-type (n=20), black bar; sibling (n=10), blue bar; *daedalus/fgf10* mutant (n=20), green bar. Statistical analysis carried out using one-way ANOVA; $p = < 0.0001$. Error bars represent Mean ± SEM.

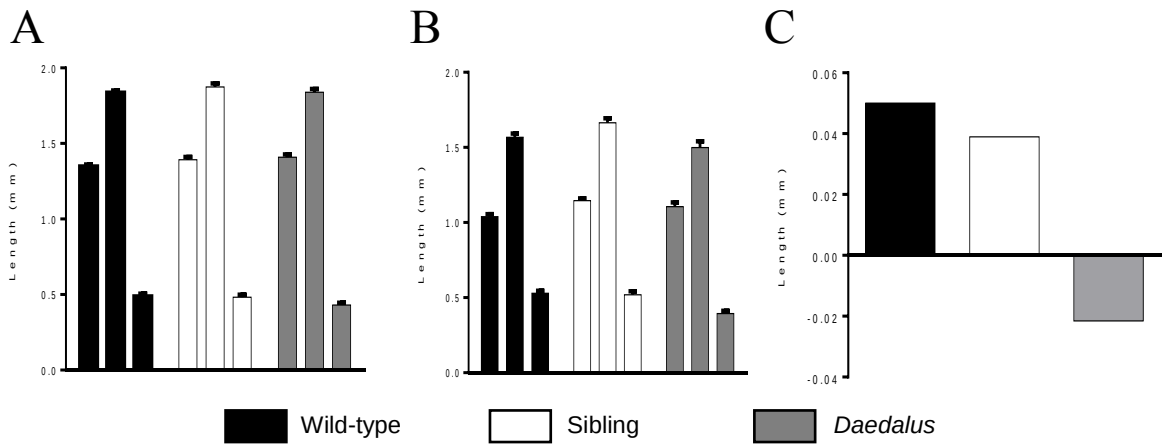

Figure 5-3. There is a net tissue loss after 3 days of tail regeneration in *daedalus* fish.
(A) A graph to show difference in anus-caudal length during development from 3 days postfertilization (dpf) (left bars of each group) to 5 days dpf (middle bars of each group). The third bar of each group represents the difference between the left and middle bars.
(B) A graph representing the change in anus-caudal length between 0 days postamputation (dpa) (left bars of each group) and 3 dpa (middle bars of each group). The third bar of each group represents the difference between the left and middle bars.
(C) A graph to show the overall anus to caudal tip length gained by 3 dpa after accounting for length gained during development. (A-C) n = 10 embryos for wild-type, sibling and *Daedalus*.

To make sure the difference in tail length after regeneration, between controls and *daedalus* mutants, wasn't due to any underlying developmental defects that could affect zebrafish body length, the average length gained during development was subtracted from the anus-caudal axis length of 3 dpa tails (Figure 5-3). Measuring the length gained between 2 and 5 dpf showed no significant difference between controls and the *daedalus*. On average, wild-type, sibling, and *daedalus* gained 0.49, 0.48, and 0.43 mm during development, respectively (Figure 5-3A). From measurements taken at 0 hpa the amount of tissue amputated was similar across sample groups (Figure 5-3B). Calculating the difference between regeneration and development length, from anus to caudal tip, there was a net increase in length for wild-type (0.05 mm) and sibling (0.04 mm), but a net loss of tissue was seen in the *daedalus* tails at 3 dpa (-0.02 mm).

5.2.3. Signal pathway activity is unchanged during *daedalus* epimorphic regeneration.

To begin to understand the possible mechanisms behind the tail regeneration phenotype of *daedalus* zebrafish I first wanted to determine any changes in its gene expression profile. *In situ* hybridisation, utilising the same probes in the two previous chapters, studying wild-type and *dackel* regeneration, was carried out on 30 hpa *daedalus* tails (Figure 5-4).

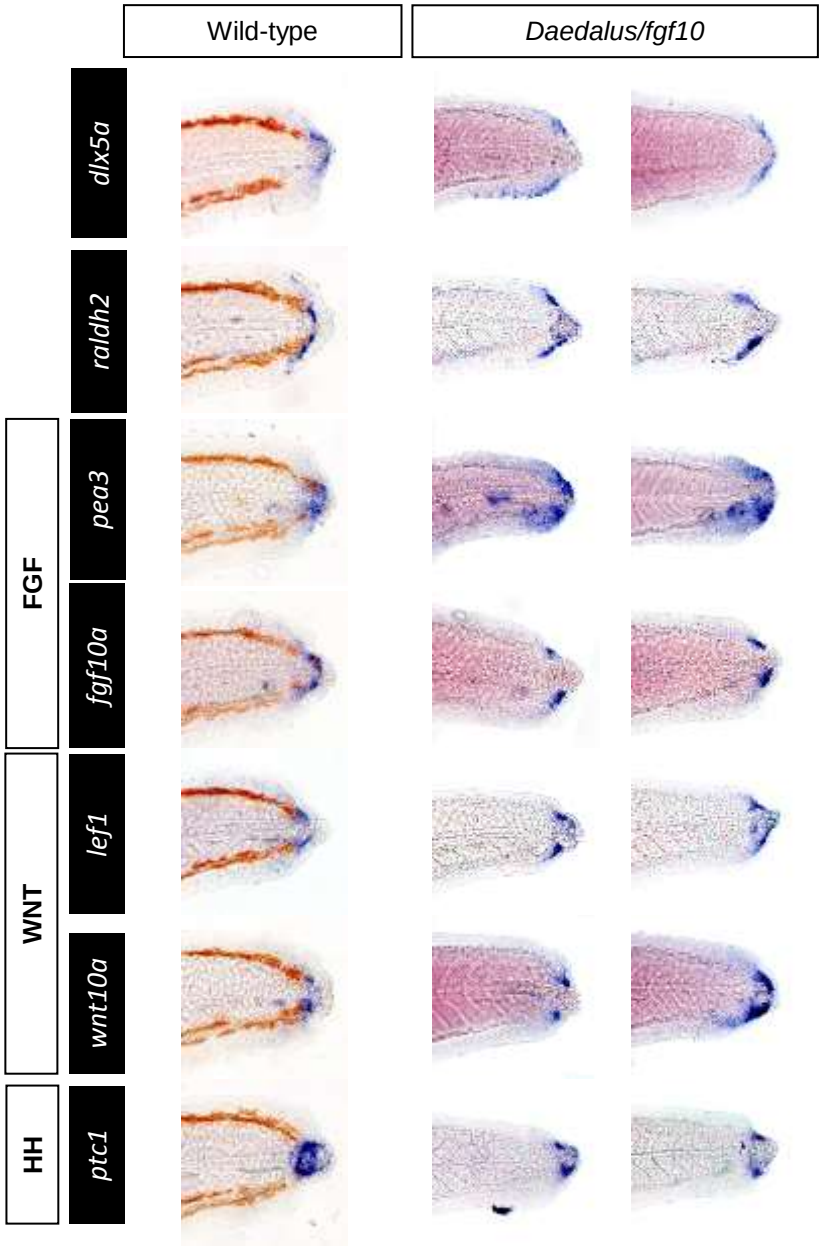

Figure 5-4. Gene expression is unaffected during *daedalus* tail regeneration.
In situ hybridisation to detect regenerate structures (*dlx5a* and *raldh2*) and developmental signal pathway activity (*lef1, pea3, ptc1*) in regenerating caudal fins of wild-type (n = 10) and *daedalus/fgf10* zebrafish (n = 10) at 30 hours postamputation (hpa). The FGF and Wnt ligand transcripts - *fgf10a* and *wnt10a* – were also detected. *Daedalus* images show two representative samples per gene.

Expression of the wound epidermis and blastema marker genes, *dlx5a* and *raldh2*, respectively, were unaffected in the late phase of larval tail regeneration. Their expression appeared to be similar to their wild-type counterparts. Similar results were seen for the FGF, Wnt and Hh read-out genes. Detection of the *fgf10a* and *pea3* RNA exhibited the same expression pattern as wild-type tails at the same time point after amputation. The reason *fgf10a* could still be detected was because the transcript for *fgf10* in the *daedalus*^{tbvbo} strain only differs by one nucleotide compared to that of the wild-type. Wnt gene expression was also normal, as probing for *wnt10a* and *lef1* RNA presented a similar staining pattern to *wnt10a* and *axin2* of regenerating wild-type tails. Overall, signal pathway activity was not altered during *daedalus* tail regeneration.

As knocking out the FGF10 ligand during tail regeneration did not lead to any changes in gene expression - more specifically the FGF pathway read-out, *pea3* – this suggested a role other than the modulation of developmental pathways during zebrafish epimorphic regeneration.

5.2.4. Proliferation is greatly reduced during *Daedalus* epimorphic regeneration in the *daedalus* mutant.

As the FGF pathway has been heavily linked with proliferation in a wide range of systems, I next decided to analyse the levels of cell proliferation during *daedalus* epimorphic regeneration. To determine whether the FGF10 ligand could act as a lone mitogen during tail regrowth, *dackel* tails were analysed alongside.

The phosphorylation of a serine residue of histone-H3 (H3P) has been shown to regulate the faithful packaging and segregation of chromosomes during mitosis (Wei *et al.*, 1999). 3-day old zebrafish were amputated in the pigment gap and allowed to recover for 12 to 48 hours. They were then fixed, and proliferating cells were detected using anti-H3P (Figure 5-5). After confocal imaging of H3P-positive cells in the tails of wild-type and both zebrafish mutants, it

was evident that there were no one obvious population of cells dedicated to proliferating at any stage during larval tail regeneration. Cells were dispersed randomly throughout all tails after amputation. The only noticeable difference was that proliferating cells of the wild-type, and arguably *dackel,* tails seemed to occupy regions further from the amputation plane (Figure 5-5 B-D). Uncut larval tails of wild-type and mutants possessed some proliferation within the pigment gap (Figure 5-5 A, E, I, white asterisks). Proliferating cells within the uncut *dackel* tail exhibited H3P-positive cells outside of the densely populated pigment gap.

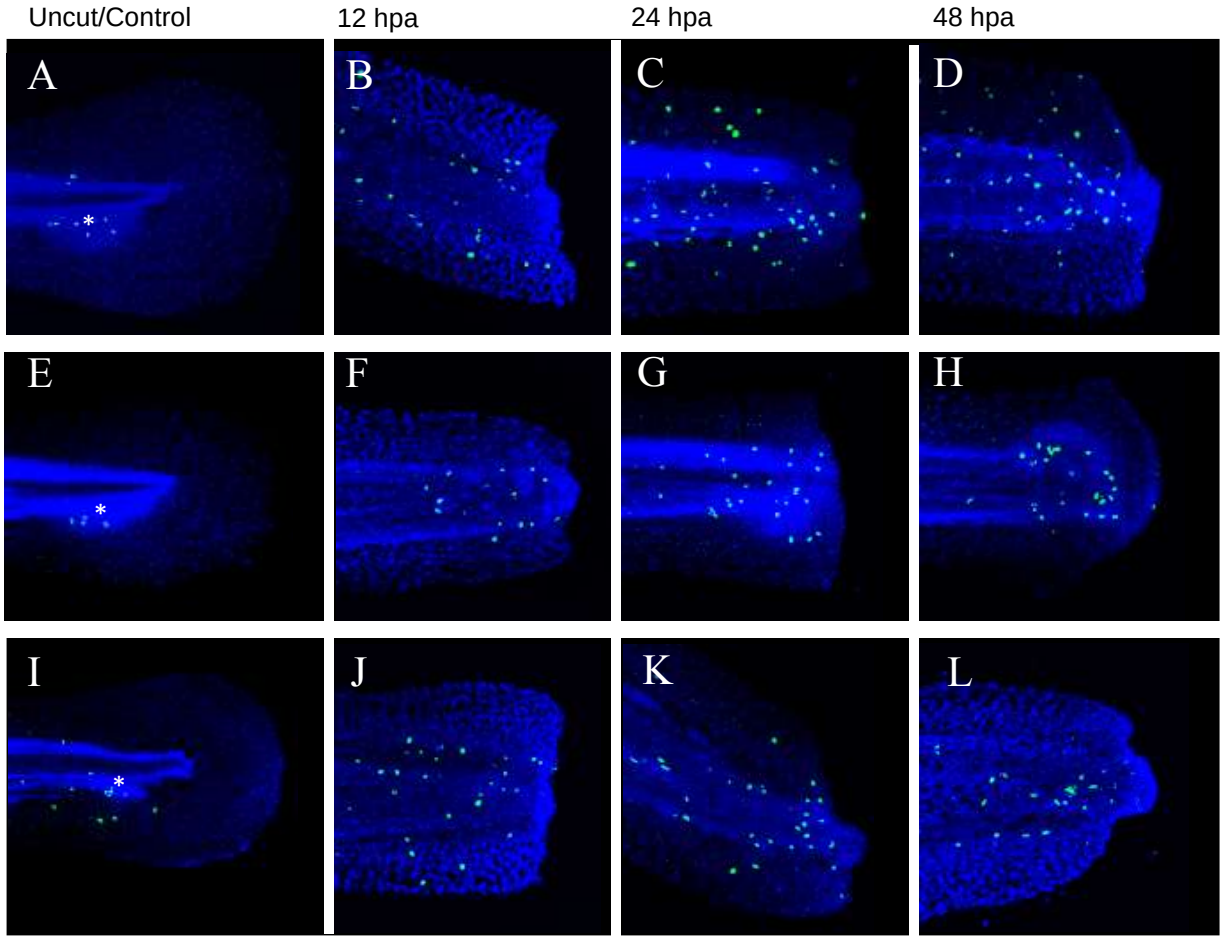

Figure 5-5. Proliferation is visibly reduced during *dackel* and *daedalus* tail regeneration.
Representative images showing the detection of proliferating cells using fluorescent immunohistochemistry and anti-phospho-histone H3 (H3P, green) in wild-type (A-D), *daedalus/fgf10* (E-H), and *dackel/ext2* (I-L) caudal fins, between 12 and 48 hours postamputation (hpa). (A, E, I) Uncut; (B, F, J) 12 hpa; (C, G, K) 24 hpa; (D, H, L) 48 hpa. DAPI (blue) was used as a counterstain. White asterisk mark the pigment gap. All images were captured using an Olympus confocal microscope, and edited using ImageJ.

As well as analysing the pattern of proliferation, I also counted the number of H3P-positive cells within a predefined region of the regenerating tails, using the PerkinElmer Volocity software (Figure 5-6). After I compared the counts of each mutant to the wild-type, significant differences were evident from 24 hpa onwards. Wild-type tails exhibited a steady increase in the number of H3P-positive cells between 12 and 48 hpa; from an initial 17 to a peak of 35. However, throughout *daedalus* regeneration, the number of stained cells, between 12 and 48 hpa, was maintained around 20, and peaked at 23. A similar result was seen in *dackel* zebrafish after amputation, however, the number of H3P-positive cells at 48 hpa was significantly reduced to 12.

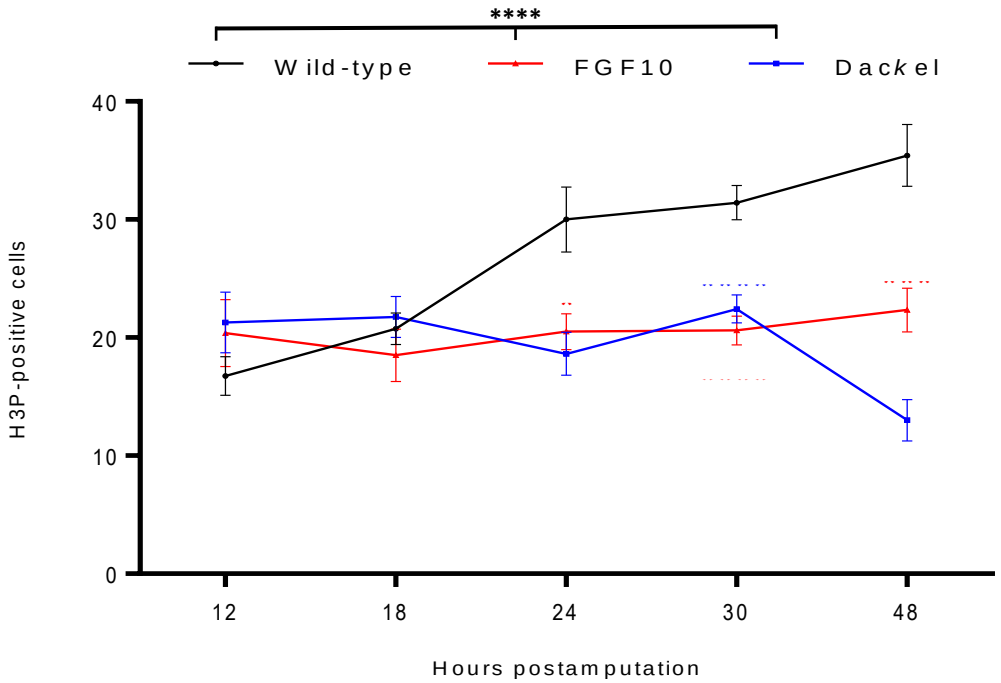

Figure 5-6. FGF10 acts as a mitogen during caudal fin regeneration.
A graph quantifying the change in the number of mitotic cells (H3P-positive) in the caudal fin of wild-type, *daedalus* and *dackel* after amputation between 12 and 48 hours postamputation (hpa). n = 20 per sample per time point. Statistical analysis carried out using two-way ANOVA; p = < 0.0001. Error bars represent mean ± SEM.

Identification of proliferation in wild-type, *daedalus*, and *dackel* tails undergoing regeneration highlighted differences between all strains; least variation was seen between both –*dackel* and *daedalus* - mutants until the final time point of 48 hpa. Even though proliferation

was induced after amputation in all three zebrafish strains, there was a significant difference between mutants and wild-types when tracking changes across a range of time points.

5.3. Discussion

The evidence provided for the FGF ligand, FGF10a, having a role during larval zebrafish tail regeneration came after the analysis of the *dackel* mutant. The loss of the *fgf10* transcript in the region of the blastema suggested it was important during or after blastema formation. This chapter used the *daedalus/fgf10*^{tbvbo} mutant to understand more about the role for this ligand during epimorphic regeneration.

Quantification of regeneration length, using the anus-caudal axis, with or without taking into consideration the length gained during development, highlighted a reduction in the *daedalus/fgf10* mutant's ability to regenerate its tail (Figure 5-2 and 5-3). This suggested that FGF10a was not a crucial factor during the opening stages of epimorphic regeneration, but functions after the initial responses following tail amputation, such as WE and blastema formation. This went against studies carried out using *Xenopus laevis* to understand the role of FGF10 during limb regeneration - defining it as a factor able to induce regeneration during a period of development characterised by their inability to mount a regenerative response. Yokoyama *et al*. (2001) showed that the application of an FGF10-soaked bead to amputated *Xenopus* forelimbs, during the refractory – non-regenerative – period, induced regrowth of the limb. After this refractory period *Xenopus* are only able to regenerate a structure known as a 'spike' – a poorly patterned cartilaginous protrusion - after limb amputation. It would be interesting to see whether FGF10-soaked beads could rescue regeneration in fully developed frogs, but also what the effects are of applying an *fgf10* morpholino to regenerating limbs, prior to the refractory period, in froglets. Christensen *et al*. (2002) came to the conclusion that the mesenchymal expression profile of *Fgf10* and *Fgf8* suggested the role of FGF10 during limb

development is not simply recapitulated during its regeneration. More experiments, using mutagenesis, are required in the *Xenopus* and axolotl to determine the role of FGF10 during epimorphic regeneration of the limb.

As FGF10 is important during the development of vertebrate limbs (Min *et al.*, 1998), there could be a conserved function for this ligand in lower vertebrates during regeneration. In the present study it was evident that the FGF10a ligand was crucial for pectoral fin development (Figure 5-1), which, during the early stages, requires a structure analogous to that of the vertebrate limb bud (Ng *et al.*, 2002). However, because the unpaired fins – caudal, anal, and dorsal – don't develop using this bud structure, and because FGF10 has not been well documented during their development, it is difficult to postulate the ligand's role during larval tail regeneration. Using *in situ* hybridisation to detect gene expression in 30 hpa *daeadalus* tails it was apparent that the FGF10 ligand was not able to modulate the three developmental pathways – FGF, Hh and Wnt – during tail regeneration (Figure 5-4). Also, the genes demarcating the WE and blastema presented temporospatial expression akin to their wild-type counterparts. This fits with the data measuring regeneration length: shorter regeneration length than those seen in the *daedalus/fgf10* mutant, for example the *dackel*, are more likely to exhibit defects in these two features of regeneration. Interestingly, knocking out *fgf10* did not prevent the expression of *pea3*, suggesting FGF10 is amongst other FGF ligands expressed during larval tail regeneration. Likely candidates include *fgf20a*, which has been linked with blastema formation (Whitehead *et al.*, 2005), and *fgf24*, previously known as *wfgf*, which is expressed within the wound epidermis (Poss *et al.*, 200a).

FGF10 seems to be expressed predominantly in the mesenchyme during the development of various organs, including the eye and pancreas (Bhushan *et al.*, 2001; Tao *et al.*, 2005). The same studies show FGF10 signals from the mesenchyme to epithelium in order to maintain proliferation during organogenesis. This function seems to be conserved during the

regenerative response in the model of this present study (Figure 5-5 and Figure 5-6). However, I did not identify the cell types that were H3P-positive. I could have started to answer this question by carrying out double-staining for H3P and a marker expressed during development, such as keratin 8 (Gong *et al.*, 2002). The FGF10 ligand seems to become integral for driving proliferation beyond 24 hpa, which is consistent with its gene expression during wild-type regeneration.

Analysis of cells undergoing mitosis during wild-type, *dackel* and *daedalus* tail regeneration provided evidence for another, HS-independent, regulator of proliferation. As the *dackel* and *daedalus* H3P counts were almost identical between 18 and 30 hpa suggests FGF10 to be the predominant, HS-dependent, mitogen at these time points. If all signals inducing proliferation were HS-dependent then I would not have expected to visualise any H3P-positive cells within *dackel* tails during regeneration. However, the remaining H3P-positive cells could be due to the presence of residual HS chains synthesised by Ext1, as it still functions at a lower capacity after the loss of Ext2. After 48 hpa, there is a further reduction in the number of proliferating cells during *dackel* regeneration to around 10, which, one could deduce as being a switch to a more HS-dependent regulation of proliferation at that time. If this were the case then I would have expected to see a rise in *daedalus* proliferation at the same time point, however the number of H3P-positive cells did not increase significantly (30 hpa, 20.6; 48 hpa, 22.33). This could be due to an increase in dependency on FGF10 at 48 hpa but another, HS-dependent, factor could compensate for this in *daedalus* tails, but not *dackel*, causing a negligible shift in the number of proliferating cells. This other factor could be Wnt10a, which had been identified to be expressed between 18 and 24 hpa (Figure 3-3), however this could be too early to fit this hypothesis.

In this chapter I believe I have reported, for the first time in zebrafish, a role for FGF10 during larval tail regeneration. It would be interesting to see if the properties of this ligand are

maintained during adult caudal fin regeneration. Creating a Cre-lox recombinant line for the conditional knock-out the *fgf10* gene following amputation, and immunohistochemistry to detect H3P-positive cells would provide some answers to this question.

5.4. Conclusion

Analysis of *daedalus/fgf10* tail regeneration has not only highlighted what a powerful animal model we have in the zebrafish but also the ability of other transgenic lines to identify potential candidates involved during epimorphic regeneration. It was, after all, the work in the previous chapter, using the *dackel* mutant to understand signalling pathways perturbed during epimorphic regeneration, in the absence of HS chains, which brought me to study it in the *daedalus/fgf10* mutant.

In this chapter, *in situ* hybridisation showed larval *daedalus* tail regeneration was identical to that of the wild-type. However, previous literature identified a role for the FGF10 ligand during organogenesis; providing me with the idea to analyse proliferation, during regeneration in zebrafish larval tails unable to express the ligand. As seen during the development of many anatomical structures, FGF10 seems to be expressed in the mesenchyme, and overlapped with the blastema marker, *raldh2*, in larval tails, signalling to a dispersed population of – what I assume to be epithelial – cells during tail regeneration.

It is in this chapter that I can draw to a close the identification of the molecular interactions during larval zebrafish epimorphic regeneration, how the absence of HS chains affects these pathways during tail regeneration, and the role of a ligand – FGF10 - identified through the analysis of regeneration in the *dackel*, and thus I have proposed a model for zebrafish larval tail regeneration (Figure 5-7).

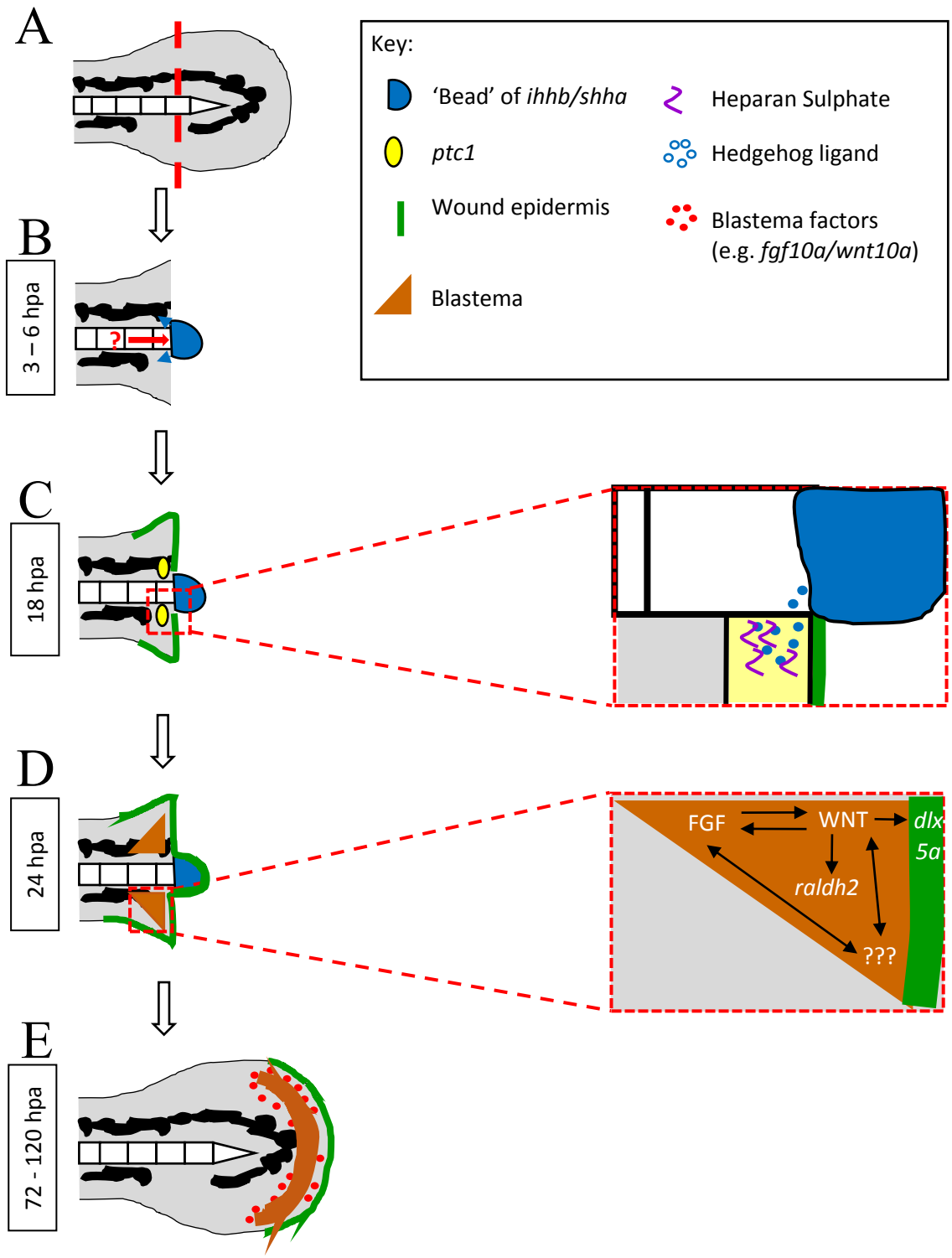

Figure 5-7. Our proposed model of larval zebrafish tail regeneration.
(A) After amputation of 2- or 3-day old tails there is an early expression – between 3 and 6 hours postamputation - of *shha* and *ihhb* in the distal most 'bead' – possibly notochord derived (B). The hedgehog pathway is active after 18 hpa (C), which seems to depend strongly on the presence of heparan sulphate chains. The blastema is identifiable after 24 hpa (D), and along with the wound epidermis is maintained by the Wnt pathway. Finally, various factors are released from the blastema for transition into the regenerative outgrowth phase (E).

Immediately after amputation comes the induction, through an unidentified source (hypothesised to be increasing levels of reactive oxygen species; Roehl Lab, unpublished data), of *shha* and *ihhb* expression within cells presumed to originate from the notochord – based on regeneration studies in *Xenopus* and newt tails. Hedgehog ligands then signal, regulated, in part, by the faithful synthesis of HS chains, to a region where the blastema eventually formed. Evidence from Chapter 3 suggested the Hedgehog pathway could regulate signalling events that orchestrate the formation of the WE and blastema. At 30 hpa, the Wnt pathway was shown to regulate the expression of, *dlx5a* and *raldh2*, and thus could have had a role in their induction, or as a maintenance signal during regenerative outgrowth. Wnt10a could have a role in blastema formation: as its expression was detected in the same region as the blastema prior to the expression of *raldh2*. Also, the FGF pathway might be able to directly interact with the Wnt pathway. Furthermore, the FGF ligand, FGF10, was able to contribute towards proliferation during and after blastema formation.

6 HPLC Isolation and *in vitro* characterisation of a Hedgehog-binding HS fraction.

6.1. Introduction

In Chapter 3, I was able to provide evidence for the early initiation of the Hedgehog signalling pathway and that its ability to progress zebrafish tail regeneration relied heavily upon the faithful synthesis of heparin sulphate (HS) chains. Firstly, through *in situ* hybridisation, I was able to identify early – 3 hours postamputation - upregulation of genes encoding the Hedgehog ligands, *shha* and *ihhb* (Figure 3-4). Also, the detection of the Hedgehog pathway read-out, *ptc1*, prior to the expression of the FGF and Wnt read-out genes, *pea3* and *axin2*, respectively (Figure 3-3). I was also able to provide evidence, using short-term exposure to Cyclopamine, GSK3-inhibitor or SU5402, during tail regeneration, for the Hedgehog pathway acting upstream of the FGF and Wnt pathways (Figure 3-8, 3-9 and 3-10). Furthermore, using *dackel/ext2* zebrafish mutants, which lack the function of one of the two glycosyltransferases – Ext2 - responsible for HS chain polymerisation, I was able to see a visible reduction in *ptc1* gene expression during tail regeneration (Figure 4-5). Also, in the same mutants, *shha* and *ihhb* expression was slightly delayed compared to wild-type regenerating tails (Figure 4-6). To this end, I hypothesise that there is a breakdown in communication, due to a diminished supply of HS, between Hedgehog ligand-expressing cells and their targets, leading to a reduction in the *dackel* mutants' ability to regenerate their tails. Therefore, this chapter focuses on the isolation, using high performance liquid chromatography (HPLC), of a purified HS fraction to target the Hedgehog pathway by restoring stable ligand-receptor interactions.

HPLC is a powerful tool which is able to separate a complex starting mixture into separate fractions. To extract a population of HS chains that could target a specific Hedgehog

ligand, first, I would have to identify, then recapitulate, a predefined peptide sequence of the HS-binding region within the protein. The HS-binding domain of murine Sonic hedgehog (Shh) has been identified as a Cardin-Weintraub sequence – a previously characterised cluster of basic amino acid residues - within the N-terminal region (Figure 6-1, red box) (Farshi et al., 2011). Removal of the CW domain through site-directed mutagenesis prevented Shh from binding to HS, but still maintained its ability to bind the highly sulphated HS analogue, heparin. This suggests Shh has multiple sites for binding to heparin, but only one for HS.

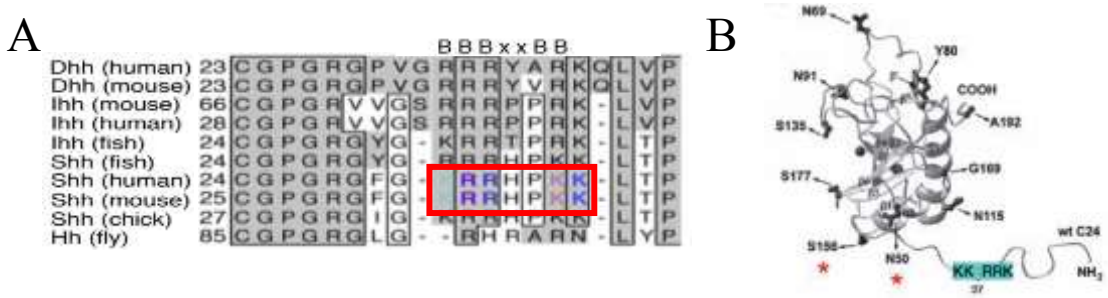

Figure 6-1. The HS-binding region of various Hedgehog ligands is a highly-conserved N-terminal Cardin-Weintraub (CW) sequence.
(A) The heparin-binding sequence of various Hedgehog ligands in different animals. The CW domain consists of five basic amino acids (BBBXXBB), KRRHPKK in the mouse and human Shh ligand (red box). Figure source: (Farshi et al., 2011).
(B) The CW domain highlighted (blue) in the N-terminus of SHH.
Image source: (Rubin *et al.*, 2002).

The isolation step should provide two fractions – a positive and negative – that will hopefully differ in their abilities to bind Shh. To test this, several biochemical techniques will be used; one such method being ELISA-based, GAG plates. These would allow me to compare the two HS fractions' Shh-binding ability by measuring the relative amount of ligand bound through enzyme-linked antibody detection. A bio-assay will also be used to determine the ability of the positive, Hedgehog-binding, fraction to augment a Shh response within a cell line. A good candidate for this is the MC3T3-E1 pre-osteoblast cell line; it has been shown to increase alkaline phosphatase (ALP) activity when exposed to exogenous Shh, in a dose-

dependent manner (Yuasa et al., 2002); which means these same cells should also be able to respond well to exogenous Shh through the upregulation of its target genes, *Gli1* and *Patched1*.

This chapter will describe the isolation of a novel HS fraction, isolated through HPLC, using HS from porcine mucosa (HS^{pm}) and a peptide sequence, to target the Shh ligand. Furthermore, biochemical tests will be used to assess the Shh-binding properties of the new, positive and negative, fractions.

6.2. Results

6.2.1. The peptide sequence for the Shh HS-binding domain interacts with heparin and heparan sulphate.

Purification of a HS fraction that preferentially binds to the Shh ligand exploited the GAG's affinity for a defined HS-binding domain of that protein. This took the form of a biotinylated 18-amino acid peptide to be applied to a column for isolation through affinity chromatography. These peptides came in two forms; with a biotin on the N- or C-terminus (Figure 6-2A), and I had to first select one for the isolation step. This required initial analysis of the binding properties of these two amino-acid chains – ISP1 and ISP2 - for heparin and HS (Figure 6-2).

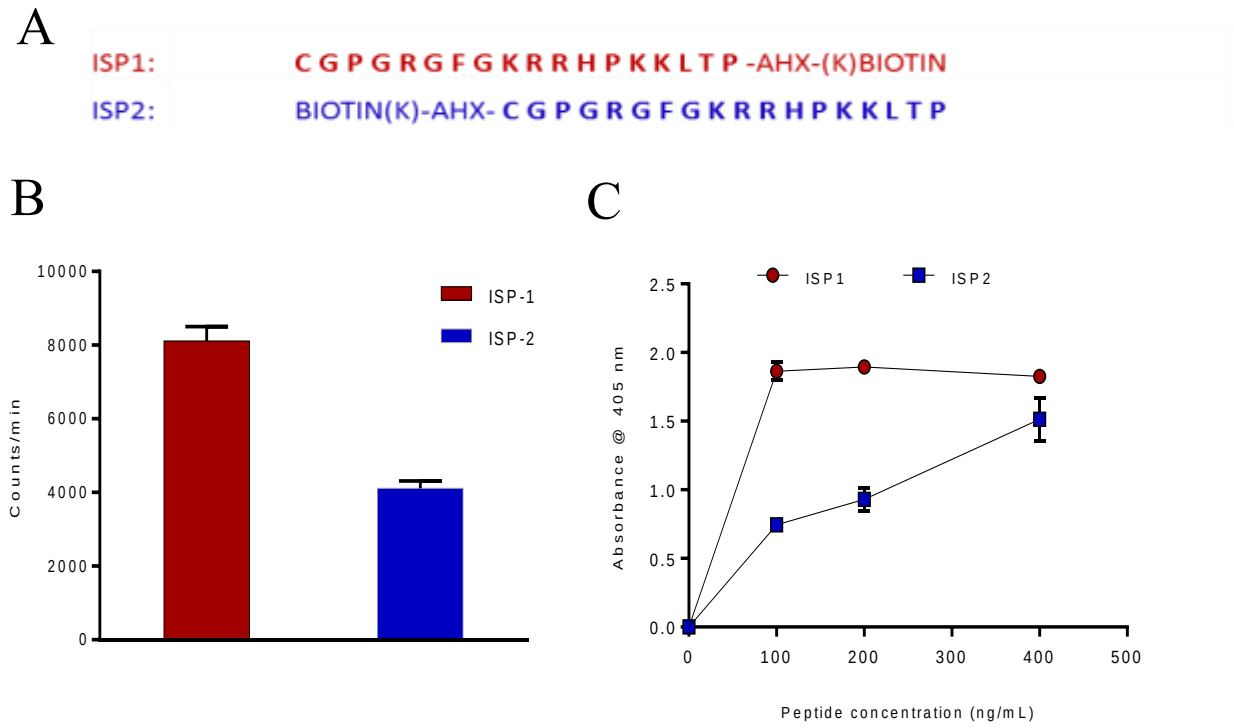

Figure 6-2. The isolation peptides, ISP1 and 2, bind to heparin and HS.

(A) The 18-amino acid peptides for the HS-binding domain of the Shh ligand. (B) Quantification of the amount of tritiated heparin bound to ISP1 or 2 on a dot blot assay. (C) GAG-binding plate to show the binding ability of ISP1 or 2 with heparan sulphate. (B, C) Graphs representative of two independent experiments, each ran as triplicate dot blots; data presented as mean ± SEM.

Detecting the amount of radio-labelled heparin bound to ISP-1 and ISP-2 exhibited significant differences in their binding abilities. ISP-1 and 2 showed 8000 and 4000 counts/min, respectively, when exposed to tritiated heparin (Figure 6-2B). Furthermore, GAG-binding plate analysis detected differences between these peptides for the binding of HS. When ISP-1 and 2 were added, at various concentrations, to wells coated with HS from the porcine mucosa (HS^{pm}) the absorbance differed significantly (Figure 6-2C). At 100 ng/mL ISP-1 absorbance readings reached maximum levels of 1.8, which was maintained until 400 ng/mL peptide. On the other hand, ISP-2 showed a gradual increase in the amount bound: rising steadily between 100 ng/mL (0.75) and 400 ng/mL (1.5). This shows that ISP-1 harbours a higher potential for binding HS^{pm}

and, therefore, I hypothesise that it might provide the bait for the isolation of a HS fraction more inclined to bind the protein of interest.

6.2.2. HS sourced from porcine mucosa (HS^{pm}) can be separated into two distinct populations using HPLC.

As heparin/HS binding analysis of ISP-1 and 2 suggested the former possessed a potentially greater affinity for the population of HS chains I was interested in, I bound ISP-1 to a streptavidin column, followed by the application of HS^{pm}, and then introduced increasing concentrations of sodium chloride whilst simultaneously collecting HS leaving the column into separate wells (Figure 6-3). HS chains that were immediately washed through the column - flow-through – at low salt concentrations will be known as the negative fraction, or $HS23^{-ve}$ (Figure 6-3, Y peak). The fractions that were collected after increasing the salt concentration, suggesting they have a greater affinity for the bait peptide, and thus the Hedgehog ligand, will be known as the positive fraction, or $HS23^{+ve}$ (Figure 6-3, Z peak). I was able to identify two clear peaks during all of the 33 HPLC runs, and next had to identify differences between these two populations; starting with the analysis of disaccharide composition.

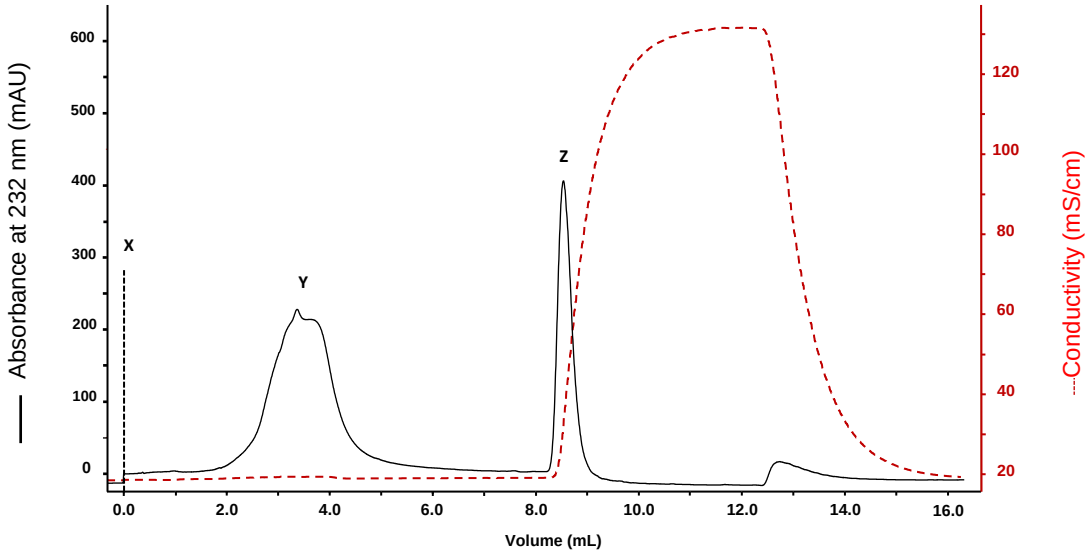

Figure 6-3. A Chromatogram showing the isolation of two HS fractions using HPLC.
A sensorgram to show the first run of heparan sulphate isolation using ISP1. X, Injection of heparan sulphate starting material – HS^{pm}; Y, HS flow-through/unbound fraction ($HS23^{-ve}$); Z, HS bound fraction ($HS23^{+ve}$). Black line represents carbohydrate detection. Red dashed line represents NaCl concentration.

To determine how disaccharide composition differed between the newly isolated GAG fractions, HS23^{+ve} and HS23^{-ve}, they were sent to IRL (New Zealand) for compositional analysis by HPLC. First, the HS chains of each fraction were digested into their basic disaccharide repeats and subjected to HPLC-SEC-RI to identify disaccharides with various levels of sulphation (Figure 6-4).

The chromatogram showed elevated levels of tri- and di-sulphated disaccharides within H
c
f
h
a

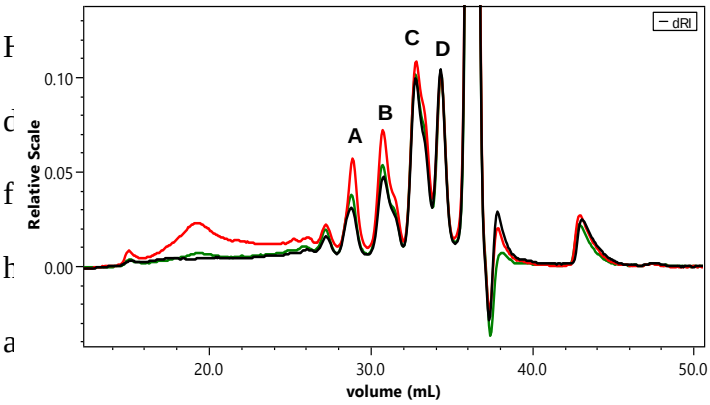

Figure 6-4: HPLC-SEC-RI chromatograms of mono- and un-sulphated HS23^{+ve}, HS23^{-ve} and HS^{pm}.
Identification of the varying levels of disaccharide sulphation of HS fractions. Peak A, trisulfated; Peak B, disulphated; Peak C, mono-sulphated; and peak D, un-sulphated disaccharides. The large signal at approximately 39 mL is from salts in the buffer.

Next, disaccharide analysis of GAG determined disaccharide standards of n of each (Table 6-1), and then plotted

	ΔUA-GlcNAc	ΔUA-GlcNS	ΔUA-GlcNAc,6S	ΔUA-GlcNS,6S	ΔUA,2S-GlcNS	ΔUA,2S-GlcNS,6S	ΔUA,2S-GlcNAc
HS^{pm}	33.8	26.2	12.1	10.8	6.4	10.2	0.5
HS23 +ve	31.1	22.4	11.6	12.8	5.7	16.1	0.6
HS23 -ve	34.6	28.2	12.0	10.0	6.9	7.8	0.5

Table 6-1. Disaccharide composition of the different Heparan Sulphate fractions.
The disaccharide composition, represented in percent, of isolated GAGs.

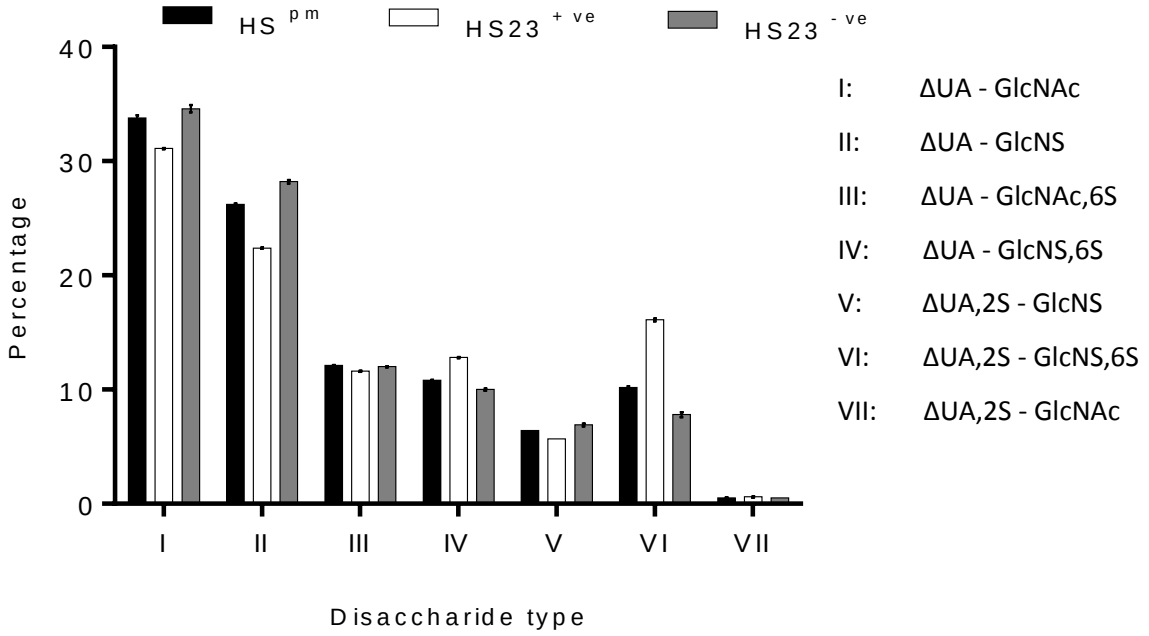

Figure 6-5. HS23^{+ve} is enriched in sulphated disaccharides compared to starting material and HS23^{-ve}, flow-through fraction.

A graph presenting the composition of various disaccharides within the three HS fractions: HS^{pm}, HS23^{+ve}, and HS23^{-ve}. ΔUA, uronic acid; GlcNAc, N-acetylated glucosamine; GlcNS, N-sulphated glucosamine 2S and 6S; 2-O-sulphation and 6-O-sulphation, respectively. Data presented as mean (error bars = SD).

Of the seven disaccharides detected the composition of four varied between HS23^{+ve} and HS23^{-ve}. Whereas HS23^{-ve} and HS^{pm} showed comparable levels of the unsulphated and monosulphated disaccharides, ΔUA–GlcNAc and ΔUA–GlcNS (HS23^{-ve}: 34.6 and 28.2%, respectively; HS^{pm}: 33.8 and 26.2%, respectively), HS23^{+ve} presented reduced levels at 31.1 and 22.4%, respectively. On the other hand, HS23^{+ve} showed enriched levels of the di- and tri-sulphated disaccharides, ΔUA–GlcNS,6S (12.8 %) and ΔUA,2S–GlcNS,6S (16.1%), when compared to HS23^{-ve} (10 and 7.8%, respectively) or HS^{pm} (10.8 and 10.2%, respectively). This data is comparable to the HPLC-SEC-RI analysis of sulphated

disaccharides: HS23^{+ve} exhibited increased levels of sulphation, whereas HS23^{-ve} presented levels comparable to those of HS^{pm}.

6.2.3. HS23^{+ve} exhibits preferential binding for Shh.

To investigate the Shh-binding ability of the positive fraction I started with a relatively simple ELISA-based technique known as the GAG-binding plate. It is a 96-well plate which allows for charged GAGs to be presented within their individual wells, without the requirement of modifications to their chains. To this end, I applied 5 µg/mL of the three GAG fractions to separate wells, followed by equal amounts of rh-SHH; which were detected through the addition of a substrate after the application of an enzyme-antibody conjugate (Figure 6-6).

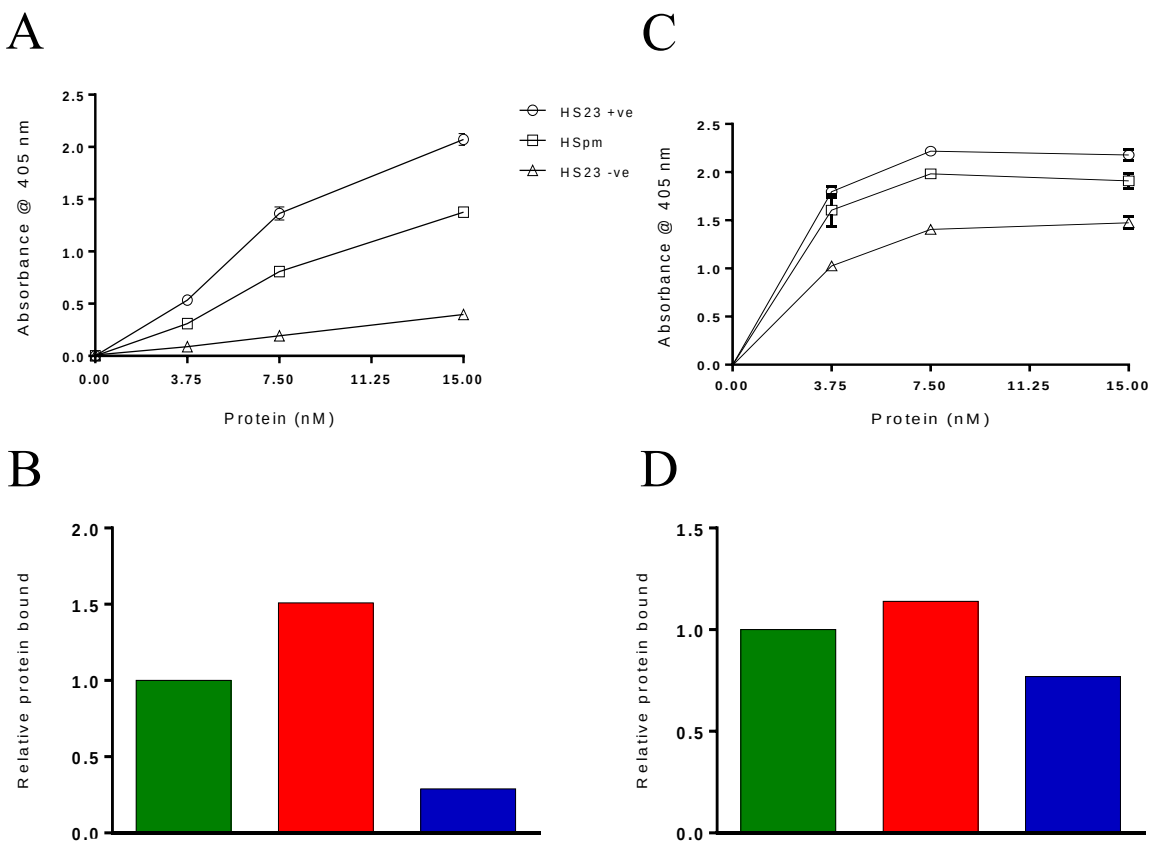

Figure 6-6. HS23^{+ve} has an increased preference for the Shh ligand.
Protein binding assay of rh-SHH (A) or BMP2 (C) for HS starting matieral (HS^{pm}), HS23^{+ve} or HS23^{-ve}. All readings normalized against blank wells. Binding of rh-SHH (B) or BMP2 (D) to HS23^{+ve} or HS23^{-ve} relative to HS^{pm}. Green bar, HS^{pm}; Red bar, HS23^{+ve}; blue bar, HS23^{-ve}. (A, C) Data presented as mean ± SEM. Graphs represent triplicate wells of individual experiments.

The ability of the positive fraction to bind to rh-SHH was significantly greater than that of the negative fraction (Figure 6-6A). Upon application of the same concentrations of rh-SHH to $HS23^{+ve}$ and $HS23^{-ve}$, absorbance levels were consistently higher in positive GAG wells. At the maximum concentration, 15 nM, $HS23^{+ve}$ gave a reading of 2.07±0.06, and $HS23^{-ve}$ a value of 0.4±0.03. The positive fraction also showed higher absorbance when compared to 15 nM of starting HS material (1.38±0.02). Relative binding ability of the positive and negative fractions was calculated using absorbance at 15 nM protein relative to HS^{pm} (Figure 6-6B). $HS23^{+ve}$ showed a 50% increase in absorbance, whereas $HS23^{-ve}$ yielded only 29% absorbance of the initial HS mix.

To further highlight differences in specificity for Shh between the positive and negative HS fractions, another protein, BMP-2, was added to each, at the same concentrations as rh-SHH – 3.75, 7.5, and 15 nM. Readings from the BMP-2 GAG plate showed plots that were more tightly packed than those analysing rh-SHH binding. At 15 nM BMP-2, $HS23^{+ve}$ and $HS23^{-ve}$ gave a reading of 2.18±0.05 and 1.48±0.06, respectively. Starting material exhibited an absorbance of 1.9±0.08. Positive and negative fractions, in the presence of 15 nM BMP-2, showed a 15% increase and 23% decrease relative to HS^{pm}, respectively (Figure 6-6D).

Another technique used exploited the natural phenomenon of surface plasmon resonance (SPR) to provide evidence for the preferential binding of Shh by $HS23^{+ve}$. This experiment utilised the BIAcore T100 to detect changes in SPR angle upon binding of an analyte – rh-SHH - to a surface-bound ligand, such as heparin. I used the system to detect the effect on levels of rh-SHH, bound to a heparin-coated chip, when applied with 5 or 10 µg/mL of the HS fractions. This would cause a direct competition between surface-bound heparin and the freely diffusible HS chains for the binding of Shh (Figure 6-8).

Before carrying out the competition assay using the BIAcore, first, I had to determine a concentration of rh-SHH that was detectable, but had not yet reached maximum response. Applying increasing concentrations of the protein over a heparin-coated chip showed a dose-dependent response (Figure 6-7). At 50 nM the reading had not reached its maximum response, which was seen at 200 nM, giving a reading well above 25 A.U; high enough for me to be able to detect an increase or decrease in response upon addition of the HS fractions.

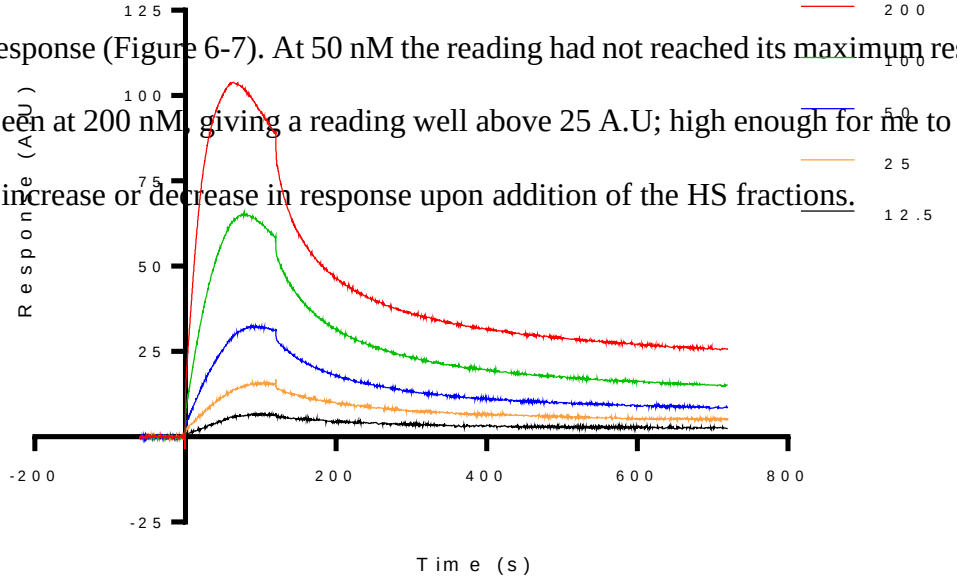

Figure 6-7. Shh binds to a heparin-coated chip in a dose-dependent manner.
A sensorgram to show the response of a heparin-coated streptavidin sensor chip to increasing concentrations of rh-SHH.

After determining that 50 nM of rh-SHH provided an adequate reading, GAG fractions were preincubated at 5 or 10 µg/mL with the ligand - competing Shh away from the heparin-coated sensor chip (Figure 6-8). Using the highly sulphated GAG, heparin, as a positive control, protein bound to the heparin of the sensor chip was all but abolished (Figure 6-8A). The HS fractions showed differing abilities to compete against heparin for rh-SHH (Figure 6-8E). $HS23^{+ve}$ reduced the response of the sensor chip to rh-SHH in a dose-dependent manner, and 10 µg/mL halved the levels of heparin-bound protein. In contrast, $HS23^{-ve}$ at 5 and 10 µg/mL could only prevent the binding of 13.7 and 18.7% of the Shh to heparin, respectively. The

negative fraction only performed slightly better than HS^{pm}, which only began to see a loss of Shh bound to the sensor chip at 10 µg/mL – 92% of the rh-SHH still remained.

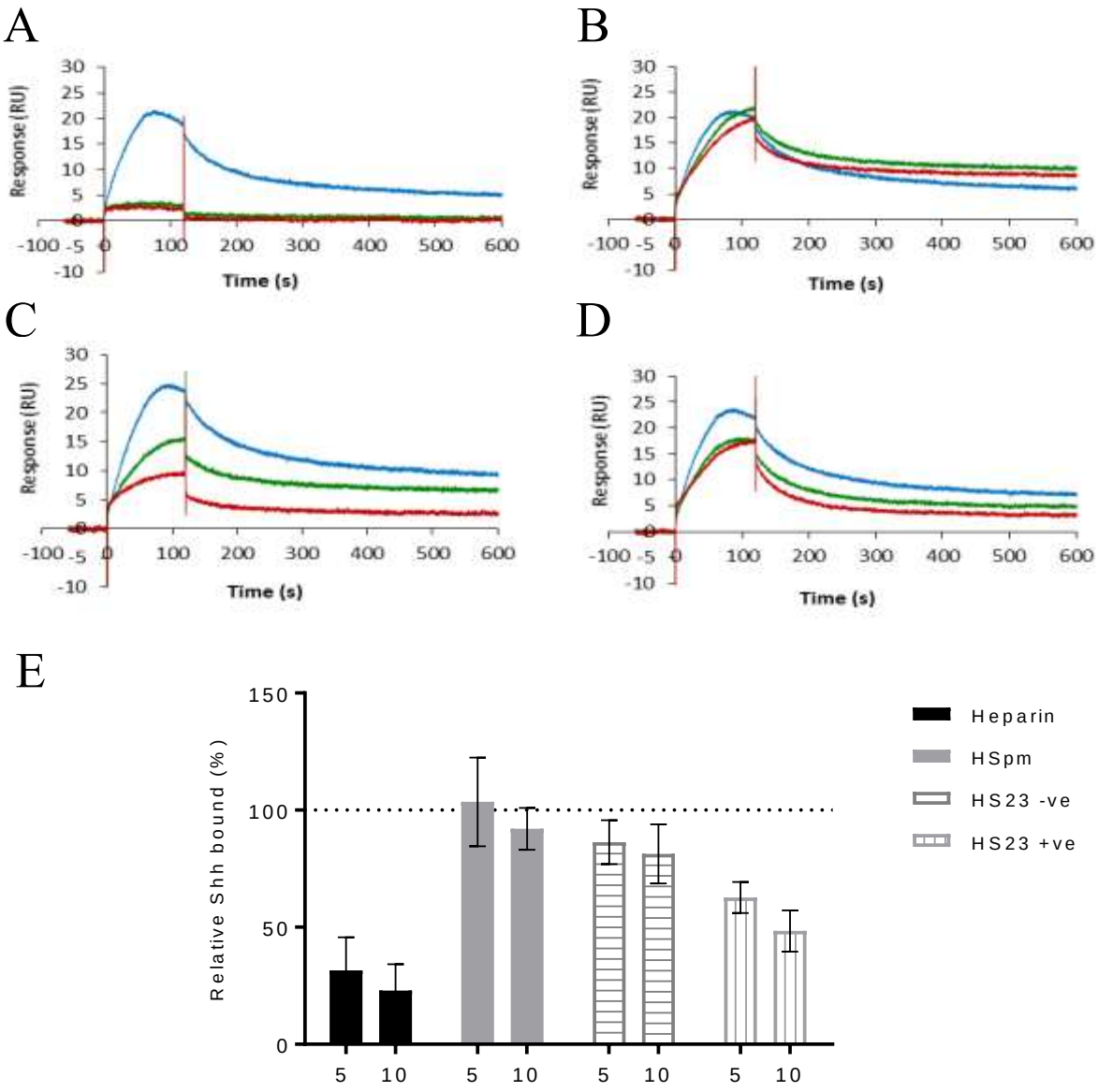

Figure 6-8. HS23^{+ve} is able to compete against heparin for the binding of Shh.
(A-D) Sample sensorgrams depicting the response when 50 nM SHH – incubated with, or without 5 or 10 µg/mL of the HS fractions - injected over a heparin-coated streptavidin chip: (A) heparin; (B) HS^{pm}; (C) HS23^{+ve}; (D) HS23^{-ve}. Red plot, 10 µg/mL GAG; green plot, 5 µg/mL GAG; blue plot, no GAG (E) A bar chart to show the amount of Shh bound to the heparin-coated chip after competition with four different GAG fractions, relative to protein bound in the absence of GAG fractions. (E) Bar chart represents three independent experiments, each run with triplicate wells. Data presented as mean ± SEM (Two-way ANOVA, ** p = 0.0052).

6.2.4. HS23^{+ve} does not alter the expression of Hedgehog target genes in mouse pre-osteoblasts.

Binding studies suggested that, using a peptide sequence of the Shh HS-binding domain with affinity chromatography, a HS fraction with preferential binding for the ligand of interest can be selected for from a mixed population of HS chains. However, understanding how this binding potential translates into a more biological context was the next important objective. Using MC3T3-E1 pre-osteoblasts, I was able to show that they could responded to increasing doses of exogenous rh-SHH (Figure 6-9), and also any effects the addition of HS fractions had on the expression of Hedgehog target genes, *Gli1* and *Patched1* (Figure 6-10 and 6-11).

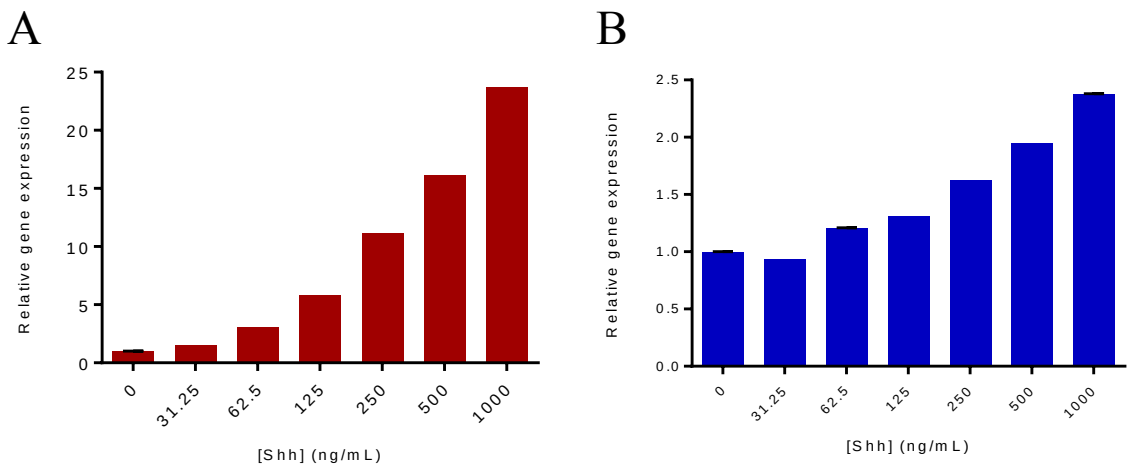

Figure 6-9. Relative expression of *Gli-1* and *Ptch1* increases in MC3T3-E1 cells exposed to Shh. MC3T3-E1 cells incubated for 24 hours with increasing concentrations of rh-SHH (A, B). Relative levels of *Gli-1* (A) and *Patched 1* (B) gene expression. Housekeeping gene: Actinb. Graphs representative of triplicate wells of one experiment. Data presented as mean ± SEM.

MC3T3-E1 pre-osteoblast cells have been shown to respond to Hedgehog signalling, when exposed to Shh, through the upregulation of the *Gli1* and *Patched1* genes (Zunich *et al*., 2009). Using the same cells, incubated with increasing concentrations of rh-SHH for 24 hours (Figure 6-9), there was a dose-dependent increase in relative *Gli1* and *Patched1* - neither genes ever reached their maximum expression levels up to 1000 ng/mL (Figure 6-9).

Next, gene expression was analysed after increasing concentrations of HS23^{+ve} were introduced to MC3T3-E1 media, alongside rh-SHH at the concentration required for half-maximum gene expression (250 ng/mL) (Figure 6-10).

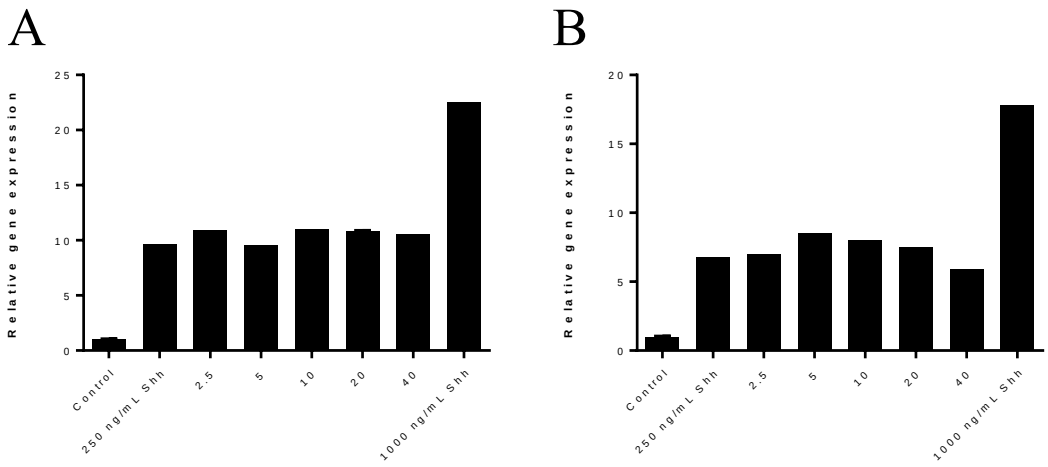

Figure 6-10. HS23^{+ve} does not significantly alter *Gli1* expression in MC3T3-E1 cells.
Relative *Gli1* gene expression of MC3T3-E1 cells incubated with increasing concentrations of HS23^{+ve} (ug/mL) in the presence of 250 ng/mL Shh for (A) 24 or (B) 48 hours (housekeeping gene: Actinb). Graphs representative of triplicate wells of one experiment. Data presented as mean ± SEM.

After the incubation of MC3T3-E1 cells for 24 or 48 hours in the presence of both rh-SHH and HS23^{+ve}, *Gli1* expression did not change significantly. Addition of 10 µg/mL of the positive fraction for 24 hours increased the expression to 11.02 ± 0.165^{-3}, compared to rh-SHH alone at 9.67 ± 0.72^{-4}. However, incubation of 5 µg/mL HS23^{+ve} for 48 hours induced a slightly bigger increase in *Gli1* expression (8.56 ± 0.97^{-4}) when compared to ligand alone (6.82 ± 0.64^{-4}).

Finally, Figure 6-11 represents the difference in *Gli1* and *Patched1* expression after MC3T3-E1 cells were incubated with both of the newly isolated GAG fractions for 48 hours. Changes in relative RNA levels were dependent upon the fraction.

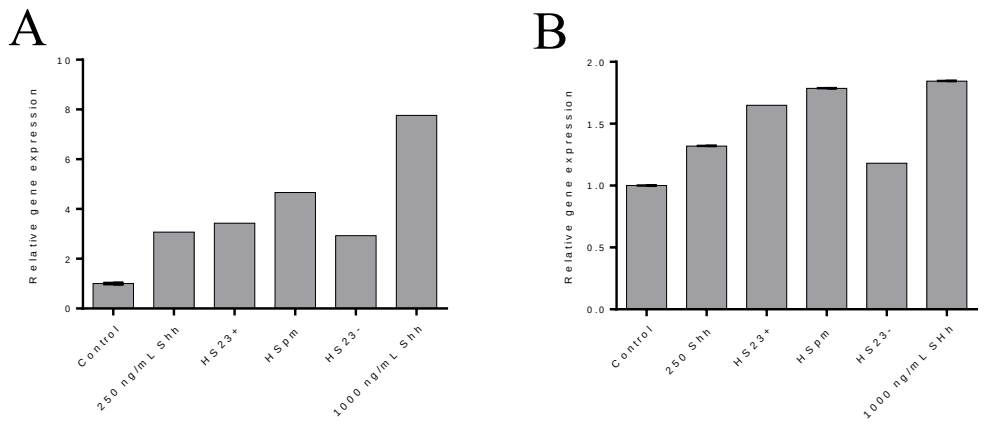

Figure 6-11. Positive and negative fractions show different abilities to modulate *Gli1* and *Patched1* gene expression.
Gli-1 (A) and *Patched1* (B) expression in MC3T3-E1 cells incubated, for 48 hours, with 5 µg/mL HS fractions in the presence of 250 ng/mL SHH. (Housekeeping gene: Actinb). Data presented as mean ± SEM. Graphs representative of triplicate wells of one experiment.

None of the fractions were able to augment target gene expression above the levels of the positive control - 1000 ng/mL rh-SHH alone. Surprisingly, HS^{pm} increased expression of both *Gli1* and *Patched1* more so than the positive and negative fractions. $HS23^{+ve}$ performed slightly better than $HS23^{-ve}$ for both genes, however this was not a significant change. Interestingly, when compared to 250 ng/mL rh-SHH alone, the expression levels of both genes were reduced after cells were incubated with $HS23^{-ve}$ for 48 hours.

6.2.5. ALP activity of MC3T3-E1 cells is augmented in the presence of $HS23^{+ve}$.

The final assay to determine the HS fractions' ability to modulate Hedgehog pathway activity used MC3T3-E1 cells to detect changes in alkaline phosphatase (ALP) activity when exposed to rh-SHH in the presence, or absence, of HS fractions. First, I had to determine the best rh-SHH concentration for two different time courses - to determine when to change the media (Figure 6-12).

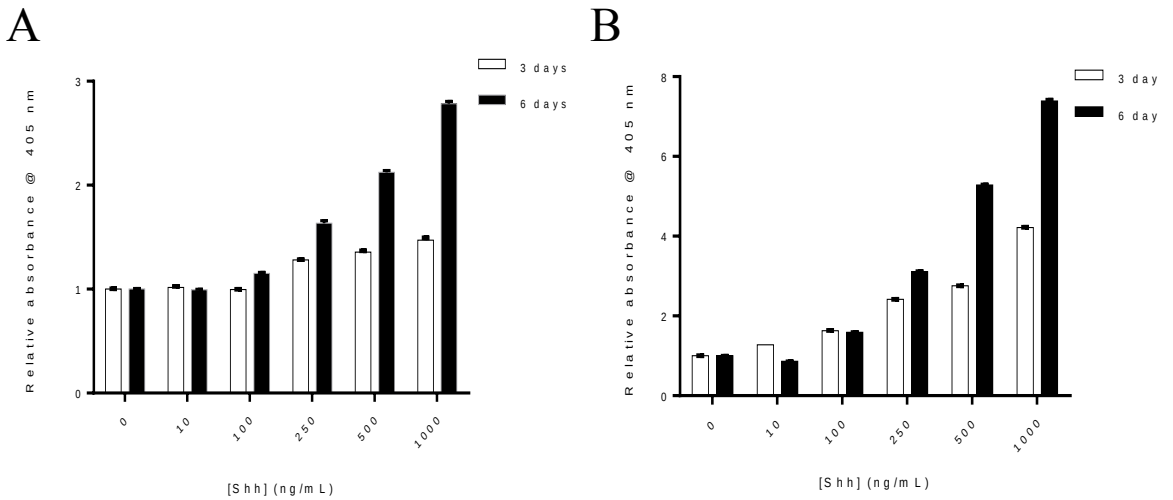

Figure 6-12. MC3T3-E1 alkaline phosphatase (ALP) activity increases dose-dependently in response to Shh.

MC3T3-E1 cells treated with rh-SHH for 3 or 6 days with media changes after every three days (A), or every other day (B). Graphs representative of triplicate wells of one experiment. Data presented as mean ± SEM.

The cells exhibited dose-dependent increases in ALP activity under all conditions; however, 3-day continuous treatments only showed an increase after 250 ng/mL rh-SHH (Figure 6-12A, white bars), all other time courses responded by 100 ng/mL. MC3T3-E1 cells incubated for 6 days with 250 ng/mL SHH, changing the media after 3 days, exhibited a robust increase in their ALP activity – enough to visualise any changes after the addition of each fraction. Next, supplementing MC3T3-E1 medium with or without rh-SHH, and 2.5 to 20 µg/mL $HS23^{+ve}$ for 6 days – changing media once - led to an increase in ALP activity (Figure 6-13).

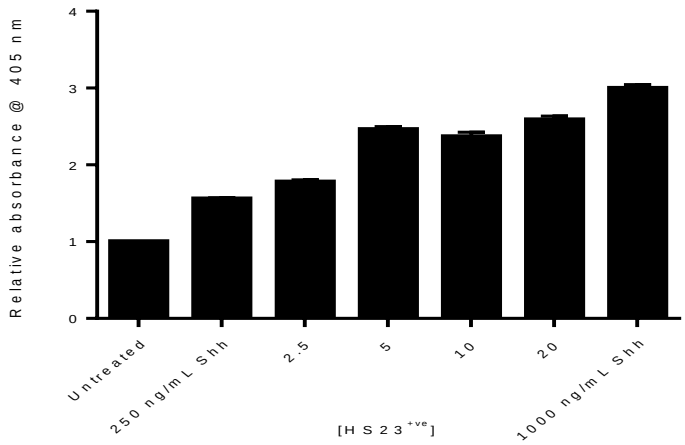

Figure 6-13. HS23^{+ve} augments the ALP activity of MC3T3-E1 cells
Relative ALP activity after MC3T3-E1 cells were exposed to increasing doses (2.5 – 20 ug/mL) of HS23^{+ve} in the presence of 250 ng/mL rh-SHH for 6 days – media changed on the third day. Graph representative of triplicate wells of one experiment; data presented as mean ± SEM.

MC3T3-E1 reached maximum phosphatase activity after only 5 µg/mL HS23^{+ve} was added with 250 ng/mL rh-SHH: ALP activity after 20 µg/mL was almost identical to 5 µg/mL HS23^{+ve} treatments. None of the treatments were able to match the positive control of 1000 ng/mL rh-SHH alone.

Furthermore, when MC3T3-E1 cells were incubated with either the positive or negative fractions in the presence of rh-SHH, HS23^{+ve} induced relative ALP activity levels above those of HS23^{-ve} treated cells. (Figure 6-14). Similarities can be drawn between *Gli1* and *Patched1* RT-PCR results and the ALP activity after supplementing media with HS23^{-ve}: in MC3T3-E1 cells, ALP activity and Hedgehog regulated genes were downregulated when incubated in the presence of rh-SHH and negative fraction.

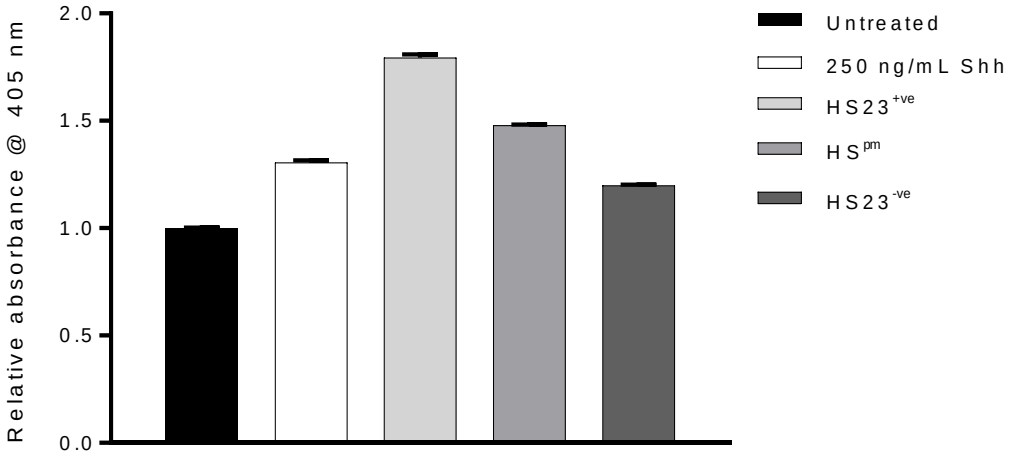

Figure 6-14. HS23^{+ve} increases ALP activity more so than the starting and negative fractions.
MC3T3-E1 cells exposed to 5 µg/mL of the GAG fractions for 6 days – media changed on the third – in the presence of 250 ng/mL Shh. Graph representative of triplicate wells of one experiment; data presented as mean ± SEM.

As the BMP-2 ligand has been reported, in coordination with Shh, to augment ALP activity of MC3T3-E1 and C3H10T pre-osteoblast cells, and is likely to be present within the media supplement, bovine serum, it was important to understand whether the ALP response was due to the positive fraction's ability to specifically modulate Hedgehog pathway activity, or it was affecting ALP activity through the binding of other factors within the media. To this end, the hedgehog inhibitor, cyclopamine, was added to the cells exposed to HS23^{+ve} and rh-SHH, and ALP activity determined (Figre 6-15).

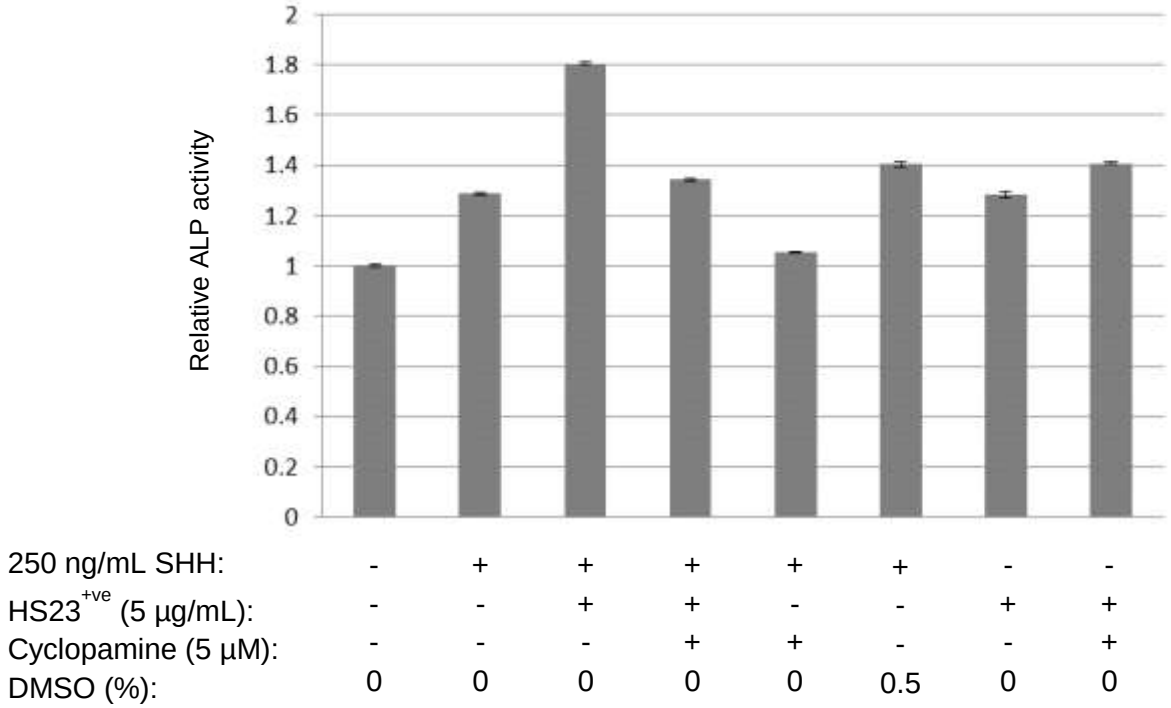

Figure 6.15. HS23^{+ve} induction of ALP activity is not entirely Hedgehog-dependent.
ALP activity in MC3T3-E1 cells detected after their exposure to 250 ng/mL rh-SHH with 5 µg/mL HS23^{+ve}, and the addition of 5 µM cyclopamine. HS23^{+ve} was also added alone, in the presence or absence of 5 µM cyclopamine. 0.5 % DMSO was used as a vehicle control. Graph represents triplicate wells of one experiment; data presented as mean ± SEM.

As previously reported, ALP activity increased after MC3T3-E1 cells were incubated with rh-SHH and 5µg/mL HS23^{+ve}, however, after introducing 5 µM cyclopamine, to the same treatment, phosphatase activity only dropped to levels achieved after exposure to 250 ng/mL rh-SHH alone. There was a slight increase after rh-SHH was introduced to cells alongside the vehicle control (0.5 % DMSO). Unexpectedly, HS23^{+ve} alone was able to induce an ALP response, and was further increased when in the presence of 5 µM cyclopamine – similar to activity levels of rh-SHH in the presence of 0.5 % DMSO. The positive control of 250 ng/mL rh-SHH and 5 µM cyclopamine gave a relative ALP reading similar to that of untreated MC3T3-E1 cells.

6.3. Discussion

In this chapter I used a peptide sequence, identified as the heparin/HS-binding domain of the Hedgehog ligands, alongside affinity chromatography, in an attempt to isolate a population of Shh-binding HS chains. This is the first time such a method has been used to fractionate a mixed population of HS chains, from the porcine mucosa, to target this protein. As there was a high degree of homology between the fish and mammalian HS-binding domains across the ligand family, and recombinant human Shh could be easily sourced, I chose the human peptide sequence for HPLC isolation. Besides this tightly packed sequence of basic amino acid residues, another, single amino acid – Lysine 178 - had been shown to be important for Shh to interact with HS chains (Chang *et al.*, 2011). However, this group only used the hyper-sulphated and highly charged analogue of HS, heparin, which could bind more strongly to the ligand, possibly through the use of additional amino acids.

As an N-terminus biotinylated peptide could fold more or less favourably than a C-terminus peptide with the same modification for interactions with GAG chains; prior to carrying out affinity chromatography with the 18-amino acid sequence of Shh, I analysed differences between the peptides' binding abilities for both heparin and HS chains (Figure 6-2). Comparing ISP-1 and 2, I saw a more potent ability for the C-terminal – ISP-1 - biotinylated peptide to bind both GAG chains; suggesting a more efficient return on the quantity within the positive fraction, and could also provide HS chains with a potentially higher specificity for the ligand of interest. On the other hand, utilising the peptide with a stronger binding profile could isolate HS chains with adverse properties, such as a more promiscuous binding profile after biochemical analysis. I decided that the first interpretation provided the promise of more positives than potential negatives.

After applying the peptide to a streptavidin column and running the HS starting mix (Heparan sulphate from porcine mucosa) over it, I was able to identify two well-defined peaks. One showing a typical flow-through – negative – fraction, and the other a strongly bound HS chains - positive fraction - requiring high salt concentrations for their elution (Figure 6-3). This short, sharp peak is indicative of a defined population of GAGs which can be biochemically tested against its unbound, flow-through counterpart seen as an earlier peak with a small plateau on the chromatograph.

Next, disaccharide composition of all three HS populations – starting (HS^{pm}), positive ($HS23^{+ve}$), and negative ($HS23^{-ve}$) – was analysed to determine how these fractions differed at a molecular level. Understanding the proportions of each disaccharide subunit could narrow down which modifications were integral to invoking a response from the desired target – the Hedgehog pathway in this instance. $HS23^{+ve}$ showed an increase in its tri- and di-sulphated disaccharide levels compared to the other two fractions. This suggests, for a GAG chain to interact with its ligand may require an increase in sulphate modifications, which would lead to an overall elevated negative charge. Further analysis to determine the relative levels of several predetermined disaccharides within each fraction showed an increase in the proportion of disaccharides containing a 6-O-sulphation - UA-GlcNS,6S and UA,2S-GlcNS,6S - within the positive fraction. However, in the developing external granule cell layer of the cerebellum, it has been shown to be the 2-O-sulfo-iduronic (UA,2S) acid component of the disaccharides that play an important role in modulating Shh-dependent proliferation (Witt *et al.*, 2013). Also, it seems the 6-O-sulphated glucosamine (GlcNS,6S) could have a crucial role in the regulation of Shh distribution and availability within the chick neural tube during development (Danesin *et al.*, 2006). In the study, temporospatial expression of the *Sulf1* gene, encoding an enzyme involved in the removal of 6-O-sulphates from heparin/HS chains (Morimoto-Tomita *et al.*, 2002), suggested a role in regulating neurogenesis through changing HS chain interactions with

Shh. This was shown to be the case after electroporation of a Sulf1-expression vector: the Shh ligand distribution and activity extended dorsally, determined via the detection of *ptc1* and the neuronal progenitor marker, Nkx2.2, expression (Danesin *et al.*, 2006). Even more interesting was that the suggested substrate for Sulf1 was the trisulphated UA2S-GlcNS,6S (Morimoto-Tomita *et al.*, 2002). Therefore, a combined role could exist for disaccharides containing the 2-O- and 6-O-sulphate groups during Hedgehog ligand interactions. After the Shh ligand is sequestered at the cell surface by trisulphated disaccharides, removal of the 6-O-sulphate group, through extracellular Sulf1 activity, could lead to the presentation of the ligand to its receptor, patched, through the 2-O- and N-sulphate groups continued interaction with the ligand, and possibly the receptor, leading to the activation of the pathway (Figure 6-16). This model has also been suggested by Dhoot *et al.*, (2001) during a study identifying Sulf1 as a regulator of Wnt activity in myogenic cell cultures.

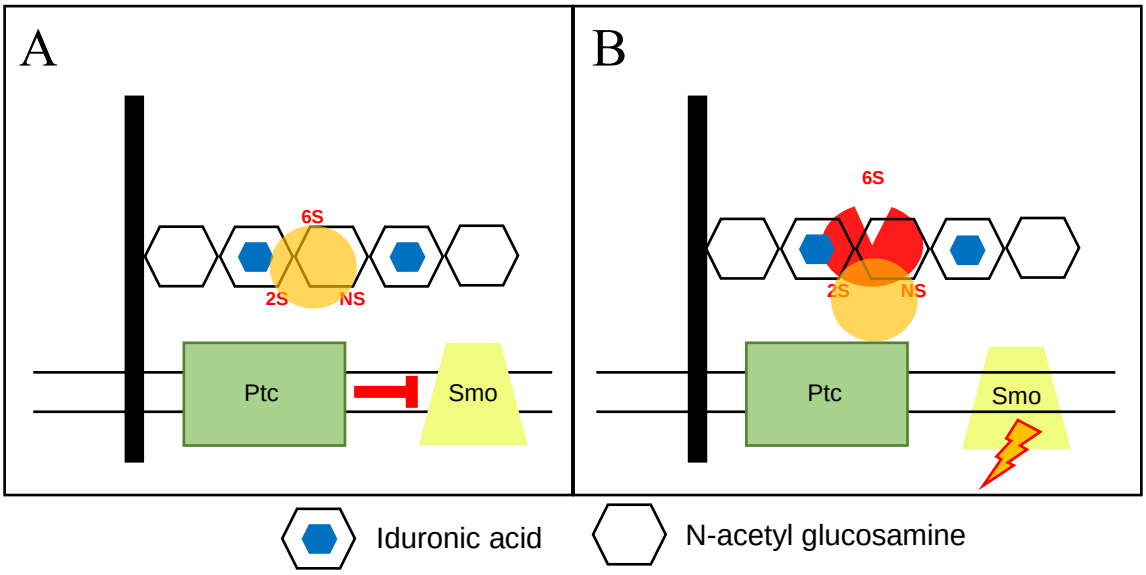

Figure 6-16. A model for the interaction of the Hedgehog ligands with HS chains before and after their modification.
(A) The Hedgehog ligand (orange circle) interacts with the trisulphated disaccharide, IdoA2S-GlcNS,6S, which prevents its interaction with the patched receptor.
(B) After Sulf1 (red symbol) removal of the 6-O-sulphate group from GlcNS,6S the Hedgehog ligand is able to interact with both the receptor and HS chain, inducing pathway activity.

I have, thus far, shown that the positive HS fraction, when compared to the negative and starting material, contained a higher proportion of tri- and di-sulphated disaccharides, which, during development, could be the primary units for Shh distribution. Therefore, when applying rh-SHH exogenously to each fraction of HS, I would expect to see a stronger preference for the positive fraction over the negative, and slightly more so than the starting fraction, which contains both populations. This, indeed, was the case after GAG plate analysis (Figure 6-6). Not only was the relative binding of Shh to $HS23^{+ve}$ greater than that of $HS23^{-ve}$ but after the addition of BMP-2, at the same molar concentrations, the difference in the amount of protein bound to positive and negative fractions was greatly reduced. This result shows that there is some Shh-binding preference exhibited by the HS chains of the positive fraction, and that ligand-binding is, arguably, not determined solely by charge alone. Some specificity must come from how the various disaccharide units within the linear polysaccharide are positioned, causing HS to change conformation, thus lining up with complementary regions of an interacting protein. As HS synthesis has no clear template, like DNA replication, and the number of saccharide combinations in a 200 saccharide long GAG chain reaches into the thousands, it is extremely difficult to create a HS sequence that only binds the protein of interest. To be able to adapt the method known as protect and label, which exploits heparin's ability to block chemical alterations of an interacting amino acid, to instead label the saccharides bound to amino acids, followed by a sequencing step, might be able to unlock protein-binding GAG chains with higher specificity for their predetermined target.

I analysed further the binding preference of both HS fractions for the Shh ligand using a heparin competition assay and SPR detection (Figure 6-8). The ability of 10 µg/mL $HS23^{+ve}$ chains to compete away up to 50% of the rh-SHH from the highly charged, promiscuous binder, heparin, showed that this fraction has the potential to form strong GAG-ligand interactions. However, heparin exhibited all the hallmarks of a strong protein binder in this assay, much

more so than $HS23^{+ve}$. Although, as eluded to earlier, heparin binds to another amino acid - Lysine 178 – of the ligand, which is yet to be reported for HS; therefore heparin might have a slight advantage due to potentially novel binding sites. The negative population, and starting material - HS^{pm} - weren't able to compete large amounts of Shh away from the heparin-coated chip. Surprisingly, the negative fraction appeared to compete for the binding of the protein more effectively than HS^{pm}. This could be due to the fact that HS^{pm} has not had any fractions isolated from it, causing off-target effects, such as the binding of HS chains with one another. These results provided further evidence that the positive fraction had a stronger binding preference for Shh compared to the negative fraction and starting material. They also showed that heparin could still bind Shh in the presence of $HS23^{+ve}$, possibly due to its higher negative charge or ability to interact with amino acids not recognised by HS. This could be tested through protect and label; comparing the differences between Shh amino acids protected by heparin and HS. Carrying on from this, to understand the importance of specific amino acids identified for protein-GAG interactions, affinity chromatography could be carried out to analyse how the HS-binding ability of Shh changes after the substitution of one amino acid – identified during protect and label - for another, uncharged one. However, as these experiments are too time consuming for the short amount of time spent in the Singapore lab, these were beyond the scope of this project.

As shown above, through GAG-binding plates and SPR-based analysis, $HS23^{+ve}$ exhibited a stronger preference for the binding Shh compared to $HS23^{-ve}$. This, I thought, could translate to augmented Hedgehog activity, and therefore upregulated target gene expression. However, this was not the case: *Ptc1* and *Gli1* levels were not significantly altered in MC3T3-E1 cells exposed to exogenous rh-SHH with increasing concentrations of $HS23^{+ve}$. When comparing equal amounts of the two fractions and starting material, it was the starting material that presented the biggest increase in both genes. $HS23^{+ve}$ performed slightly better, but not

significantly, when compared to $HS23^{-ve}$ (Figure 6-10 and 6-11). This could be due to a larger proportion of the positive population of HS chains within HS^{pm}, as it is unlikely that affinity chromatography isolated the entire population of Shh-binding chains. Another theory could be that HS^{pm} does not contain enough GAG chains able to bind Shh and thus the pathway is upregulated more so than the other fractions; however, this would make $HS23^{-ve}$ the most able fraction to induce higher levels of *Ptc1* and *Gli1* expression. Another explanation for the poor performance by the positive fraction could be due to the lack of the HS chain modifier, Sulf1. As outlined above, Sulf1 might be required for $HS23^{+ve}$ chains to present the HS-bound ligand to its receptor on the cell-surface of MC3T3-E1 cells. However, as Shh induces MC3T3-E1 osteoblast differentiation (Yuasa *et al*., 2002), which has been shown to lead to a reduction in Sulf1 expression (Pugdee *et al.*, 2007), the HS chains might not function as they would have done within their developmental context. Transfection of MC3T3-E1 cells to overexpress Sulf1 could develop our understanding of the possible role played by this enzyme in modulating HS-Shh interactions. Finally, as the HS chains used during these experiments were not attached to their core proteins, nor were they part of the cell membrane or a well-organised extracellular matrix, could have hindered their ability to modulate the activity of the Hedgehog pathway. If I was able to attach HS fractions to a core protein and introduced them into a 3D-matrix for cell culture; I would have taken a step towards a more physiological representation of these HS chains, and could have provided a more relevant, and favourable, bioassay.

Due to the underwhelming RT-PCR results I decided to carry out another bioassay to analyse the activity of alkaline phosphatase (ALP) in MC3T3-E1 cells after exposure to the HS fractions in the presence of exogenous Shh. Application of the Shh ligand to MC3T3-E1 cells has been reported to induce differentiation, determined by an increase in ALP activity, of these osteoblasts. I was able to verify this through the addition of rh-SHH to MC3T3-E1 media for 3 or 6 days and seeing a dose-dependent increase in ALP activity (Figure 6-12). Also, addition

of 5 µg/mL $HS23^{+ve}$, for 6 days, induced a notable increase in ALP activity, which was surprising, because the same concentration did not augment the expression of Hedgehog target genes after 48 hours of exposure. However, differences in the timespan of each assay could be an explanation for this. Even more interesting were the results that came after comparing the ability of each HS fraction to modulate ALP activity. $HS23^{+ve}$ at 5 µg/mL increased the activity ALP significantly more so than $HS23^{-ve}$ or HS^{pm}. This was surprising, because Hedgehog gene expression suggested HS^{pm} would induce ALP more so than the positive or negative fractions. This could be due to the HS chains being able to interact with other ligands, or extracellular proteins on MC3T3-E1 cells, during the incubation period, leading to increases in ALP activity through other pathways. Previous experiments have identified BMP-2 as another ligand that can enhance the effects of Shh on differentiating MC3T3-E1 cells to their osteoblast fate (Yuasa *et al*., 2002). It is possible that the foetal bovine serum (FBS) used to supplement the media contained this factor, and when HS chains were added they would bind and augment pathway activity. There was a correlation between the ALP activity of MC3T3-E1 cells and previous results analysing the ability of each HS fraction to bind BMP2 through GAG-binding plate analysis. Further evidence for the presence of other factors in the serum came after RT-PCR analysis showed that the Hedgehog target genes, *Gli1* and *Ptc1*, were dose-dependently reduced after dilution of the FBS content in MC3T3-E1 media (Page 52, Figure 2-8). Therefore, it is likely that the positive fraction is able to interact sufficiently with BMP-2, as well as Shh, to significantly increase ALP activity in MC3T3-E1 cells. Time permitting, it would have been advantageous to analyse ALP activity after application of the BMP inhibitor, Noggin, to cells cultured in $HS23^{+ve}$, $HS23^{-ve}$, or HS^{pm}, in the absence of rh-SHH; however, it was nearing the end of my time in Singapore.

Priority was given to determining the relative amount of ALP activity that was a direct consequence of $HS23^{+ve}$ increasing the activity of the Hedgehog pathway (Figure 6-15).

Application of 5 µM cyclopamine with 250 ng/mL rh-SHH for 6 days was enough to reduce ALP activity back to the levels seen in untreated cells. This showed that I could directly influence MC3T3-E1 differentiation in a Shh-dependent manner. However, when $HS23^{+ve}$ was introduced on its own there was a detectable increase in ALP activity, which was comparable to those levels seen after the administration of rh-SHH alone; but also, upon addition of cyclopamine there was no visible reduction in the activity of ALP. Furthermore, the increase in ALP activity in MC3T3-E1 cells when rh-SHH and $HS23^{+ve}$ were combined boosted levels above Shh alone, however, upon addition of cyclopamine to the same treatment ALP activity was reduced to levels similar to Shh alone. This evidence points to the presence of another factor, within the medium, being targeted by the $HS23^{+ve}$ chain, causing a false-positive increase in ALP activity. The most likely candidate, as mentioned above, is BMP-2.

6.4. Conclusion

Information gathered here has provided us an insight into our abilities, using affinity chromatography, to purify a HS population to target a ligand of interest. I was able to isolate two fractions – positive and negative - of HS that presented differing abilities to bind with Shh, but also presented slight differences when asking the same question using BMP-2. As the scope of this project was to determine the preference of these fractions for Shh I did not have the time or resources to carry out extensive analysis of how these HS fractions interacted with other proteins. Using disaccharide analysis to detect variations between the compositions of each HS fraction, it was evident that the 2-O- and 6-O-sulphate modifications were important to the Shh-binding properties of $HS23^{+ve}$. Finally, as eluded to in the ALP assay, I postulate that $HS23^{+ve}$ could be having off-target effects, through interactions with BMP-2 in the bovine serum of the media.

It is clear that, through affinity chromatography and analysis using biochemical techniques, we were able to isolate two distinct HS fractions. They differed in disaccharide composition but also their ability to bind the Shh ligand. However, it is up for debate whether the positive HS fraction is truly specific to Shh, or whether there is a stronger preference towards the protein whilst still maintaining the ability to interact with some others. It is most likely the latter, due to the length of an individual HS chain and the complexity of their synthesis. It would be incredibly difficult, if at all possible, to isolate a HS fraction with such a high degree of specificity through affinity chromatography alone. It may have been beneficial to synthesise an isolation peptide after using protect and label experiments to identify any other amino acids of the Shh ligand able to bind to HS. However, there is still no guarantee that these HS chains would show an enhanced specificity for Shh. Until we are able to identify unique HS-binding domains of a protein, and also efficiently synthesise our own GAG chains to our predefined length and sequence, it will be incredibly difficult to obtain HS chains that are specific binders of one protein.

7 *In vivo* Analysis of a HS Fraction Designed to Target the Hedgehog Pathway.

7.1. Introduction

In Chapter 6, I was able to isolate, using affinity chromatography, a HS fraction – $HS23^{+ve}$ – that exhibited a stronger preference for Shh binding than its flow-through counterpart, $HS23^{-ve}$, and also presented differences between their disaccharide compositions. They provided promising biochemical results through GAG-binding plate and SPR competition assays. However, cell-based assays provided less promise. Expression of Hedgehog target genes, *Gli1* and *Ptc1*, was not significantly altered in MC3T3-E1 cells exposed to either fraction. On the other hand, analysis of ALP activity provided more promising results, but, whether these were due to the specific modulation of the Hedgehog pathway remains a point of contention. Therefore, testing these two – positive and negative – fractions *in vivo* might shed more light on the abilities of these HS chains to regulate various pathways.

In this chapter I exposed early-stage embryos to HS fractions in an attempt to identify any effects on the expression of read-out genes responsive to Hedgehog, FGF, or Wnt signalling. Furthermore, using the *dackel* zebrafish mutant, which lacks the ability to synthesise normal levels of HS, and fails to regenerate, I attempted to recover this phenotype by applying the newly isolated HS fractions to amputated zebrafish tails.

From the identification of an early requirement for the Hedgehog pathway during wild-type epimorphic regeneration (Chapter 3), and its disruption during HS mutant zebrafish

(Chapter 4) led me to isolate and characterise a HS chain designed to target this pathway (Chapter 6). In this, the final experimental chapter, I am aiming to draw on all this previous knowledge in an attempt to show that glycotherapeutics could work in a zebrafish model.

7.2. Results

7.2.1. HS from the porcine mucosa is not toxic to zebrafish

Before I was able to start using the HS fractions – HS^{pm}, $HS23^{+ve}$ and $HS23^{-ve}$ – in the planned experiments it was important to first determine the toxicity of the GAG to zebrafish. This was done by exposing one-cell stage zebrafish to increasing concentrations of HS^{pm}, in fish water, for 5 days (Figure 7-1).

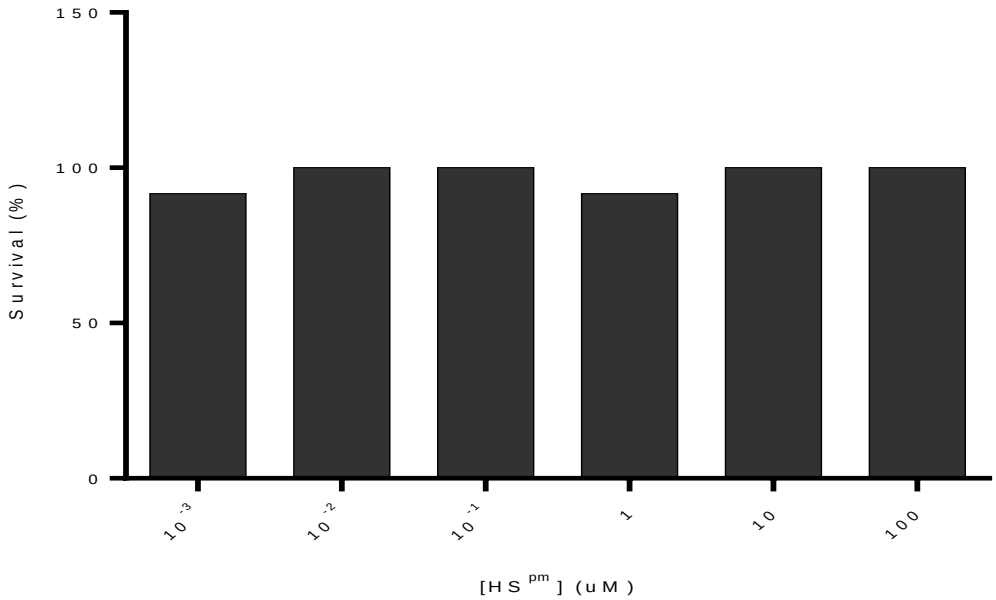

Figure 7-1. Continuous exposure of zebrafish embryos to HS^{pm} is not lethal.
Zebrafish exposed for 5 days – from one-cell stage - to increasing doses of heparan sulphate isolated from porcine mucosa (HS^{pm}). n = 12 embryos per treatment.

The zebrafish embryos were unaffected during early development after continuous exposure to HS. There was an almost consistent 100 % survival rate, even at the highest concentration of 100 µM.

7.2.2. HS23^{+ve} does not affect gene expression during zebrafish development.

The next step was to determine any effects on Hedgehog, FGF, and Wnt pathway activity during zebrafish development after the addition of the HS fractions. Due to limited stock availability HS^{pm} was first used to screen for the ability of 10 or 50 µM to alter pathway read-out transcripts. Therefore, 10 hpf zebrafish were incubated for 14 hours in the presence of HS^{pm}. After this time the embryos were fixed and stained for the Hedgehog, FGF, and Wnt pathway read-outs: *ptc1*, *pea3*, and *axin2*, respectively (Figure 7-2).

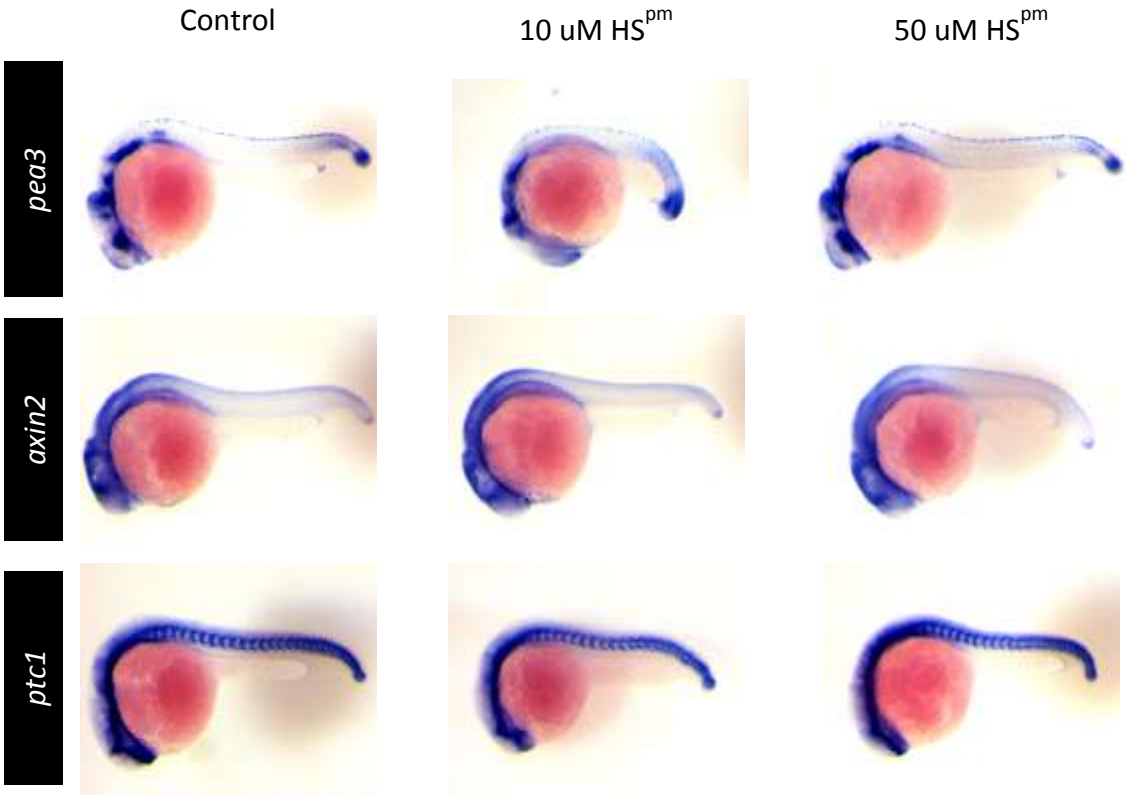

Figure 7-2. Development pathways are unaffected in zebrafish larvae exposed to HS^{pm}.
In situ hybridization to detect the expression of developmental pathway read-outs after HS^{pm} was added to 10-hour post-fertilization (hpf) zebrafish for 14 hours in fish water. Signal pathways detected: FGF (*pea3*); Wnt (*axin2*); Hedgehog (*ptc1*). n = 10 per gene per treatment.

After exposure to the HS starting material there were no obvious changes to developmental pathway activity. *Pea3* in the tail bud and developing brain remained at levels comparable to

control treatments. This was also true when detecting *axin2* and *ptc1* – control zebrafish staining was identical to HS-treated samples. Therefore, the next treatment, applying positive and negative fractions, used the lower of the two concentrations.

There were no detectable changes in developmental pathway activity upon the addition of 10 µM HS23^{+ve} or HS23^{-ve} to fish the water of 10 hpf zebrafish for 14 hours (Figure 7-3).

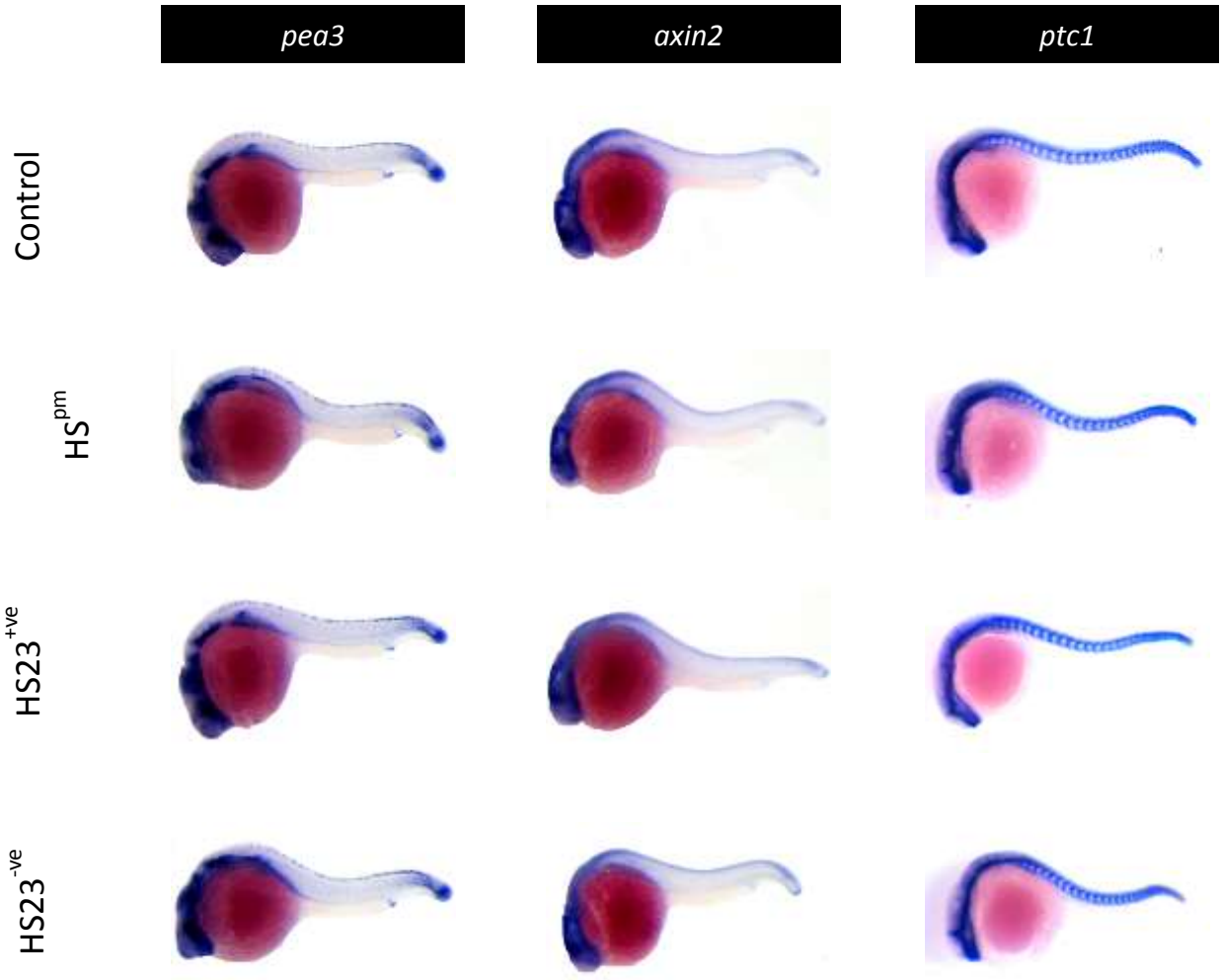

Figure 7-3. HS fractions do not affect gene expression during the early stages of zebrafish development.

In situ hybridization of read-out transcripts for developmental pathways, after 10-hour post fertilization zebrafish were exposed to 10 µM GAG fractions for 14 hours in fish water. Developmental pathways detected: FGF (*pea3*); Wnt (*axin2*); Hedgehog (*ptc1*). n = 10 per gene per treatment.

The HS fractions showed no ability to increase the intensity of any of the read-out transcripts during zebrafish development. All HS treatments showed levels comparable to controls in both

the tail bud and rostral structures, such as the forebrain and hindbrain. Even though this was the case, it was still important to expose the *dackel* zebrafish to these GAG fractions during regeneration.

7.2.3. The HS fractions are unable to rescue *dackel/ext2* tail regeneration.

To determine the effects of GAG exposure during *dackel* tail regeneration, zebrafish were transferred to fish water containing 10 µM of the HS fractions immediately after amputation (Figure 7-4). This would hopefully increase the exposure of cells within the damaged tissues to exogenous heparan sulphate chains, and therefore enable the activation of any molecular cues unable to transduce signals in the absence of endogenous HS.

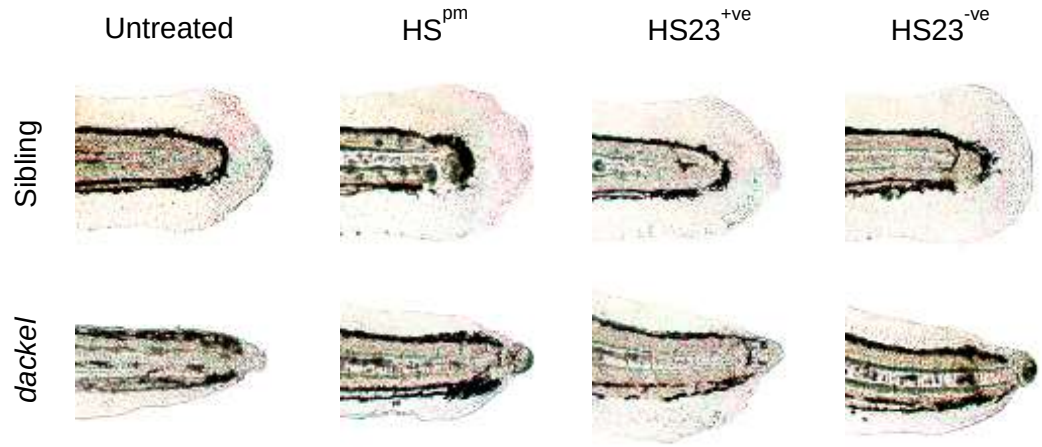

Figure 7-4. Tail regeneration cannot be rescued in *dackel* zebrafish exposed to exogenous HS. Amputated *dackel* and sibling zebrafish tails after recovering for 3 days in the presence, or absence, of 10 µM: HS^{pm}, HS23^{+ve} or HS23^{-ve-}. n = 10 per gene per treatment.

To this end, 2 dpf mutant and sibling zebrafish were amputated and immediately exposed to HS fractions in fish water. The gross morphology of 3 dpa sibling zebrafish tails were not affected after exposure to exogenous HS chains. The same was seen during *dackel* regeneration; I was unable to rescue the regeneration phenotype, presented by the mutant, after application of any of the HS fractions.

7.3. Discussion

After analysing the newly isolated HS23^{+ve} and HS23^{-ve}, and finding differences between their disaccharide composition and Shh-binding abilities, but showing an inability to modulate the Hedgehog pathway through RT-PCR analysis of target genes, I decided to apply these fractions into the larval zebrafish regeneration model to see if there were any effects *in vivo*. I hoped that exogenous HS would incorporate into the extracellular matrix (ECM) to replace the chains lost in *dackel* mutants, enabling ligand-receptor interactions and thus rescue their truncated regeneration phenotype. However, all the results came back negative, with none of the HS fractions able to alter gene expression within developing zebrafish, and also unable to rescue regeneration in *dackel* mutants.

To determine any toxic effects of HS^{pm} on zebrafish I first had to apply increasing concentrations to one-cell stage embryos. The main obstacle to overcome was that of the chorion. During the first 48 hours the zebrafish are supported within a transparent membrane, protecting the developing, fragile embryo from a potentially damaging environment. Kais *et al*. (2013) identified the chorion to become more permeable to relatively low molecular weight (332 and 401 Da), water insoluble fluorescein in the presence of dimethyl sulfoxide (DMSO). However, with the average molecular weight of these HS fractions to be 15,000 Da, I was unsure, and had no way of telling, whether these negatively charged macromolecules would penetrate the chorion, even in the presence of higher concentrations of DMSO. To this end, I decided to compromise the chorion through mechanical disruption, using a surgical blade, after the application of HS^{pm} into the fish water. After this, I did not detect any changes to survivability of embryos exposed to HS chains, or control embryos – pierced chorions in fish water containing molecular water (Figure 7-1, control data not included).

Next, application of these HS fractions to early-stage - 10 hpf - embryos, showed no detectable differences in the expression levels of *pea3*, *axin2* or *ptc1* transcripts. This could be

due to the innate inability of these fractions to modulate developmental pathways, or, as highlighted in the toxicity screen, a permeability issue. Much like the toxicity screen, there was another physical barrier in the way of the highly charged, high molecular weight HS chains – the epithelium. One study showed the outer cell layer to be dependent on the presence of claudin-b (Kwong and Perry. 2013), and upon knockdown the 4 kDa fluorescein, FD-4, was able to accumulate within the yolk sac and pericardial cavity. To alter gene expression within the wild-type fish could have compromised our results, therefore I was unwilling to take this route. Again, DMSO could have been utilised, however this method would most likely be futile as the chemical is usually applied to increase the permeability to low molecular weight drugs.

Finally, in an attempt to rescue *dackel* mutant regeneration, I applied the HS fractions to fish water, in the hope that an open wound could allow some of the chains to enter and bind proteins between cells. The rescue of the mutant zebrafish was unsuccessful, but might not have been due to the inability of HS to penetrate this time; instead, the concentrations might not have been high enough. However, as the quantities of each fraction left were significantly diminished, I was unable to increase concentrations above 10 µM. On the other hand, it could have remained an issue with permeability. To combat this, one method could involve the injection of these fractions directly into the blood stream of uncut zebrafish, and upon amputation the caudal vein and aorta would be severed - allowing for HS chains to leave from the open end, or to exude from any leaky vessels close to the wound site. Time permitting, this would have been the most promising avenue to explore. However, it would have required the injection, into an incredibly narrow vessel, of HS conjugated to a fluorescent label to track the GAGs before and after injury – this would have been technically challenging to pull off, and time did not permit such an ambitious task.

7.4. Conclusion

Above all else, the present study has highlighted problems faced when applying charged macromolecules to whole embryos. Unless the zebrafish could be manipulated, using a technique yet to be discovered, to express the crucial domain of our positive HS fraction, there doesn't seem to be another way to properly expose cells to these GAGs. In the short-term this final chapter was not entirely successful, however in the grand scheme of things it has provided interesting insight into overcoming problems faced during this type of experiment.

8 General Discussion and Future Directions

8.1. General Discussion

In nature a regenerative response depends entirely upon its context. For example, mammalian gut epithelium will continuously rejuvenate itself through the activation of stem cells within the crypts. However, animals such as the newt, salamander, and zebrafish are amongst the elite in harbouring a powerful form of regeneration, known as epimorphic regeneration, to replace their limbs, or caudal fins. The complex process utilises a special mass of cells recruited close to the site of injury called the blastema. Also, developmental pathways, such as the Hh, FGF, and Wnt, are known to be required during the regeneration of the zebrafish caudal fins, and limbs of the aforementioned lower vertebrates. However, no studies allude to the role played by the extracellular matrix in regulating these pathways during regeneration. Understanding this could be a step into an era of molecular manipulation for regenerative therapies. The present study sets out to identify pathways that rely on the presence of an extracellular GAG, HS, and to isolate a HS fraction to rescue regeneration in a zebrafish mutant unable to synthesise its own.

Heparan sulphates (HS) have been described as secondary, extracellular receptors to many ligands, due to their ability to interact with, and augment a response from the bound protein. These polysaccharide chains have been mimicked to assist, through the stabilisation of molecular cues, in the healing of chronic skin wounds, such as diabetic sores (Slim *et al*., 2012). The area of glycotherapeutics has the potential to become a major player in the regenerative field, but at the moment it is in the early stages of its development. However, expanding our knowledge of how HS fits into the regenerative process could assist us in moving towards harbouring that potential for our own gains.

Therefore, I set out to understand the effects of disrupting HS synthesis has on signal pathways during zebrafish tail regeneration. Prior to this study the adult zebrafish had become a well-established model organism in the regenerative field, because of its genetic tractability, and availability of a wide-ranging portfolio of molecular techniques used for experimental analysis. It has assisted in providing insights into the signalling events that can orchestrate epimorphic regeneration. As my study centred on the identification of the *dackel/ext2* mutant's inability to regenerate its caudal fin/tail, and it was unable to survive past 10 dpf, I was restricted to working within its short life span. The most common time point when using larval zebrafish to study regeneration was between 2 and 5 dpf, and so I analysed the process after the amputation of 2 and 3 dpf tails. Also, previous studies amputated larvae within the caudal fin fold, which consists, predominantly, of epithelial tissue, and therefore is less representative of the loss of a multi-tissue structure, such as a limb. I therefore decided to amputate within a feature of the larval tail known as the pigment gap, and analysed the regenerative process through the detection of gene transcripts normally up regulated after the activation of their respective pathways. However, as I was using a relatively new amputation plane within zebrafish larval tails I was interested in determining whether several of the development - Hh, FGF, or Wnt – signal pathways, and also gene markers of the wound epidermis (*dlx5a*) and blastema (*raldh2*), were upregulated in this larval model – which they were. And, as the present study had set out to identify a possible target of a new HS fraction that I would eventually come to isolate, I was particularly interested in determining which pathway was induced the earliest. Through *in situ* hybridisation, and the exposure of regenerating tails to various chemical modulators of the development pathways, I was able to identify Hh to be the first signal to be induced.

Having determined all pathways were upregulated, and the wound epidermis and blastema were present during wild-type regeneration, I next wanted to see the effects of reduced

HS synthesis on these pathways during zebrafish tail regeneration. The *dackel* was an ideal genetic model for targeted HS disruption during regeneration, because the gene mutated - Ext2 – encodes an enzyme reported to only be involved in HS synthesis. Another way I could have disrupted normal HS chain synthesis was through the application of sodium chlorate. However, as a broad-spectrum inhibitor of sulphation, all GAG chains, not just HS, will be disrupted, such as chondroitin sulphate. Through the repetition of *in situ* hybridisation identifying the upregulation of read-out transcripts, I saw that all signal pathways had been disrupted during *dackel/ext2* tail regeneration. Surprisingly, the Hedgehog pathway was the least affected; *ptc1* was still expressed, but at levels lower than in the wild-types. However, as this was still the earliest signal activated I decided that the HS fraction I wanted to isolate would target this pathway, through the binding of a Hedgehog ligand.

During the analysis of *dackel* regeneration I was able to identify ligands – FGF10a and Wnt10a - that, when removed, could lead to a reduced regenerative ability in zebrafish. Due to strain availability, and also literature highlighting the importance of HS-dependent FGF10 signalling during pectoral fin development, I assessed the regenerative capacity of *daedalus/fgf10*^{tbvbo} mutants. Initial 3 dpa results hinted that FGF10 was important for later stages of tail regeneration. This was the case, because gene expression appeared normal, but proliferation was significantly reduced at roughly the time regenerative outgrowth is initiated. Regeneration in *dackel* and *daedalus* mutants exhibited similar levels of proliferation until 48 hpa, at which point the *dackel* had half the number of cells undergoing proliferation. I postulated that this might be due to the expression of another HS-dependent ligand able to induce proliferation, however, this would also mean an increase for *deadalus* mutants; unless FGF10 became as crucial to regeneration as the unidentified factor at the same time, or FGF10 controlled the expression of the mitogen.

The penultimate section of this present study was dedicated to the isolation and biochemical analysis of a new fraction of HS to target the Hh pathway. I was following previous studies carried out by the Cool Lab, using affinity chromatography to isolate BMP-2- and VEGF-binding HS fractions for their use in bone and vascular therapies, respectively (Murali *et al.*, 2013; Wang *et al.*, 2014). Through affinity chromatography, using a peptide sequence for the HS-binding domain of Shh, I was able to see a clearly defined peak on the sensorgram; suggesting a new fraction had been isolated successfully. This was later confirmed by the difference between disaccharide composition of the two – positive and negative – fractions of HS. Binding analysis through GAG-binding plates and SPR competition assays provided strong evidence that the positive, $HS23^{+ve}$, fraction could preferentially bind the Shh ligand. However, MC3T3-1 cells did not show an upregulation in the Hedgehog target genes after the introduction of rh-SHH with $HS23^{+ve}$. Analysis of the ALP activity in the same cells provided more promising data: showing an increase in activity after the positive, but not the negative, fraction was added to culture medium. However, this could have been due to the presence of other HS-binding factors within the serum that could induce osteoblast differentiation, which was further supported after the introduction of the hedgehog inhibitor, cyclopamine.

Finally, I wanted to see if some of the promising *in vitro* data could translate to positive results in the zebrafish model. Unfortunately, adding the HS fractions to the fish water had no effects on gene expression, and did not rescue regeneration in *dackel* mutants. I put this down to the impermeable nature of the epithelium to negatively charged macromolecules. As, to my knowledge, HS chains have not been applied directly to the zebrafish in this way before. I have, at the very least, ruled out this as a valid method, and suggested that HS could have been injected intravenously for release after tail amputation. Therefore, for future novel

glycotherapeutics the route of administration is as crucial to the study as the peptide sequence used for the initial isolation of the GAG fractions.

8.2. Future Directions

The present study made good use of a zebrafish mutant line that was initially intended for studying the causes behind human multiple exostosis (HME). I was able to analyse, in the absence of proper HS synthesis, the process of epimorphic regeneration, and identify key molecular pathways that depend upon these HS chains to mount a regenerative response. However, this was only done in the zebrafish larval model. Therefore, the next logical step would be to determine whether HS synthesis is important for the regeneration of adult zebrafish caudal fins. This would be difficult to achieve, because *dackel* mutants are unable to survive beyond 10 dpf, and so would require the use of morpholino knockdown to target *ext1* or *ext2*, or both. The genetic technique, Cre:Lox, could also be used to induce the over-expression of enzymes involved in the digestion of HS chains, such as heparinise I, II, and III, after amputation. Moreover, their expression could be targeted to the golgi apparatus where HS synthesis takes place.

Identification of zebrafish mutant unable to synthesise HS chains provided an intriguing tool with which to study the early stages of regeneration. As the *dackel* tail still expressed the transcripts for Ihhb and Shha but failed to show any activation of other ligands during regeneration, it would be interesting to see if any other ligands are expressed around the time of the Hedgehog family, such as BMPs or TGFs. And following on from that, studying the possible HS-independent mechanisms behind their induction. A strong candidate that has recently come to light is that of the reactive oxygen species (ROS). Experiments to manipulate ROS synthesis after amputation are underway in the Roehl Lab, and preliminary data is showing promising results. Upon inhibition of the ROS-synthesising enzyme, dual oxidase,

ihhb expression was lost at 6 hpa (data not shown). Furthermore, after amputated larval tails were exposed to the translation-blocking chemical, cyclohexamide, the expression of *ihhb* RNA remained (data not shown). This provides evidence for the presence of a protein, or proteins, that, when activated through wounding, regulate the transcription of crucial, early genes during the regenerative response – most likely of the kinase family. Screening is currently underway to identify any kinases activate during the first hours following resection of zebrafish larval tails.

The present study shows that HS chain synthesis is an important factor during epimorphic regeneration. It would be interesting to screen zebrafish with mutations in other, stage-specific, enzymes during HS synthesis to help identify which modification is the most important one. For example, 6-O-sulphotransferase mutant zebrafish might show a weaker phenotype to the *dackel*, but analysis through *in situ* hybridisation could show which pathway requires that modification during epimorphic regeneration. Instead of manipulating the HS chains, one could look to the core proteins. Disrupting the expression of these proteins could allow us to identify the ones harbouring a specific HS chain required for the progression of regeneration. Finally, it would be interesting to compare regeneration in the UDP-glucose dehydrogenase mutant zebrafish, *jekyll*, to *dackel*. UDP-glucose dehydrogenase is an important enzyme in the synthesis of both HS and chondroitin sulphate (CS). If *Jekyll* presented a more severe regenerative phenotype than *dackel* it could provide evidence for the role of CS during epimorphic regeneration.

As this study used the larval zebrafish, exclusively, to analyse epimorphic regeneration, there was a risk that I was overlapping two major branches of biology – development and regeneration. Evidence for the regrowth of zebrafish tails through epimorphic regeneration, and not just the induction of redevelopment, came after the detection of *dlx5a* and *raldh2*, genetic markers of the WE and blastema, respectively. Their temporospatial expression was

archetypal of a regenerative response: *dlx5a* was upregulated in the distal-most region first, followed by *raldh2* expression in the more proximal blastema. Also, as I saw the expression of *raldh2* within regenerating tails but not within developing zebrafish tail buds (data not shown). Furthermore, the fact that *dackel* zebrafish are able to develop a relatively normal caudal fin fold, but unable to regenerate them following tail amputation, provided more support towards this being epimorphic regeneration.

It seems that 3-day old zebrafish have developed enough of their caudal fin to warrant, after amputation, the initiation of a regenerative response. Experiments recently carried out in the Roehl lab to identify the differences between developmental pathways during tail development and regeneration have provided mixed results. Application of the Hedgehog pathway inhibitor, cyclopamine, to developing larval tails did not affect their development but, as shown in this study, the addition of the same chemical to amputated tails blocks early stages of its regeneration. However, inhibition of the Wnt pathway, after heat shock-induced Dkk1 expression, during development and regeneration halted the progress of both. This could mean the Wnt pathway is conserved during both processes, but Hedgehog seems to have a pivotal role during regeneration only. It would be interesting to determine whether pathways shown to be conserved during development and regeneration use the same branches. If regeneration utilises a different branch, of the same signal, it could support the use of larval zebrafish as a more viable model for the studying the process of epimorphic regeneration.

During the present study, through chemical treatments and *in situ* hybridisation, I was able to identify an interaction between the Wnt and FGF pathways. However, I did not determine which pathway was upstream of the other, or whether these pathways acted in parallel - modulating one another during the entire process of tail regeneration. After chemical treatment of tails prior to 30 hpa, I saw that the manipulation of one pathway altered the expression of the opposing pathway's read-out gene, and therefore could only deduce that they

can act upon each other at this stage, with no obvious linear interaction. But, to determine which influenced which first, I could have carried out a classic inhibitor-activator epistasis experiment. This was recently carried out by the Roehl lab, and identified Wnt to be upstream of the FGF pathway.

The isolation and analysis of a novel HS fraction, $HS23^{+ve}$, to bind a Hedgehog ligand, provided more questions than answers. The positive fraction exhibited an increase in disaccharide subunits containing 2- and 6-O-sulphate modifications, which hinted at a dependency upon them for Shh-binding. To determine the importance of each HS modification, in place of HS fractions, predefined heparin oligomers modified exclusively with either of the two sulphate modifications, could have been applied to an SPR competition assay. The amount of Shh competed away would be directly influenced by which modification was the most critical for the binding of Shh.

A method, highlighted in Chapter 6, exploiting the protection given to amino acids, preventing their chemical modification, could be used to identify the HS-binding sequence of a protein, and then applied to a column for the HPLC isolation of HS fractions. Prior to the synthesis of an isolation peptide, analysis could be carried out to identify which amino acids provide the ligand with its ability to bind to HS. After replacing each amino acid, protected after binding HS, for nonpolar ones, and analysing changes in Shh's affinity for HS, would help to determine which are indispensable for HS binding. This could have provided a less promiscuous Shh-binding fraction of HS. After its isolation, instead of testing the HS fractions in a zebrafish model, it might be beneficial to apply them to a critical-sized bone defect in rabbits – a model often used by the Cool Lab (Singapore). As the Hedgehog ligands play an important role during osteogenesis, they could have a role during bone repair. Applying the positive fraction to a scaffold – as opposed to freely diffusible HS in fish water - prior to implantation could also provide the HS chains a medium to enhance their biological activity.

The main long-term conclusion of the future studies would be to develop a glycotherapeutic that could rescue the regenerative phenotype of the *dackel* zebrafish. As this study presented the importance of the Hedgehog pathway during the early stages of regeneration, but failed to provide a suitable HS fraction to target a ligand, further work towards the detection of novel HS-binding regions of the Hedgehog ligands could assist in the isolation of more biologically active HS chains. Also, identifying a novel way to apply newly isolated HS fractions to the zebrafish model, so that they are more accessible to cells contributing to regeneration, for example, administered intravenously before or after tail amputation. Beyond the scope of this study, glycotherapeutics able to initiate regeneration in the *dackel* could eventually lead to their application in higher vertebrate studies for the same purpose.

8.3. Conclusion

The molecular mechanisms behind epimorphic regeneration in several organisms have been studied extensively, however, the role played by the extracellular matrix (ECM) is not well characterised. The present study has successfully identified several pathways – Hh, FGF, and Wnt - that rely upon the presence of HS during epimorphic regeneration. Loss of faithful HS synthesis caused a down regulation in Hh activity, and the loss of downstream FGF and Wnt pathway activity. In an attempt to rescue the *dackel/ext2*, I successfully isolated a new population of HS chains using the HS-binding sequence of the Shh protein. However, application *in vivo* provided no positive results during the analysis developmental pathway activity, and gross morphology of regenerating *dackel* tails. Therefore, the isolation of a highly specific Hedgehog-binding HS fraction, alongside a more calculated approach to its application, could eventually provide enough data in zebrafish for its application, as a regenerative factor, to higher vertebrate models.

References

- Bai. S., Thummel. R., Godwin. A., Nagase. H., Itoh. Y., Li. L., Evans. R., McDermott. J., Seiki. M. and Sarras. M. (2005). Matrix metalloproteinase expression and function during fin regeneration in zebrafish: Analysis of MT1-MMP, MMP2 and TIMP2. *Matrix Biology*, 24(4), pp.247-260.
- Bellusci. S., Grindley. J., Emoto. H., Itoh. N and Hogan. B. (1997). Fibroblast Growth Factor 10 (FGF10) and branching morphogenesis in the embryonic mouse lung. *Development*, 124, pp.4867-4878.
- Bhushan. A., Itoh. N., Kato. S, Thiery. J., Czernichow. P, Bellusci. S and Scharfmann. R. (2001) Fgf10 is essential for maintaining the proliferative capacity of epithelial progenitor cells during early pancreatic organogenesis. *Development,* 128, pp.5109-5117.
- Bloechlinger. S., Karchewski. L and Woolf. C. (2004). Dynamic changes in glypcan-1 expression in dorsal root ganglion neurons after peripheral and central axonal injury. *European Journal of Neuroscience*, 19, pp.1119-1132.
- Blum, N. and Begemann, G. (2011). Retinoic acid signaling controls the formation, proliferation and survival of the blastema during adult zebrafish fin regeneration. *Development*, 139(1), pp.107-116.
- Bornemann, D. Duncan. J., Staatz. W., Selleck. S and Warrior. R. (2004). Abrogation of heparan sulfate synthesis in Drosophila disrupts the Wingless, Hedgehog and Decapentaplegic signaling pathways. *Development,* 131(9), pp.1927-1938.
- Brockes, J. (1997). Amphibian Limb Regeneration: Rebuilding a Complex Structure. *Science*, 276(5309), pp.81-87.
- Burke, R., Nellen, D., Bellotto, M., Hafen, E., Senti, K., Dickson, B. and Basler, K. (1999). Dispatched, a Novel Sterol-Sensing Domain Protein Dedicated to the Release of Cholesterol-Modified Hedgehog from Signaling Cells. *Cell*, 99(7), pp.803-815.
- Busse, M., Feta, A., Presto, J., Wilen, M., Gronning, M., Kjellen, L. and Kusche-Gullberg, M. (2007). Contribution of EXT1, EXT2, and EXTL3 to Heparan Sulfate Chain Elongation. *Journal of Biological Chemistry*, 282(45), pp.32802-32810.
- Casar. J., Cabello-Verrugio. C., Olguin. H., Aldunate. R., Inestrosa. N and Brandan. E (2004). Heparan sulfate proteoglycans are increased during skeletal muscle regeneration: requirement of syndecan-3 for successful fiber formation. *Journal of Cell Science*, 117(1), pp.73-84.
- Chang. S., Mulloy. B., Magee. A. and Couchman. J. (2011). Two Distinct Sites in Sonic Hedgehog Combine for Heparan Sulfate Interactions and Cell Signaling Functions. *Journal of Biological Chemistry*, 286(52), pp.44391-44402.
- Christensen, R., Weinstein, M. and Tassava, R. (2002). Expression of fibroblast growth factors 4, 8, and 10 in limbs, flanks, and blastemas ofAmbystoma. *Dev. Dyn.*, 223(2), pp.193-203.
- Clément, A., Wiweger, M., von der Hardt, S., Rusch, M., Selleck, S., Chien, C. and Roehl, H. (2008). Regulation of Zebrafish Skeletogenesis by ext2/dackel and papst1/pinscher. *PLoS Genetics*, 4(7), p.e1000136.
- Dailey, L., Ambrosetti, D., Mansukhani, A. and Basilico, C. (2005). Mechanisms underlying differential responses to FGF signaling. *Cytokine & Growth Factor Reviews*, 16(2), pp.233-247.
- Danesin, C. Agius. E., Escalas. N., Ai. X., Emerson. C., Cochard. P and Soula. C. (2006). Ventral Neural Progenitors Switch toward an Oligodendroglial Fate in Response to Increased

Sonic Hedgehog (Shh) Activity: Involvement of Sulfatase 1 in Modulating Shh Signaling in the Ventral Spinal Cord. *Journal of Neuroscience*, 26(19), pp.5037-5048.

- Desbordes, S and Sanson. B. (2003). The glypican Dally-like is required for Hedgehog signalling in the embryonic epidermis of Drosophila. *Development*, 130(25), pp.6245-6255.
- Dhoot. G., Gustafsson. M., Ai. X., Sun. W., Standiford. D and Emerson Jr. C (2001). Regulation of Wnt Signaling and Embryo Patterning by an Extracellular Sulfatase. *Science*, 293(5535), pp.1663-1666.
- Dierker, T., Dreier, R., Petersen, A., Bordych, C. and Grobe, K. (2009). Heparan Sulfate-modulated, Metalloprotease-mediated Sonic Hedgehog Release from Producing Cells. *Journal of Biological Chemistry*, 284(12), pp.8013-8022.
- Dierker, T., Dreier, R., Petersen, A., Bordych, C. and Grobe, K. (2009). Heparan Sulfate-modulated, Metalloprotease-mediated Sonic Hedgehog Release from Producing Cells. *Journal of Biological Chemistry*, 284(12), pp.8013-8022.
- Dinsmore, C. (1996). Urodele limb and tail regeneration in early biological thought: an essay on scientific controversy and social change. *Int. J. Dev. Bio.*, 40: 621-627.
- Dixon, G., Elks, P., Loynes, C., Whyte, M. and Renshaw, S. (2012). A Method for the In Vivo Measurement of Zebrafish Tissue Neutrophil Lifespan. *ISRN Hematology*, 2012, pp.1-6.
- Dorey, K. and Amaya, E. (2010). FGF signalling: diverse roles during early vertebrate embryogenesis. *Development*, 137(22), pp.3731-3742.
- Echeverri, K., Clarke, J. and Tanaka, E. (2001). In Vivo Imaging Indicates Muscle Fiber Dedifferentiation Is a Major Contributor to the Regenerating Tail Blastema. *Developmental Biology*, 236(1), pp.151-164.
- Endo. K., Takino. T., Miyamori. H., Kinsen. H., Yoshizaki. T., Furukawa. M and Sato. H. (2003). Cleavage of Syndecan-1 by Membrane Type Matrix Metalloproteinase-1 Stimulates Cell Migration. *Journal of Biological Chemistry*, 278(42), pp.40764-40770.
- Endo. K., Takino. T., Miyamori. H., Kinsen. H., Yoshizaki. T., Furukawa. M., and Sato. H. (2003). Cleavage of Syndecan-1 by Membrane Type Matrix Metalloproteinase-1 Stimulates Cell Migration. *Journal of Biological Chemistry*, 278(42), pp.40764-40770.
- Esko, J. and Lindahl, U. (2001). Molecular diversity of heparan sulfate. *Journal of Clinical Investigation*, 108(2), pp.169-173.
- Esko, J. and Selleck, S. (2002). Order Out of Chaos: Assembly of Ligand Binding Sites in Heparan Sulfate 1. *Annu. Rev. Biochem.*, 71(1), pp.435-471.
- Farshi. P., Ohlig. S., Pickhinke. U., Hoing. S., Jochmann. K., Lawrence. R., Dreier. R., Dierker. T. and Grobe. K. (2011). Dual Roles of the Cardin-Weintraub Motif in Multimeric Sonic Hedgehog. *Journal of Biological Chemistry*, 286(26), pp.23608-23619.
- Fischer. S., Filipek-Gorniok. B. and Ledin, J. (2011). Zebrafish Ext2 is necessary for Fgf and Wnt signaling, but not for Hh signaling. *BMC Developmental Biology*, 11(1), pp.53.
- Fuerer, C., Habib, S. and Nusse, R. (2010). A study on the interactions between heparan sulfate proteoglycans and Wnt proteins. *Dev. Dyn.*, 239(1), pp.184–190.
- Gibert. Y., Gajewski. A., Meyer. A and Begemann. G. (2006). Induction and prepatterning of the zebrafish pectoral fin bud requires axial retinoic acid signaling. *Development*, 133(14), pp.2649-2659.
- Gong. Z., Ju. B., Wang. X., He. J., Wan. H., Sudha. P and Yan. T. (2002). Green Fluorescent Protein Expression in Germ-Line Transmitted Transgenic Zebrafish Under a Stratified Epithelial Promoter From *Keratin8. Dev. Dyn*, 223, pp.204-215.
- González-Rubio. M., Voit. S., Rodríguez-Puyol. D., Eber. M. and Marx. M. (1996). Oxidative stress induces tyrosine phosphorylation of PDGF α- and β-receptors and pp60$^{c\text{-}src}$ in mesangial cells. *Kidney International,* 50, pp.164-173.

- Grandel. H., Draper. B and Schulte-Merker. S. (2000). dackel acts in the ectoderm of the zebrafish pectoral fin bud to maintain AER signalling. *Development*, 127, pp.4169-4178.
- Han, C. Belenkaya. T., Khodoun. M., Tauchi. M., Lin. X and Lin. X. (2004). Distinct and collaborative roles of Drosophila EXT family proteins in morphogen signalling and gradient formation. *Development*, 131(7), pp.1563-1575.
- Han, C. Yan. D., Belenkaya. T and Lin. X (2005). Drosophila glypicans Dally and Dally-like shape the extracellular Wingless morphogen gradient in the wing disc. *Development*, 132(4), pp.667-679.
- Heude. É., Shaikho. S. and Ekker. M. (2014). The dlx5a/dlx6a Genes Play Essential Roles in the Early Development of Zebrafish Median Fin and Pectoral Structures. *PLoS ONE*, 9(5), p.e98505.
- Hynes. R. (2009). The Extracellular Matrix: Not Just Pretty Fibrils. *Science*, 326(5957), pp.1216-1219.
- Ingham, P., Nakano, Y. and Seger, C. (2011). Mechanisms and functions of Hedgehog signalling across the metazoa. *Nat Rev Genet*, 12(6), pp.393-406.
- Iovine, M., Higgins, E., Hindes, A., Coblitz, B. and Johnson, S. (2005). Mutations in *connexin43* (*GJA1*) perturb bone growth in zebrafish fins. *Developmental Biology*, 278(1), pp.208-219.
- Jackman, W., Yoo, J. and Stock, D. (2010). Hedgehog signaling is required at multiple stages of zebrafish tooth development. *BMC Developmental Biology*, 10(1), pp.119.
- Jho, E., Zhang, T., Domon, C., Joo, C., Freund, J. and Costantini, F. (2002). Wnt/ -Catenin/Tcf Signaling Induces the Transcription of Axin2, a Negative Regulator of the Signalling Pathway. *Molecular and Cellular Biology*, 22(4), pp.1172-1183.
- Kais. B., Schneider. K., Keiter. S., Henn. K., Ackermann. C and Braunbeck. T. (2013). DMSO modifies the permeability of the zebrafish (Danio rerio) chorion-Implications for the fish embryo test (FET). *Aquatic Toxicology*, 140-141, pp.229-238.
- Kawakami. A., Fukazawa. T and Takeda. H. (2004). Early Fin Primordia of Zebrafish Larvae Regenerate by a Similar Growth Control Mechanism with Adult Regeneration. *Dev. Dyn.*, 231, pp.693-699.
- Kim, B., Kitagawa, H., Tanaka, J., Tamura, J. and Sugahara, K. (2003). In Vitro Heparan Sulfate Polymerization: Crucial Roles of Core Protein Moieties of Primer Substrates in Addition to the EXT1-EXT2 Interaction. *Journal of Biological Chemistry*, 278(43), pp.41618-41623.
- Kimmel, C., Ballard, W., Kimmel, S., Ullmann, B. and Schilling, T. (1995). Stages of embryonic development of the zebrafish. *Dev. Dyn.*, 203(3), pp.253-310.
- Koziel, L., Kunath, M., Kelly, O. and Vortkamp, A. (2004). Ext1-Dependent Heparan Sulfate Regulates the Range of Ihh Signaling during Endochondral Ossification. *Developmental Cell*, 6(6), pp.801-813.
- Kwong. R and Perry. S. (2013). The tight junction protein claudin-b regulates epithelial permeability and sodium handling in larval zebrafish, Danio rerio. *Am J Physiol Regul Integr Comp Physiol*, 304(7), pp.R504-R513.
- Lee, J., von der Hardt, S., Rusch, M., Stringer, S., Stickney, H., Talbot, W., Geisler, R., Nüsslein-Volhard, C., Selleck, S., Chien, C. and Roehl, H. (2004). Axon Sorting in the Optic Tract Requires HSPG Synthesis by ext2 (dackel) and extl3 (boxer). *Neuron*, 44(6), pp.947-960.
- Lee, Y. Grill. S., Sanchez. A., Murphy-Ryan. M and Poss. K. (2005). Fgf signaling instructs position-dependent growth rate during zebrafish fin regeneration. *Development*, 132(23), pp.5173-5183.

- Lee, Y., Hami, D., De Val, S., Kagermeier-Schenk, B., Wills, A., Black, B., Weidinger, G. and Poss, K. (2009). Maintenance of blastemal proliferation by functionally diverse epidermis in regenerating zebrafish fins. *Developmental Biology*, 331(2), pp.270-280.
- Lin, G. and Slack, J. (2008). Requirement for Wnt and FGF signaling in Xenopus tadpole tail regeneration. *Developmental Biology*, 316(2), pp.323-335.
- Lin. X., Buff2. E., Perrimon. N and Michelson. A. (1999). Heparan sulfate proteoglycans are essential for FGF receptor signalling during Drosophila embryonic development. *Development*, 126, pp3715-3723.
- Lobb, R. and Fett, J. (1984). Purification of two distinct growth factors from bovine neural tissue by heparin affinity chromatography. *Biochemistry*, 23(26), pp.6295-6299.
- Logan, C. and Nusse, R. (2004). The Wnt Signaling Pathway in Development and Disease. *Annual Review of Cell and Developmental Biology*, 20(1), pp.781-810.
- Love, N., Chen, Y., Ishibashi, S., Kritsiligkou, P., Lea, R., Koh, Y., Gallop, J., Dorey, K. and Amaya, E. (2013). Amputation-induced reactive oxygen species are required for successful Xenopus tadpole tail regeneration. *Nature Cell Biology*, 15(2), pp.222-228.
- MacDonald, B., Tamai, K. and He, X. (2009). Wnt/β-Catenin Signaling: Components, Mechanisms, and Diseases. *Developmental Cell*, 17(1), pp.9-26.
- Mathew, L., Sengupta, S., Franzosa, J., Perry, J., La Du, J., Andreasen, E. and Tanguay, R. (2009). Comparative Expression Profiling Reveals an Essential Role for Raldh2 in Epimorphic Regeneration. *Journal of Biological Chemistry*, 284(48), pp.33642-33653.
- Meeker, N., Hutchinson, S., Ho, L. and Trede, N. (2007). Method for isolation of PCR-ready genomic DNA from zebrafish tissues. *BioTechniques*, 43(5), pp.610-614.
- Mills. A., Zheng. B., Wang. X., Vogelk. H., Roop. D & Bradley. A. (1999). p63 is a p53 homologue required for limb and epidermal morphogenesis. *Nature*, 398, pp.708-713.
- Min, H., Danilenko, D., Scully, S., Bolon, B., Ring, B., Tarpley, J., DeRose, M. and Simonet, W. (1998). Fgf-10 is required for both limb and lung development and exhibits striking functional similarity to Drosophila branchless. *Genes & Development*, 12(20), pp.3156-3161.
- Monaghan, J. and Maden, M. (2012). Visualization of retinoic acid signaling in transgenic axolotls during limb development and regeneration. *Developmental Biology*, 368(1), pp.63-75.
- Morimoto-Tomita. M., Uchimura. K., Werb. Z., Hemmerich. S and Rosen. S. (2002). Cloning and Characterization of Two Extracellular Heparin-degrading Endosulfatases in Mice and Humans. *Journal of Biological Chemistry*, 277(51), pp.49175-49185.
- Murakami, K., Namikawa, K., Shimizu, T., Shirasawa, T., Yoshida, S. and Kiyama, H. (2006). Nerve injury induces the expression of EXT2, a glycosyltransferase required for heparan sulfate synthesis. *Neuroscience*, 141(4), pp.1961-1969.
- Murali. S., Rai. B., Dombrowski. C., Lee. J., Lim. Z., Bramono. D., Ling. L., Bell. T., Hinkley. S., Nathan. S., Hui. J., Wong. H., Nurcombe. V and Cool. S. (2013). Affinity-selected heparan sulfate for bone repair. *Biomaterials*, 34, pp.5594-5605.
- Nakato. H., Futch. T and Selleck. S. (1995). The division abnormally delayed (dally) gene: a putative integral membrane proteoglycan required for cell division patterning during postembryonic development of the nervous system in Drosophila. *Development*, 121, pp.3687-3702.
- Nechiporuk. A and Keating. M. (2002). A proliferation gradient between proximal and msxb-expressing distal blastema directs zebrafish fin regeneration. *Development*, 129, pp.2607-2617.
- Ng. J., Kawakami. Y., Büscher. D., Raya. Á., Itoh. T, M. Koth. C., Esteban. C., Rodríguez-León. J., Garrity. D., Fishman. M and Belmonte. J. (2002). The limb identity gene Tbx5

promotes limb initiation by interacting with Wnt2b and Fgf10. *Development,* 129, pp.5161-5170.

- Norton, W., Ledin. J., Grandel. H and Neumann. C. (2005). HSPG synthesis by zebrafish Ext2 and Extl3 is required for Fgf10 signalling during limb development. *Development*, 132(22), pp.4963-4973.
- Nusse, R. (2003). Wnts and Hedgehogs: lipid-modified proteins and similarities in signaling mechanisms at the cell surface. *Development*, 130(22), pp.5297-5305.
- Nüsslein-Volhard. C and Wieschaus. E. (1980). Mutations affecting segment number and polarity in Drosophila. *Nature*, 287(5785), pp.795-801.
- Ohuchi. H., Nakagawa. T., Yamamoto. A., Araga. A., Takeshi Ohata. T., Ishimaru. Y., Yoshioka. H., Kuwana. T., Nohno. T., Yamasaki. M., Itoh. N and Noji. S. (1997). The mesenchymal factor, FGF10, initiates and maintains the outgrowth of the chick limb bud through interaction with FGF8, an apical ectodermal factor. *Developmental*, 124, pp.2235-2244.
- Page-McCaw, A., Ewald, A. and Werb, Z. (2007). Matrix metalloproteinases and the regulation of tissue remodelling. *Nature Reviews Molecular Cell Biology*, 8(3), pp.221-233.
- Pan, Y., Woodbury, A., Esko, J., Grobe, K. and Zhang, X. (2006). Heparan sulfate biosynthetic gene Ndst1 is required for FGF signaling in early lens development. *Development*, 133(24), pp.4933-4944.
- Pearse, R., Vogan, K. and Tabin, C. (2001). Ptc1 and Ptc2 Transcripts Provide Distinct Readouts of Hedgehog Signaling Activity during Chick Embryogenesis. *Developmental Biology*, 239(1), pp.15-29.
- Perathoner, S., Daane, J., Henrion, U., Seebohm, G., Higdon, C., Johnson, S., Nüsslein-Volhard, C. and Harris, M. (2014). Bioelectric Signaling Regulates Size in Zebrafish Fins. *PLoS Genetics*, 10(1), p.e1004080.
- Pfefferli, C. and Jaźwińska, A. (2015). The art of fin regeneration in zebrafish. *Regeneration*, 2(2), pp.72-83.
- Poleo, G., Brown, C., Laforest, L. and Akimenko, M. (2001). Cell proliferation and movement during early fin regeneration in zebrafish. *Dev. Dyn.*, 221(4), pp.380-390.
- Poss, K., Keating, M. and Nechiporuk, A. (2003). Tales of regeneration in zebrafish. *Dev. Dyn.*, 226(2), pp.202-210.
- Poss, K., Shen, J. and Keating, M. (2000b). Induction of lef1 during zebrafish fin regeneration. *Dev. Dyn.*, 219(2), pp.282-286.
- Poss, K., Shen, J., Nechiporuk, A., McMahon, G., Thisse, B., Thisse, C. and Keating, M. (2000a). Roles for Fgf Signaling during Zebrafish Fin Regeneration. *Developmental Biology*, 222(2), pp.347-358.
- Poss, K., Wilson, L., Keating, M. (2002). Heart Regeneration in Zebrafish. *Science*, 298(5601), pp.2188-2190.
- Pugdee. K., Shibata. Y., Yamamichi. N., Tsutsumi. H., Yoshinari. M., Abiko. Y and Hayakawa. T. (2007). Gene Expression of MC3T3-E1 Cells on Fibronextin-immobilized Titanium Using Tresyl Chloride Activation Technique. *Dental Materials Journal*, 26(5), pp.647-655.
- Pye, D., Vives, R., Turnbull, J., Hyde, P. and Gallagher, J. (1998). Heparan Sulfate Oligosaccharides Require 6-O-Sulfation for Promotion of Basic Fibroblast Growth Factor Mitogenic Activity. *Journal of Biological Chemistry*, 273(36), pp.22936-22942.
- Quint, E., Smith, A., Avaron, F., Laforest, L., Miles, J., Gaffield, W. and Akimenko, M. (2002). Bone patterning is altered in the regenerating zebrafish caudal fin after ectopic expression of sonic hedgehog and bmp2b or exposure to cyclopamine. *Proceedings of the National Academy of Sciences*, 99(13), pp.8713-8718.

- Rapraeger, A., Krufka, A. and Olwin, B. (1991). Requirement of heparan sulfate for bFGF-mediated fibroblast growth and myoblast differentiation. *Science*, 252(5013), pp.1705-1708.
- Roehl, H. and Nüsslein-Volhard, C. (2001). Zebrafish pea3 and erm are general targets of FGF8 signaling. *Current Biology*, 11(7), pp.503-507.
- Roelink, H., Porter, J., Chiang, C., Tanabe, Y., Chang, D., Beachy, P. and Jessell, T. (1995). Floor plate and motor neuron induction by different concentrations of the amino-terminal cleavage product of sonic hedgehog autoproteolysis. *Cell*, 81(3), pp.445-455.
- Rubin. J., Choi. Y and Segal. R. (2002). Cerebellar proteoglycans regulate sonic hedgehog responses during development. *Development*, 129, pp.2223-2232.
- Rubin. J., Choi. Y and Segal. R. (2002). Cerebellar proteoglycans regulate sonic hedgehog responses during development. *Development*, 129, pp.2223-2232.
- Sarrazin, S., Lamanna, W. and Esko, J. (2011). Heparan Sulfate Proteoglycans. *Cold Spring Harbor Perspectives in Biology*, 3(7), pp.a004952-a004952.
- Schebesta, M., Lien, C., Engel, F. and Keating, M. (2006). Transcriptional Profiling of Caudal Fin Regeneration in Zebrafish. *The Scientific World JOURNAL*, 6, pp.38-54.
- Schlessinger, J., Plotnikov, A., Ibrahimi, O., Eliseenkova, A., Yeh, B., Yayon, A., Linhardt, R. and Mohammadi, M. (2000). Crystal Structure of a Ternary FGF-FGFR-Heparin Complex Reveals a Dual Role for Heparin in FGFR Binding and Dimerization. *Molecular Cell*, 6(3), pp.743-750.
- Schnapp, E. Kragl. M., Rubin. L and Tanaka. E. (2005). Hedgehog signaling controls dorsoventral patterning, blastema cell proliferation and cartilage induction during axolotl tail regeneration. *Development*, 132(14), pp.3243-3253.
- Sekine. K., Ohuchi. H., Fujiwara. M., Yamasaki. M., Yoshizawa. T., Sato. T., Yagishita. N., Matsui. D., Koga. Y., Itoh. N and Kato. S. (1999). *Nature Genetics*, 21, pp.138-141.
- Shimokawa, T., Yasutaka, S., Kominami, R. and Shinohara, H. (2012). Wound epithelium function in axolotl limb regeneration. *Okajimas Folia Anat. Jpn.*, 89(3), pp.75-81.
- Singh, B., Doyle, M., Weaver, C., Koyano-Nakagawa, N. and Garry, D. (2012). Hedgehog and Wnt coordinate signaling in myogenic progenitors and regulate limb regeneration. *Developmental Biology*, 371(1), pp.23-34.
- Slim. I., Tajouri. H., Barritault. D., Njah. M., Ach. K., Chaie. M and Chaieb. L. (2012). Matrix Protection Therapy in Diabetic Foot Ulcers: Pilot Study of CACIPLIQ20. *Journal of Wound Technology*, (17), pp.16-20.
- Solomon. L. (1963). Hereditary Multiple Exostosis. *The Journal of Bone and Joint Surgery*, 45(2), pp.292-304.
- Song, H. Shi. W, Xiang. Y and Filmus. J. (2005). The Loss of Glypican-3 Induces Alterations in Wnt Signaling. *Journal of Biological Chemistry*, 280(3), pp.2116-2125.
- Stark, D. and Kulesa, P. (2007). An in vivo comparison of photoactivatable fluorescent proteins in an avian embryo model. *Dev. Dyn.*, 236(6), pp.1583-1594.
- Stickens, D., Zak. B., Rougier. N., Esko. J., and Werb. Z. (2005). Mice deficient in Ext2 lack heparan sulfate and develop exostoses. *Development*, 132(22), pp.5055-5068.
- Stoick-Cooper, C., Weidinger, G., Riehle, K., Hubbert, C., Major, M., Fausto, N. and Moon, R. (2006). Distinct Wnt signaling pathways have opposing roles in appendage regeneration. *Development*, 134(3), pp.479-489.
- Tanaka, E., Gann. A., Gates. P. and Brockes. J. (1997). Newt Myotubes Reenter the Cell Cycle by Phosphorylation of the Retinoblastoma Protein. *The Journal of Cell Biology*, 136(1), pp.155-165.
- Taniguchi, Y., Watanabe, K. and Mochii, M. (2014). Notochord-derived hedgehog is essential for tail regeneration in Xenopus tadpole. *BMC Developmental Biology*, 14(1), pp.27-35.

- Taniguchi, Y., Watanabe, K. and Mochii, M. (2014). Notochord-derived hedgehog is essential for tail regeneration in Xenopus tadpole. *BMC Developmental Biology*, 14(1), p.27.
- Tao, H. Shimizu. M., Kusumoto. R., Ono. K., Noji. S and Ohuchi. H. (2005). A dual role of FGF10 in proliferation and coordinated migration of epithelial leading edge cells during mouse eyelid development. *Development,* 132(14), pp.3217-3230.
- Thornton, C. (1957). The effect of apical cap removal on limb regeneration in Amblystoma larvae. *J. Exp. Zool.*, 134(2), pp.357-381.
- Thummel, R., Bai, S., Sarras, M., Song, P., McDermott, J., Brewer, J., Perry, M., Zhang, X., Hyde, D. and Godwin, A. (2006). Inhibition of zebrafish fin regeneration using in vivo electroporation of morpholinos against fgfr1 and msxb. *Dev. Dyn.*, 235(2), pp.336-346.
- Tu, S. and Johnson, S. (2011). Fate Restriction in the Growing and Regenerating Zebrafish Fin. *Developmental Cell*, 20(5), pp.725-732.
- Van Eeden. FJ., Granato. M., Schach. U., Brand. M., Furutani-Seiki. M., Haffter. P., Hammerschmidt. M., Heisenberg. CP., Jiang. YJ., Kane. DA., Kelsh. RN., Mullins. MC., Odenthal. J., Warga. RM and Nüsslein-Volhard. C. (1996). Genetic analysis of fin formation in the zebrafish, Danio rerio. *Development,* 123, pp.255-262.
- Wang. C., Poon. S., Murali. S., Koo. C., Bell. T., Hinkley. S., Yeong. H., Bhakoo. K., Victor Nurcombe. V and Cool. S. (2014). Engineering a vascular endothelial growth factor 165-binding heparan sulfate for vascular therapy. *Biomaterials,* 35(25), pp.6776–6786.
- Wassmer, S., Beddaoui, M., Rajai, P., Munger, R. and Tsilfidis, C. (2013). A Focus on the Optical Properties of the Regenerated Newt Lens. *PLoS ONE*, 8(8), p.e70845.
- Wehner, D., Cizelsky, W., Vasudevaro, M., Özhan, G., Haase, C., Kagermeier-Schenk, B., Röder, A., Dorsky, R., Moro, E., Argenton, F., Kühl, M. and Weidinger, G. (2014). Wnt/β-Catenin Signaling Defines Organizing Centers that Orchestrate Growth and Differentiation of the Regenerating Zebrafish Caudal Fin. *Cell Reports*, 6(3), pp.467-481.
- Wei. Y., Yu. L., Bowen. J., Gorovsky. M and C. Allis. (1999). Phosphorylation of Histone H3 Is Required for Proper Chromosome Condensation and Segregation. *Cell,* 97, pp.99-109.
- White. J., Boffa. M., Jones. B., and Petkovich. M. (1994). A zebrafish retinoic acid receptor expressed in the regenerating caudal fin. *Development,* 120, pp.1861-1872.
- Whitehead, G., Makino. S., Lien. C and Keating. M. (2005). Fgf20 Is Essential for Initiating Zebrafish Fin Regeneration. *Science*, 310(5756), pp.1957-1960.
- Witt, R., Hecht, M., Pazyra-Murphy, M., Cohen, S., Noti, C., van Kuppevelt, T., Fuller, M., Chan, J., Hopwood, J., Seeberger, P. and Segal, R. (2013). Heparan Sulfate Proteoglycans Containing a Glypican 5 Core and 2-O-Sulfo-iduronic Acid Function as Sonic Hedgehog Co-receptors to Promote Proliferation. *Journal of Biological Chemistry*, 288(36), pp.26275-26288.
- Xu. X., Weinstein. M., Li. C., Naski. M., Cohen. R., Ornitz. D., Leder. P and Deng. C. (1998). Fibroblast growth factor receptor 2 (FGFR2)-mediated reciprocal regulation loop between FGF8 and FGF10 is essential for limb induction. *Development,* 125, pp. 753-765.
- Yokoyama, H., Ide, H. and Tamura, K. (2001). FGF-10 Stimulates Limb Regeneration Ability in Xenopus laevis. *Developmental Biology*, 233(1), pp.72-79.
- Yokoyama, H., Maruoka, T., Ochi, H., Aruga, A., Ohgo, S., Ogino, H. and Tamura, K. (2011). Different Requirement for Wnt/β-Catenin Signaling in Limb Regeneration of Larval and Adult Xenopus. *PLoS ONE*, 6(7), p.e21721.
- Yokoyama, H., Ogino, H., Stoick-Cooper, C., Grainger, R and Moon, R. (2007). Wnt/β-catenin signaling has an essential role in the initiation of limb regeneration. *Developmental Biology*, 306(1), pp.170-178.

- Yokoyama, H., Yonei-Tamura, S., Endo, T., Izpisúa Belmonte, J., Tamura, K. and Ide, H. (2000). Mesenchyme with fgf-10 Expression Is Responsible for Regenerative Capacity in Xenopus Limb Buds. *Developmental Biology*, 219(1), pp.18-29.
- Yoo, S., Freisinger, C., LeBert, D. and Huttenlocher, A. (2012). Early redox, Src family kinase, and calcium signaling integrate wound responses and tissue regeneration in zebrafish. *The Journal of Cell Biology*, 199(2), pp.225-234.
- Yoshinari, N., Ishida, T., Kudo, A. and Kawakami, A. (2009). Gene expression and functional analysis of zebrafish larval fin fold regeneration. *Developmental Biology*, 325(1), pp.71-81.
- Yuasa, T., Kataoka, H., Kinto, N., Iwamoto, M., Enomoto-Iwamoto, M., Iemura, S., Ueno, N., Shibata, Y., Kurosawa, H. and Yamaguchi, A. (2002). Sonic hedgehog is involved in osteoblast differentiation by cooperating with BMP-2. *J. Cell. Physiol.*, 193(2), pp.225-232.
- Yuasa. T., Kataoka. H., Kinto. N., Iwamoto. M., Enomoto-Iwamoto. M., Iemura. S., Ueno. N., Shibata. Y., Kurosawa. H and Yamaguchi. A. (2002). Sonic hedgehog is involved in osteoblast differentiation by cooperating with BMP-2. *J. Cell. Physiol.*, 193(2), pp.225-232.
- Zunich, S., Douglas, T., Valdovinos, M., Chang, T., Bushman, W., Walterhouse, D., Iannaccone, P. and Lamm, M. (2009). Paracrine sonic hedgehog signalling by prostate cancer cells induces osteoblast differentiation. *Molecular Cancer*, 8(1), pp.12-22.

Acknowledgements

Firstly, I would like to extend my thanks to Dr. Henry Roehl for his excellent supervision, guidance and support over the last four years. Thanks also goes to the amazing members of the Roehl lab (Montse, Kunal, Calvin, Gareth, Luis, and Sarah – apologies if I have missed anyone!), without them I would not have enjoyed the long days as much as I have.

I would like to also thank my supervisors during my time in Singapore, Dr. Simon Cool and Dr. Victor Nurcombe, who made the transition to life in South East Asia incredibly easy. I would also like to extend my thanks to the members of their lab, who gave up their time to teach me the many techniques whilst there.

During my time as a PhD student I have had the opportunity to meet many incredible people, in wonderful places, who were not just great colleagues, but amazing friends.

Last but not least, I would like to thank my family (Susan, George, Jay and Dan), and fiancée Sarah; without you by my side, through the highs and lows, I would never have made it this far! For that I am eternally grateful.

Thank you all for the support!